Re-evaluation of LRFD Resistance Factors of Driven Piles

Final Report

December 2018

Florida Department of Transportation Project BDV25-977-53

Project Manager: Larry Jones, P.E.

State Geotechnical Engineer

SUBMITTED BY

M Gunaratne, Ph.D., P.E.,
G. Mullins, Ph.D., P.E.,

Dept. of Civil & Environment Engineering,
University of South Florida
4202 E. Fowler Avenue, ENB 118,
Tampa, FL 33620.
(813) 974 5818
Email: gunaratn@eng.usf.edu

And

S. Wasman, Ph.D.

Engineering School of Sustainable Infrastructure and Environment
University of Florida
1949 Stadium Road, 365 Weil Hall
Gainesville FL 32611
(352) 273-4609
Email: scott.wasman@essie.ufl.edu

DISCLAIMER

The opinions, findings, and conclusions expressed in this publication are those of the authors and not necessarily those of the Florida Department of Transportation. This document is disseminated under the sponsorship of the Department of Transportation in the interest of information exchange. The United States Government assumes no liability for the contents or use thereof.

STANDARD TABLE OF CONVERSION

To convert	U.S. Customary unit	SI unit	multiply by
Acceleration	ft/s^2	m/s^2	3.048E-1
Area	ft^2	m^2	9.290E-2
Load	(kip) kilo-pound force	N	9.80665
Length	Ft	M	3.048E-1
Pressure	lb/ft^2	N/m^2	4.788E+1
Velocity	ft/s	m/s	3.048E-1

TECHNICAL REPORT DOCUMENTATION PAGE

1. Report No.	2. Government Accession No.	3. Recipient's Catalog No.	
4. Title and Subtitle Re-evaluation of LRFD Resistance Factors of Driven Piles		5. Report Date December 11, 2018	
		6. Performing Organization Code	
7. Author(s) M. Gunaratne, G. Mullins, and S. Wasman		8. Performing Organization Report No.	
9. Performing Organization Name and Address Department of Civil and Environmental Engineering University of South Florida, 4202, East Fowler Avenue, Tampa, FL 33620 Engineering School of Sustainable Infrastructure and Environment, University of Florida, 575I Weil Hall, Gainesville FL 32611		10. Work Unit No. (TRAIS)	
		11. Contract or Grant No. BDV25-977-53	
12. Sponsoring Agency Name and Address Florida Department of Transportation 605 Suwannee St. MS 30 Tallahassee, FL 32399		13. Type of Report and Period Covered Final report January 2018 – December 2018	
		14. Sponsoring Agency Code	
15. Supplementary Notes Prepared in cooperation with the Federal Highway Administration			
16. Abstract The objective of this project was to evaluate the predicted capacity based on the embedded data collector(EDC) and the pile driving analyzer (PDA) compared to the corresponding static load test capacity of driven piles for the purpose of establishing appropriate Load and Resistance Factor Design (LRFD) resistance factors for use with the EDC-FDOT method and the PDA-CAPWAP method. To this end, University of South Florida (USF) and University of Florida (UF) researchers analyzed the static load test results and the corresponding capacity predictions based on EDC-FDOT and PDA-CAPWAP methods for 27 test piles driven and tested between 2008 and 2017. In addition, PDA-CAPWAP predictions and corresponding static load test results from a number of previously available test piles were also considered to supplement the above database. The resistance factors were computed based on the three traditional methods, namely the First-order second moment (FOSM) method, the Advanced first-order second moment (AFOSM) method and the Monte Carlo (MC) method. EDC-FDOT method predictions produced marginally higher resistance factors than the PDA-CAPWAP method. An approximate confidence interval analysis of the sample data set showed that with the number of test piles available, both PDA and EDC-FDOT methods provided a satisfactory margin of error for bias factors with high confidence levels.			
17. Key Words EDC, PDA, driven, piles		18. Distribution Statement- No restrictions. This document is available to the public through the National Technical Information Service, Springfield, VA 22161	
19. Security Classif. (of this report) Unclassified	20. Security Classif. (of this page) Unclassified	21. No. of Pages 136	22. Price

ACKNOWLEDGMENTS

EXECUTIVE SUMMARY

The objective of this project was to evaluate the predicted capacity based on the embedded data collector (EDC) and the pile driving analyzer (PDA) compared to the corresponding static load test capacity of driven piles for the purpose of establishing appropriate Load and Resistance Factor Design (LRFD) resistance factors for use with the EDC-FDOT method and the PDA-CAPWAP method. To this end, University of South Florida (USF) and University of Florida (UF) researchers analyzed the static load test results and the corresponding capacity predictions based on EDC-FDOT and PDA-CAPWAP methods for 27 test piles driven and tested between 2008 and 2017. In addition, PDA-CAPWAP predictions and corresponding static load test results from a number of previously available test piles were also considered to supplement the above database. The resistance factors were computed based on the three traditional methods, namely the First-order second moment (FOSM) method, the Advanced first-order second moment (AFOSM) method and the Monte Carlo (MC) method. EDC-FDOT method predictions produced marginally higher resistance factors than the PDA-CAPWAP method. An approximate confidence interval analysis of the sample data set showed that with the number of test piles available, both PDA and EDC-FDOT methods provided a satisfactory margin of error for bias factors with high confidence levels.

.

TABLE OF CONTENTS

LIST OF FIGURES

LIST OF TABLES

CHAPTER 1

INTRODUCTION

The objective of this project was to evaluate the predicted capacity based on the embedded data collector (EDC) and the pile driving analyzer (PDA) compared to the corresponding static load test capacity of driven piles for the purpose of establishing appropriate Load and Resistance Factor Design (LRFD) resistance factors for use with the EDC-FDOT method (Tran, et al, 2011 and 2012) and the PDA-CAPWAP method (Perez, 1998). USF and UF researchers have analyzed static load tests for 27 piles tested during 2008-2017. The project objective will be achieved by carrying out the following sequence of tasks:

Task 1(a) **-** Data collection from Static load tests
Task 1(b) - Data collection from CAPWAP predictions
Task 1(c) - Statistical analysis and calculation of resistance factors from CAPWAP predictions
Task 1(d) - Data collection from EDC predictions
Task 1(e) **-** Statistical analysis and calculation of resistance factors from EDC predictions

The work performed during the above tasks are reported in Chapters 2, 3, 4, 5 and 6 respectively. Finally, the conclusions and recommendations are documented in Chapter 7 of this report.

CHAPIER 2

DATA COLLECTION FROM STATIC LOAD TESTS

USF and UF researchers have collected static load test results for 27 piles tested during 2008-2017. The static load test (SLT) results are shown in Table 2.1. The capacities were obtained using the Davisson failure criterion. Table 2.1 also displays the maximum load applied during each SLT. Notes on some values seen in Table 2.1 and preliminary comments on the results are found at the end of the table. In addition, SLT plots used to obtain the total capacity of piles are found in the Appendix A.

Table 2.1: Results of static load tests

Pile no.	Location and pile	Static load test results											
		Davisson capacity						Maximum applied load					
		USF			UF			USF			UF		
		Tip (kip)	Skin (kip)	Total (kip)	Tip (kip)	Skin (kip)	Total (kip)	Tip (kip)	Skin (kip)	Total (kip)	Tip (kip)	Skin (kip)	Total (kip)
1	Baldwin Pass-Pile 1	159	653	812	120	692	812	204	688	892	202	690	892
2	Baldwin Pass-Pile 2	56*	219	275	48.8	226.2	275	91.2	273.8	365	102	264	366
3	Turnpike Widening-Orange Ave	120*	625	745	120	625	745	134	629	763	134	629	763
4	Turnpike Widening-Ramp A2	120	557	677	120	557	677	125	578	703	125	578	703
5	Turnpike Widening-Ramp A2-A44	N/A	N/A	N/A	N/A	N/A	N/A	N/A	N/A	N/A	N/A	N/A	N/A
6	Turnpike Widening-Ramp GH	N/A	N/A	N/A	N/A	N/A	N/A	210	990	1200	210	990	1200
7	Turnpike Widening-Taft Vineland	N/A	N/A	N/A	N/A	N/A	N/A	160	940	1100	160	940	1100
8	Bayou Lacassine Bent 1 Pile 1	71**	389	460	71	389	460	N/A	N/A	480	N/A	N/A	480
9	Bayou Lacassine Bent 1 Pile 3	153**	703	856	153	697	850	N/A	N/A	884	N/A	N/A	880

Table 2.1: Results of static load tests (contd.)

Pile no.	Location and pile	Static load test results											
		Davisson capacity						Maximum applied load					
		USF			UF			USF			UF		
		Tip (kip)	Skin (kip)	Total (kip)	Tip (kip)	Skin (kip)	Total (kip)	Tip (kip)	Skin (kip	Total (kip)	Tip (kip)	Skin (kip)	Total (kip)
10	Caminada Bay Bent 1	194	361	555	190	365	555	225	327	552	185	372	557
11	Caminada Bay TP4	N/A	N/A	N/A	N/A	N/A	N/A	N/A	N/A	1360	N/A	N/A	N/A
12	Caminada Bay Bent 7	115	503	618	115	535	650	115	575	690	115	543	658
13	US 331 Choctawhatchee Bay Pier 13	N/A	N/A	N/A	N/A	N/A	N/A	N/A	N/A	1500	N/A	N/A	1500
14	US 331 Choctawhatchee Bay Pier 25	N/A	N/A	1500	N/A	N/A	1500	N/A	N/A	1500	N/A	N/A	1500
15	US 331 Choctawhatchee Bay Pier 33	N/A	N/A	N/A	N/A	N/A	N/A	N/A	N/A	1500	N/A	N/A	1500
16	US 331 Choctawhatchee Bay Pier 59	N/A	N/A	1030	N/A	N/A	1035	N/A	N/A	1115	N/A	N/A	1103

Table 2.1: Results of static load tests (contd.)

Pile no.	Location and pile	Static load test results											
		Davisson capacity						Maximum applied load					
		USF			UF			USF			UF		
		Tip (kip)	Skin (kip)	Total (kip)	Tip (kip)	Skin (kip)	Total (kip)	Tip (kip)	Skin (kip)	Total (kip)	Tip (kip)	Skin (kip)	Total (kip)
17	US 331 Choctawhatche e Bay Pier 84	N/A	N/A	N/A	N/A	N/A	N/A	N/A	N/A	1500	N/A	N/A	1500
18	Dixie Highway Pier 4 - tension	0	212	212	0	215	215	0	222	222	0	225	225
19	Dixie Highway End Bent 1	226	202	428	306	174	480	N/A	N/A	596	375	183	558
20	Dixie Highway Pier 3	N/A	N/A	N/A	N/A	N/A	N/A	N/A	N/A	N/A	N/A	N/A	N/A
21	Dixie Highway Pier 8	184	191	375	178	185	363	N/A	N/A	510	308	217	525
22	I-95 Eau Gallie Bridge Bent 1 Pile 1	223	167	390	191	192	383	N/A	N/A	412.5	258	154.5	412.5
23	5th St Bascule Pier 2 Pile 37-tension	N/A	N/A	N/A	N/A	N/A	N/A	0	185	185	0	185	185
24	5th St Bascule Pier 2 Pile 53-tension	0	180	180	0	180	180	0	180	180	0	180	180

Table 2.1: Results of static load tests (contd.)

Pile no.	Location and pile	Static load test results											
		Davisson capacity						Maximum applied load					
		USF			UF			USF			UF		
		Tip (kip)	Skin (kip)	Total (kip)	Tip (kip)	Skin (kip)	Total (kip)	Tip (kip)	Skin (kip)	Total (kip)	Tip (kip)	Skin (kip)	Total (kip)
25	5th St Bascule Pier 3 Pile 9-tension	0	68	68	0	68	68	0	73	73	0	73	73
26	5th St Bascule Pier 3 Pile 11-tension	0	64	64	0	64	64	0	65	65	0	65	65
27	5th St Bascule Pier 3 Pile 42-tension	0	153	153	0	153	153	0	153	153	0	153	153

N/A – Not available
* Provided by the contractor at strain gauge level 2, located 24 inches from the pile tip.
**Obtained from Haque et al (2014).

Notes:

- Capacities from static load tests were obtained using the Davisson method.
- When the Davisson capacity was reached after the pile reached its maximum capacity, the maximum capacity was used as the pile capacity.
- The tip capacity was estimated based on the load observed at the bottom strain gauge at Davisson capacity.

Comments:

Table 2.1 shows that there are random (non-systematic) deviations in the capacities evaluated by UF and USF. These are suspected to be due to the graphical exercise used in evaluating the capacities using the Davisson method. The pile capacities evaluated by USF were used in the computation of bias factors.

The engineer for the static load test of Pile #2 noted in their report that there were issues with the loading jack during the test. Therefore, analysis of the top displacement versus applied load for Pile #2 considered the back calculated modulus of elasticity based on equilibrium between applied load and the measured strain at the top of the pile and not including the pile in the data set of bias. For completeness of the study, the bias statistics and resistance factors with and without Pile #2 will be presented.

CHAPTER 3

DATA COLLECTION FROM CAPWAP PREDICTIONS

USF and UF researchers have analyzed static load tests and PDA-based predictions for 27 test piles tested during 2008-2017. The PDA CAPWAP method predictions are shown in Tables 3.1-3.4. Observation of Tables 3.1-3.4 shows that there is a close agreement between the evaluations by USF and UF. Finally, Table 3.5 was developed to demonstrate the PDA-CAPWAP predictions from the closest restrike prior to the corresponding static load tests (SLT), in terms of time. Note that the PDA-based predictions for test piles #13, #16 and #1 in Table 3.5 are based on reported revised predictions (same blow), reported after the static load test, or reported revised predictions (same blow) that include the static load test results in Chapter 2.

Table 3.1: Comparison of PDA-CAPWAP pile capacities obtained by USF and UF (EOID)

Pile no	EOID							
	USF				UF			
	Date	Tip (kip)	Skin (kip)	Total (kip)	Date	Tip (kip)	Skin (kip)	Total (kip)
1	7/20/2017	147	336	483	7/20/2017	147	336	483
2	6/17/2017	N/A	N/A	N/A	6/17/2017	N/A	N/A	N/A
3	6/21/2017	77	176.9	253.9	6/21/2017	77	176.9	253.9
4	7/18/2017	N/A	N/A	N/A	7/18/2017	N/A	N/A	N/A
5	7/18/2017	N/A	N/A	N/A	7/18/2017	N/A	N/A	N/A
6	5/5/2017	144.9	152.2	297.1	5/5/2017	144.9	152.2	297.1
7	6/9/2017	243.4	878.9	1,122.3	6/9/2017	243.4	878.9	1,122.3
8	10/4/2012	76	284	360	10/4/2012	76	284	360
9	9/18/2012	172	336	508	9/18/2012	172	336	508
10	1/25/2010	198.6	251.4	450	1/25/2010	198.6	251.4	450
11	2/3/2010	315	204.2	519.2	2/3/2010	315	204.2	519.2
12	-	-	-	-	-	-	-	-
13	2/24/2014	N/A	N/A	N/A	2/24/2014	N/A	N/A	N/A
14	3/12/2014	N/A	N/A	N/A	3/12/2014	N/A	N/A	N/A
15	3/26/2014	N/A	N/A	N/A	3/26/2014	N/A	N/A	N/A
16	4/22/2014	N/A	N/A	N/A	4/22/2014	N/A	N/A	N/A
17	-	-	-	-	-	-	-	-
18	4/9/2010	1040	260	1300	4/9/2010	1040	260	1300
19	4/21/2010	391	209	600	4/21/2010	391	209	600
20	3/19/2010	217	308	525	3/19/2010*	217	308	525
21	5/6/2010	312	233	545	5/6/2010	312	233	545
22	-	-	-	-	-	-	-	-
23	8/1/2008	1464.7	197.3	1662	8/1/2008	1464.7	197.3	1662
24	7/28/2008	1415.5	230.9	1646.4	7/28/2008	1415.5	230.9	1646.4
25	8/21/2008	1728.1	128.8	1856.9	8/21/2008	1728.1	128.8	1856.9
26	9/2/2008	765	344.6	1109.6	9/2/2008	765	344.5	1109.6
27	8/26/2008	1314.3	271.1	1588.4	8/26/2008	1314.3	274.1	1588.4

EOID – End of Initial driving

*Pile 20 was initially driven on 3/16/2010 and then driven an additional 4 ft on 3/19/2010. There is not a SLT reported. UF is recommending the CAPWAP predictions reported for the blow near the end of the drive on 3/19/2010.

'-' mark indicates the a PDA-CAPWAP prediction was not made.

N/A indicates that data are not available

Table 3.2: Comparison of PDA-CAPWAP pile capacities obtained by USF and UF (Beginning of restrike - BOR-1)

Pile no	BOR-1							
	USF				UF			
	Date	Tip (kip)	Skin (kip)	Total (kip)	Date	Tip (kip)	Skin (kip)	Total (kip)
1	7/31/2017	159	535	694	7/31/2017	158.5	535.5	694
2	6/26/2017	100	409	509	6/26/2017	100	409	509
3	6/30/2017	61.6	340.6	402.2	6/30/2017	61.6	340.6	402.2
4	7/21/2017	136	360.3	496.3	7/21/2017	136	360.3	496.3
5	7/18/2017	67.7	306.2	373.9	7/18/2017	67.7	306.1	373.9
6	5/9/2017	584.9	299	883.9	5/9/2017	584.9	299	883.9
7	6/12/2017	306	1231.9	1537.9	6/12/2017	306	1231.9	1537.9
8	10/4/2012	80	290	370	10/4/2012	80	290	370
9	9/18/2012	178	416	594	9/18/2012	178	416	594
10	2/1/2010	210.2	359.8	570	2/1/2010	210.2	359.8	570
11	2/3//2010	313.4	306.6	620	2/3//2010	313.4	306.6	620
12	1/27/2010	135	230	365	1/27/2010	135	230	365
13	2/27/2014	264.9	434.7	699.6	2/27/2014	149.6 **264.9**	550 **434.7**	699.6
14	4/1/12014	317.1	649.9	967	4/1/12014	317.1	650	967
15	4/1/2014	**748.77**	**1644.4**	**2413.11**	4/1/2014	**748.77**	**1644.4**	**2413.11**
16	5/1/2014	348.5	889.6	1238.1	5/1/2014	**348.5**	**889.6**	**1238.1**
17	5/15/2014	1029.3	399.9	1429.2	5/15/2014	**1029.3**	**399.9**	**1429.2**
18	4/12/2010	310,1167	290,233	600,1400	4/12/2010*	310,1167	290,233	600,1400
19	4/26/2010	269, 278	254,182	523,460	4/26/2010**	269,278	254,182	523,460
20	-	-	-		-	-	-	-
21	5/10/2010	213.7	286.3	500	5/10/2010	213.7	286.3	500
22	-	-	-	-	-	-	-	-
23	N/A	921	243	1164	N/A	921	243	1164
24	N/A	1246	56	1302	N/A	1246	56	1302
25	-	-	-	-	-	-	-	-
26	N/A	1436	61	1497	N/A	1436	61	1497
27	N/A	1153	70	1223	N/A	1153	70	1223

Bold values are reported revised estimates (same blow), reported after the static load test, or reported revised estimates (same blow) that include the static load test results in the report.
* Two reported BOR1 CAPWAP estimates at 6-minute time interval difference.
** Two reported BOR1 CAPWAP estimates at 1-minute time interval difference.
'-' mark indicates that a PDA-CAPWAP prediction was not made.
N/A indicates that data are not available

Table 3.3: Comparison of PDA-CAPWAP pile capacities obtained by USF and UF (BOR-2)

Pile no	BOR-2							
	USF				UF			
	Date	Tip (kip)	Skin (kip)	Total (kip)	Date	Tip (kip)	Skin (kip)	Total (kip)
1	8/8/2017	171	529	700	8/8/2017	171.1	528.8	699.9
2	7/6/2017	125	500	625	7/6/2017	125.3	499.8	625.1
3	7/11/2017	55.1	465.6	520.7	7/11/2017	55.1	465.5	520.7
4	-	-	-	-	-	-	-	-
5	-	-	-	-	-	-	-	-
6	5/30/2017	487.6	918.4	1406	5/30/2017	487.6	-	1406
7	6/14/2017	206.6	1339.4	1546	6/14/2017	206.6	-	1546
8	10/5/2012	79	348	427	10/5/2012	79	348	427
9	9/19/2012	162	488	650	9/19/2012	162	488	650
10	2/21/2010	193.5	406.5	600	2/21/2010	193.5	406.5	600
11	2/21/2010	361.9	862.5	1224.4	2/21/2010	361.9	862.5	1224
12	2/24/2010	142.6	397.5	540.1	2/24/2010	142.6	397.5	540
13	4/12/2014	606.1	897.3	1503.4	4/12/2014	606.1	897.3	1503.4
14	-	-	-	-	-	-	-	-
15	-	-	-	-	-	-	-	-
16	-	-	-	-	-	-	-	-
17	-	-	-	-	-	-	-	-
18	-	-	-	-	-	-	-	-
19	-	-	-	-	-	-	-	-
20	-	-	-		-	-	-	-
21	5/14/2010	255,390.2	223,211.9	478,602.1	5/14/2010*	255,390.2	223,211.9	478, 602.1
22	-	-	-	-	-	-	-	-
23	-	-	-	-	-	-	-	-
24	-	-	-	-	-	-	-	-
25	-	-	-	-	-	-	-	-
26	-	-	-	-	-	-	-	-
27	-	-	-	-	-	-	-	-

* Two reported BOR2 CAPWAP estimates

'-' mark indicates that a PDA-CAPWAP prediction was not made.

N/A indicates that data are not available

Table 3.4: Comparison of PDA-CAPWAP pile capacities obtained by USF and UF (BOR-3)

Pile no	BOR-3							
	USF				UF			
	Date	Tip (kip)	Skin (kip)	Total (kip)	Date	Tip (kip)	Skin (kip)	Total (kip)
1	-	-	-	-	-	-	-	-
2	-	-	-	-	-	-	-	-
3	-	-	-	-	-	-	-	-
4	7/24/2017	184.3	343.3	527.6	7/24/2017	184.3	343.3	527.6
5	-	-	-	-	-	-	-	-
6	-	-	-	-	-	-	-	-
7	-	-	-	-	-	-	-	-
8	5/9/2013	102	534	636	5/9/2013	102	534	636
9	3/18/2013	172	642	814	3/18/2013	172	642	814
10	-	-	-	-	-	-	-	-
11	-	-	-	-	-	-	-	-
12	-	-	-	-	-	-	-	-
13	-	-	-	-	-	-	-	-
14	-	-	-	-	-	-	-	-
15	-	-	-	-	-	-	-	-
16	-	-	-	-	-	-	-	-
17	-	-	-	-	-	-	-	-
18	-	-	-	-	-	-	-	-
19	-	-	-	-	-	-	-	-
20	-	-	-	-	-	-	-	-
21	-	-	-	-	-	-	-	-
22	-	-	-	-	-	-	-	-
23	-	-	-	-	-	-	-	-
24	-	-	-	-	-	-	-	-
25	-	-	-	-	-	-	-	-
26	-	-	-	-	-	-	-	-
27	-	-	-	-	-	-	-	-

'-' mark indicates a PDA-CAPWAP prediction was not made.

N/A indicates that data are not available

Table 3.5: Results from PDA- CAPWAP analysis at the closest re-strike prior to SLT

Pile capacities evaluated at the closest re-strike to SLT under CAPWAP method				
Pile no.	Tip (kip)	Skin (kip)	Total Capacity (kip)	Date
1	159	535	694	7/31/2017
2	100	409	509	6/26/2017
3	61.6	340.6	402.2	6/30/2017
4	136	360.3	496.3	7/21/2017
5	67.7	306.2	373.9	7/18/2017
6	487.6	918.4	1406	5/30/2017
7	306	1231.9	1537.9	6/12/2017
8	79	348	427	10/5/2012
9	162	488	650	9/19/2012
10	210.2	359.8	570	2/1/2010
11	-	-	-	-
12	142.6	397.5	540.1	2/24/2010
13	264.9	434.7	699.6	2/27/2014
14	317.1	649.9	967	4/1/12014
15	-	-	-	4/1/2014
16	348.5	889.6	1238.1	5/1/2014
17	1029.3	399.9	1429.2	5/15/2014
18	1167	233	1400	4/12/2010
19	278	182	460	4/26/2010
20	-	-	-	-
21	213.7	286.3	500	5/10/2010
22	-	-	-	-
23	921	243	1164	-
24	1246	56	1302	-
25	1728.1	128.8	1856.9	8/21/2008
26	1436	61	1497	-
27	1153	70	1223	-

'-' mark indicates that a PDA-CAPWAP prediction was not made or that the date of the prediction is unknown.

N/A indicates that data are not available

CHAPTER 4

STATISTICAL ANALYSIS AND CALCULATION OF RESISTANCE FACTORS – CAPWAP

As documented in Chapters 2 and 3, USF and UF researchers compiled the predicted capacities from static load tests, PDA tests, and EDC tests conducted on 27 test piles tested during 2008-2017. PDA evaluations based on CAPWAP predictions were considered. It was also shown in the above chapters how close agreement was achieved between USF and UF reviews of the predictions from static load tests, PDA tests, and EDC tests. In the next task, the bias factors for CAPWAP estimated resistance were calculated based on Eqn. (4.1) for the following cases:

1. total capacity predictions at the closest re-strikes prior to the static load test
2. tip capacity predictions at the closest re-strikes prior to the SLT
3. skin friction capacity at the closest re-strikes prior to the SLT
4. skin friction capacity predictions at the closest re-strikes prior to the SLT of the compression and tension piles
5. total capacity predictions at the closest re-strikes prior to the SLT combined with the total capacity predictions in McVay et al (2000)
6. total capacity predictions at EOID (end of initial driving), combined with the total capacity predictions at EOID in McVay et al (2000).

$$\lambda_R = \frac{Measured\ resistance}{Predicted\ resistance} \tag{4.1}$$

The complete bias results of the cases 1, 2, and 3 are in Table 4.1, and the mean and the coefficient of variation (COV) of the bias factors for cases 1-6 are in Table 4.2. It must be noted that Table 4.1 does not include values for all the test piles because some piles did not reach failure according to the Davisson criterion, and hence, the corresponding bias values could not be calculated.

4.1 Fitting of data against the assumed theoretical distributions

It is known that normal distributions are not considered in reliability evaluations due to the extension of probability density function into the (unrealistic) negative value range. Furthermore, in Case 1 of these CAPWAP data for example, there is a significantly irrelevant upper tail (from 1,550 to 2,000 kip) where no measured resistances were available. Hence, the normal distribution approximation was not used for simulating the distribution of resistances (and loads). On the other hand, the range of resistances predicted by the CAPWAP method is represented by a lognormal distribution reasonably well, as seen in Figure 4.1. Figure 4.1 was constructed using the natural logarithm of the CAPWAP predicted resistances and the theoretical lognormal probability density function, which is a Gaussian distribution with the following statistics:

$$\mu_R = ln\left[\frac{(Mean)}{\sqrt{1+COV_R^2}}\right] \qquad (4.2)$$

$$\sigma_R = \sqrt{ln(1 + COV_R^2)} \qquad (4.3)$$

Table 4.1: Bias factors for CAPWAP predictions at the re-strike closest to SLT (summer 2017 FDOT data) (Cases 1,2, and 3)

Pile #	Tip (kip)	Skin (kip)	Total Capacity (kip)	λ tip	λ skin	λ total
1	159	535	694	1	1.220561	1.1700
2	100	409	509	0.56	0.535452	0.5403
3	61.6	340.6	402.2	1.948052	1.834997	1.8523
4	136	360.3	496.3	0.882353	1.545934	1.3641
5	67.7	306.2	373.9			
6	487.6	918.4	1406			
7	306	1231.9	1537.9			
8	79	348	427	0.898734	1.117816	1.0773
9	162	488	650	0.944444	1.440574	1.3169
10	210.2	359.8	570	0.922931	1.003335	0.9737
11	-	-	-			
12	142.6	397.5	540.1	0.806452	1.265409	1.1442
13	264.9	434.7	699.6			
14	317.1	649.9	967			1.5512
15	-	-	-			
16	348.5	889.6	1238.1			0.8319
17	1029.3	399.9	1429.2			
18	1167	233	1400		0.909871	
19	278	182	460	0.81295	1.10989	0.9304
20	-	-	-			
21	213.7	286.3	500	0.86102	0.667132	0.7500
22	-	-	-			
23	921	243	1164			
24	1246	56	1302		3.214286	
25	1728.1	128.8	1856.9		1.220561	
26	1436	61	1497		0.535452	
27	1153	70	1223		1.834997	

.

Table 4.2: Summary of CAPWAP bias factor statistics (Cases 1-6), including pile #2

Case	Description	Size of dataset	Mean of Bias	COV of Bias
1	CAPWAP-Closest and prior to re-strike to SLT, total capacity – 2008-2017 data	13	1.125	0.321
2	CAPWAP-Closest and prior to re-strike to SLT 2008-2017 data, tip capacity	10	0.964	0.380
3	CAPWAP -Closest and prior to re-strike to SLT 2008-2017 data, skin friction capacity	10	1.174	0.331
4	CAPWAP skin friction capacity (compression and tension) 2008-2017 data	15	1.297	0.513
5	CAPWAP- Total capacity- EOID 2008-2017 data + McVay et al (2000) data	49	1.569	0.368
6	CAPWAP-Closest and prior to re-strike to SLT, total capacity - 2008-2017 data + McVay et al (2000) data	91	1.246	0.342

Table 4.3: Summary of CAPWAP bias factor statistics (Cases 1-6), excluding pile #2

Case	Description	Size of dataset	Mean of Bias	COV of Bias
1	CAPWAP-Closest and prior to re-strike to SLT, total capacity – 2008-2017 data	12	1.178	0.277
2	CAPWAP-Closest and prior to re-strike to SLT 2008-2017 data, tip capacity	9	1.009	0.355
3	CAPWAP -Closest and prior to re-strike to SLT 2008-2017 data, skin friction capacity	9	1.245	0.270
4	CAPWAP skin friction capacity (compression and tension) 2008-2017 data	14	1.351	0.485
5	CAPWAP- Total capacity- EOID 2008-2017 data + McVay et al (2000) data	49	1.569	0.368
6	CAPWAP-Closest and prior to re-strike to SLT, total capacity - 2008-2017 data + McVay et al (2000) data	90	1.254	0.337
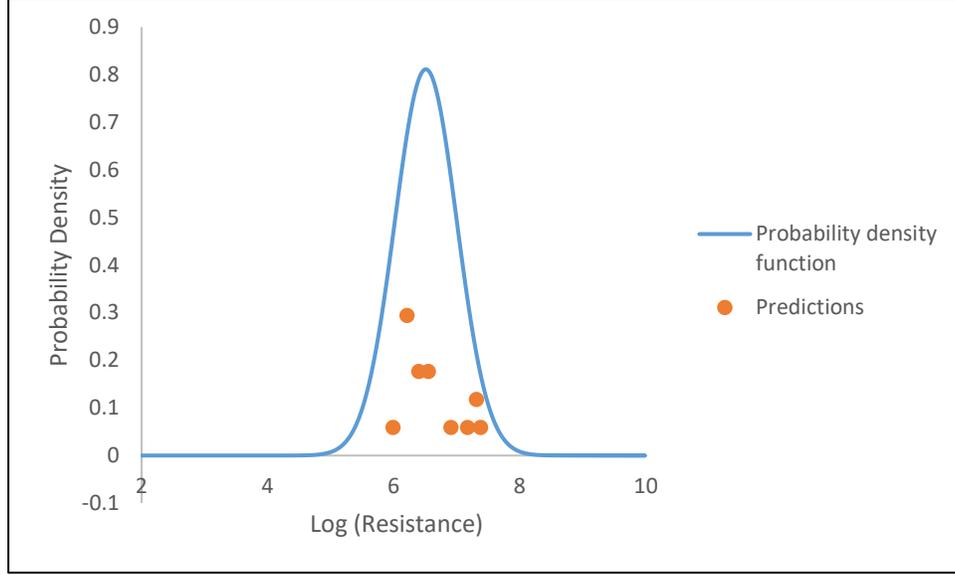
Figure 4.1: Comparison of actual data with the log-normal distribution (CAPWAP total pile capacity at the closest re-strike prior to SLT, Case 1)

Based on Figure 4.1, it can be seen that the resistances are somewhat realistically simulated by the lognormal distribution. Moreover, lognormal representations would not yield unrealistic reliability estimates as in the case of a normal distribution which is the only other option that analysts generally consider. On the other hand, since the samples are relatively small, use of t-distributions would be appropriate although they are not in common use in reliability related work.

4.2 Calculation of resistance factors

The FOSM (First-order second moment) method was used to compute the resistance factors for the CAPWAP predictions. In the FOSM method for log-normally distributed load and resistance, using a performance function of $G= ln(R/Q) = lnR\text{-}lnQ,$ where R and Q are the resistance and load respectively, the resistance factor (ϕ_R) can be calculated using the following expression:

$$\phi_R = \frac{\lambda_R[\gamma_D Q_D + \gamma_L Q_L]\sqrt{\frac{(1+COVQ_D^2+COVQ_L^2)}{(1+COVQ_R^2)}}}{[\lambda_{QD}Q_D+\lambda_{QL}Q_L]e^{\beta_T\sqrt{\ln[(1+COVQ_D^2+COVQ_L^2)(1+COVQ_R^2)]}}} \qquad (4.4)$$

where λ_R is the bias of the resistance, Q_D is the dead load, Q_L is the live load, γ_D is the dead load factor, γ_L is the live load factor, COV_{QD} is the coefficient of variation of dead load, COV_{QL} is the coefficient of variation of live load and β_T is the target reliability. The following values of the above variables obtained from Paikowsky et. al (2004) study were used in this research. Dead to live load ratio (Q_D/Q_L) = 3, *γ_D = 1.25, γ_L = 1.75, COV_{QD} = 0.1, COV_{QL} = 0.18, λ_{QD} = 1.05* and *λ_{QL} = 1.15.* For cases 1-6, the resistance factors

calculated using Equation 3.4 for a β_T = 2.33 and 2.1 (corresponding to a probabilities of failure of 1% and 1.8%) are shown in Tables 4.4-4.7. Furthermore, the calculated resistance factors for cases 1-6 (including pile #2 and excluding pile #2) for a range of target reliabilities are in Appendix B (Tables B.1-B.12). Finally, the resistance factors developed with the FOSM method were validated using Monte Carlo simulation (Appendix D) of the load and resistance probability distributions corresponding to the respective statistics. In addition, the results of the FOSM analysis was compared to those of the AFOSM method illustrated in the Appendix C.

Table 4.4: Summary of bias factor statistics and resistance factors with the FOSM method for a reliability index of 2.33, including pile #2

Case	Description	Size of dataset	Mean of Bias	COV of Bias	Resistance factor with FOSM method
1	CAPWAP-Closest re-strike prior to SLT, total capacity – 2008-2017 data	12	1.125	0.321	0.586
2	CAPWAP-Closest re-strike prior to SLT 2008-2017 data, tip capacity	10	0.964	0.380	0.442
3	CAPWAP -Closest re-strike prior to SLT 2008-2017 data, skin friction capacity	10	1.174	0.331	0.598
4	CAPWAP skin friction capacity (compression and tension) 2008-2017 data	15	1.297	0.513	0.443
5	CAPWAP- Total capacity- EOID 2008-2017 data + McVay et al (2000) data	49	1.569	0.368	0.739
6	CAPWAP-Closest re-strike prior to SLT, total capacity - 2008-2017 data + McVay et al (2000) data	91	1.246	0.341	0.62

Table 4.5: Summary of bias factor statistics and resistance factors with the FOSM method for a reliability index of 2.33, excluding pile #2

Case	Description	Size of dataset	Mean of Bias	COV of Bias	Resistance factor with FOSM method
1	CAPWAP- Closest re-strike prior to SLT, total capacity – 2008-2017 data	12	1.178	0.277	0.672
2	CAPWAP- Closest re-strike prior to SLT 2008-2017 data, tip capacity	9	1.009	0.355	0.489
3	CAPWAP - Closest re-strike prior to SLT 2008-2017 data, skin friction capacity	9	1.2452	0.270	0.719
4	CAPWAP skin friction capacity (compression and tension) 2008-2017 data	14	1.351	0.485	0.492
5	CAPWAP- Total capacity- EOID 2008-2017 data + McVay et al (2000) data	49	1.569	0.368	0.739
6	CAPWAP- Closest re-strike prior to SLT, total capacity - 2008-2017 data + McVay et al (2000) data	90	1.245	0.337	0.631

Table 4.6: Summary of bias factor statistics and resistance factors with the FOSM method for a reliability index of 2.1, including pile #2

Case	Description	Size of dataset	Mean of Bias	COV of Bias	Resistance factor with FOSM method
1	CAPWAP-Closest re-strike prior to SLT, total capacity – 2008-2017 data	12	1.125	0.321	0.638
2	CAPWAP-Closest re-strike prior to SLT 2008-2017 data, tip capacity	10	0.964	0.380	0.487
3	CAPWAP -Closest re-strike prior to SLT 2008-2017 data, skin friction capacity	10	1.174	0.331	0.653
4	CAPWAP skin friction capacity (compression and tension) 2008-2017 data	15	1.297	0.513	0.50
5	CAPWAP- Total capacity- EOID 2008-2017 data + McVay et al (2000) data	49	1.569	0.368	0.811
6	CAPWAP-Closest re-strike prior to SLT, total capacity - 2008-2017 data + McVay et al (2000) data	91	1.246	0.341	0.680

Table 4.7: Summary of bias factor statistics and resistance factors with the FOSM method for a reliability index of 2.1, excluding pile #2

Case	Description	Size of dataset	Mean of Bias	COV of Bias	Resistance factor with FOSM method
1	CAPWAP- Closest re-strike prior to SLT, total capacity – 2008-2017 data	11	1.178	0.277	0.726
2	CAPWAP- Closest re-strike prior to SLT 2008-2017 data, tip capacity	9	1.009	0.355	0.535
3	CAPWAP - Closest re-strike prior to SLT 2008-2017 data, skin friction capacity	9	1.2452	0.270	0.777
4	CAPWAP skin friction capacity (compression and tension) 2008-2017 data	14	1.351	0.485	0.552
5	CAPWAP- Total capacity- EOID 2008-2017 data + McVay et al (2000) data	49	1.569	0.368	0.811
6	CAPWAP- Closest re-strike prior to SLT, total capacity - 2008-2017 data + McVay et al (2000) data	90	1.245	0.337	0.684

4.3 Results of Monte Carlo simulation

The respective resistance factors obtained from the Monte-Carlo simulation using the above methods are given in Tables 4.8-4.11.

Table 4.8: Bias of resistance, COV of resistance and resistance factors from the MC method for a reliability index of 2.33, including pile #2

Case	Description	Size of dataset	Mean of Bias	COV of Bias	Resistance factor with MC method
1	CAPWAP-Closest re-strike to SLT, total capacity – 2008-2017 data	13	1.125	0.321	0.644
2	CAPWAP-Closest re-strike to SLT 2008-2017 data, tip capacity	10	0.964	0.380	0.48
3	CAPWAP - Closest re-strike to SLT 2008-2017 data, skin friction capacity	10	1.174	0.331	0.657
4	CAPWAP -skin friction capacity (compression and tension) 2008-2017 data	15	1.297	0.513	0.471
5	CAPWAP- Total capacity- EOID 2008-2017 data + McVay et al (2000) data	49	1.569	0.368	0.804
6	CAPWAP-Closest re-strike to SLT, total capacity - 2008-2017 data + McVay et al (2000) data	91	1.246	0.342	0.679

Table 4.9: Bias of resistance, COV of resistance and resistance factors from the MC method for a reliability index of 2.33, excluding pile #2

Case	Description	Size of dataset	Mean of Bias	COV of Bias	Resistance factor with MC method
1	CAPWAP-Closest re-strike to SLT, total capacity – 2008-2017 data	11	1.178	0.277	0.75
2	CAPWAP-Closest re-strike to SLT 2008-2017 data, tip capacity	9	1.009	0.355	0.534
3	CAPWAP - Closest re-strike to SLT 2008-2017 data, skin friction capacity	9	1.245	0.270	0.805
4	CAPWAP - tension piles, skin friction capacity 2008-2017 data	14	1.351	0.485	0.524
5	CAPWAP- Total capacity- EOID 2008-2017 data + McVay et al (2000) data	49	1.569	0.368	0.804
6	CAPWAP-Closest re-strike to SLT, total capacity - 2008-2017 data + McVay et al (2000) data	90	1.254	0.337	0.692

Table 4.10: Bias of resistance, COV of resistance and resistance factors from the MC method for a reliability index of 2.1, including pile #2

Case	Description	Size of dataset	Mean of Bias	COV of Bias	Resistance factor with MC method
1	CAPWAP-Closest re-strike to SLT, total capacity – 2008-2017 data	12	1.125	0.321	0.694
2	CAPWAP-Closest re-strike to SLT 2008-2017 data, tip capacity	10	0.964	0.380	0.524
3	CAPWAP - Closest re-strike to SLT 2008-2017 data, skin friction capacity	10	1.174	0.331	0.71
4	CAPWAP -skin friction capacity (compression and tension) 2008-2017 data	15	1.297	0.513	0.526
5	CAPWAP- Total capacity- EOID 2008-2017 data + McVay et al (2000) data	49	1.569	0.368	0.875
6	CAPWAP-Closest re-strike to SLT, total capacity - 2008-2017 data + McVay et al (2000) data	91	1.246	0.342	0.734

Table 4.11: Bias of resistance, COV of resistance and resistance factors from the MC method for a reliability index of 2.1, excluding pile #2

Case	Description	Size of dataset	Mean of Bias	COV of Bias	Resistance factor with MC method
1	CAPWAP-Closest re-strike to SLT, total capacity – 2008-2017 data	11	1.178	0.277	0.80
2	CAPWAP-Closest re-strike to SLT 2008-2017 data, tip capacity	9	1.009	0.355	0.579
3	CAPWAP - Closest re-strike to SLT 2008-2017 data, skin friction capacity	9	1.245	0.270	0.858
4	CAPWAP - tension piles, skin friction capacity 2008-2017 data	14	1.351	0.485	0.584
5	CAPWAP- Total capacity- EOID 2008-2017 data + McVay et al (2000) data	49	1.569	0.368	0.875
6	CAPWAP-Closest re-strike to SLT, total capacity - 2008-2017 data + McVay et al (2000) data	90	1.254	0.337	0.747

4.4 Reliability analysis using the AFOSM method

Based on the theoretical concepts related to the AFOSM method illustrated in the Appendix B, a performance function (g), which defines the failure region on the resistance (R) vs. load (S) space, was employed to estimate the reliability index (β) for the CAPWAP predicted capacity closest to SLT. The corresponding resistance statistics are shown in Tables 4.12-4.15 while the load statistics have been defined in the section discussing Eqn. (4.4).

Table 4.12: Bias of resistance, COV of resistance and resistance factors from AFOSM for a reliability index of 2.33, including pile #2

Case	Description	Size of dataset	Mean of Bias	COV of Bias	Resistance factor with AFOSM method
1	CAPWAP-Closest re-strike prior to SLT, total capacity – 2008-2017 data	13	1.125	0.321	0.644
2	CAPWAP-Closest re-strike prior to SLT 2008-2017 data, tip capacity	10	0.964	0.380	0.48
3	CAPWAP - Closest re-strike prior to SLT 2008-2017 data, skin friction capacity	10	1.174	0.331	0.656
4	CAPWAP -skin friction capacity (compression and tension) 2008-2017 data	15	1.297	0.513	0.471
5	CAPWAP- Total capacity- EOID 2008-2017 data + McVay et al (2000) data	49	1.569	0.368	0.804
6	CAPWAP-Closest re-strike prior to SLT, total capacity - 2008-2017 data + McVay et al (2000) data	91	1.246	0.342	0.679

Table 4.13: Bias of resistance, COV of resistance and resistance factors from AFOSM for a reliability index of 2.33, excluding pile #2

Case	Description	Size of dataset	Mean of Bias	COV of Bias	Resistance factor with AFOSM method
1	CAPWAP- Closest re-strike prior to SLT, total capacity – 2008-2017 data	11	1.178	0.277	0.749
2	CAPWAP- Closest re-strike prior to SLT 2008-2017 data, tip capacity	9	1.009	0.355	0.533
3	CAPWAP - Closest re-strike prior to SLT 2008-2017 data, skin friction capacity	9	1.245	0.270	0.805
4	CAPWAP - tension piles, skin friction capacity 2008-2017 data	14	1.351	0.485	0.524
5	CAPWAP- Total capacity- EOID 2008-2017 data + McVay et al (2000) data	49	1.569	0.368	0.804
6	CAPWAP- Closest re-strike prior to SLT, total capacity - 2008-2017 data + McVay et al (2000) data	90	1.254	0.337	0.691

Table 4.14: Bias of resistance, COV of resistance and resistance factors from AFOSM for a reliability index of 2.1, including pile #2

Case	Description	Size of dataset	Mean of Bias	COV of Bias	Resistance factor with AFOSM method
1	CAPWAP- Closest re-strike prior to SLT, total capacity – 2008-2017 data	13	1.125	0.321	0.694
2	CAPWAP- Closest re-strike prior to SLT 2008-2017 data, tip capacity	10	0.964	0.380	0.523
3	CAPWAP - Closest re-strike prior to SLT 2008-2017 data, skin friction capacity	10	1.174	0.331	0.709
4	CAPWAP -skin friction capacity (compression and tension) 2008-2017 data	15	1.297	0.513	0.527
5	CAPWAP- Total capacity- EOID 2008-2017 data + McVay et al (2000) data	49	1.569	0.368	0.874
6	CAPWAP- Closest re-strike prior to SLT, total capacity - 2008-2017 data + McVay et al (2000) data	91	1.246	0.342	0.735

Table 4.15: Bias of resistance, COV of resistance and resistance factors from AFOSM for a reliability index of 2.1, excluding pile #2

Case	Description	Size of dataset	Mean of Bias	COV of Bias	Resistance factor with AFOSM method
1	CAPWAP- Closest re-strike prior to SLT, total capacity – 2008-2017 data	11	1.178	0.277	0.80
2	CAPWAP- Closest re-strike prior to SLT 2008-2017 data, tip capacity	9	1.009	0.355	0.578
3	CAPWAP - Closest re-strike prior to SLT 2008-2017 data, skin friction capacity	9	1.245	0.270	0.858
4	CAPWAP - tension piles, skin friction capacity 2008-2017 data	14	1.351	0.485	0.584
5	CAPWAP- Total capacity- EOID 2008-2017 data + McVay et al (2000) data	49	1.569	0.368	0.874
6	CAPWAP- Closest re-strike prior to SLT, total capacity - 2008-2017 data + McVay et al (2000) data	90	1.254	0.337	0.748

4.5 Summary of calculated resistance factors for different cases of the CAPWAP data

A comparison of the calculated resistance factors using the methods presented (Tables 4.16-4.19) shows agreement between the MC and AFOSM methods and those factors are generally greater than those from the FOSM method. This has also been shown by Paikowsky (2004) and Kwak et al (2010).

Table 4.16: Comparison of resistance factors from FOSM, MC, and AFOSM methods for a reliability index of 2.33 with the data sets of the bias resistance, including pile #2

Case	Resistance factor with FOSM method	Resistance factor with MC method	Resistance factor with AFOSM method
1	0.586	0.644	0.644
2	0.442	0.48	0.48
3	0.598	0.657	0.656
4	0.443	0.471	0.471
5	0.739	0.804	0.804
6	0.62	0.679	0.679

Table 4.17: Comparison of resistance factors from FOSM, MC, and AFOSM methods for a reliability index of 2.33 with the data sets of the bias resistance, excluding pile #2

Case	Resistance factor with FOSM method	Resistance factor with MC method	Resistance factor with AFOSM method
1	0.672	0.75	0.749
2	0.489	0.534	0.533
3	0.719	0.805	0.805
4	0.492	0.524	0.524
5	0.739	0.804	0.804
6	0.631	0.692	0.691

FOSM analysis assumes Gaussian behavior of data. Therefore, FOSM analysis is strictly accurate when both the resistance and load data follow normal distributions or the logarithms of such data follow normal distributions. On the other hand, AFOSM specifies an approximation to analyze data that is not normal or lognormal.

Table 4.18: Comparison of resistance factors from FOSM, MC, and AFOSM methods for a reliability index of 2.1 with the data sets of the bias resistance, including pile #2

Case	Resistance factor with FOSM method	Resistance factor with MC method	Resistance factor with AFOSM method
1	0.638	0.694	0.694
2	0.487	0.524	0.523
3	0.653	0.71	0.709
4	0.50	0.526	0.527
5	0.811	0.875	0.874
6	0.680	0.734	0.735

Table 4.19: Comparison of resistance factors from FOSM, MC, and AFOSM methods for a reliability index of 2.1 with the data sets of the bias resistance, excluding pile #2

Case	Resistance factor with FOSM method	Resistance factor with MC method	Resistance factor with AFOSM method
1	0.726	0.80	0.80
2	0.535	0.579	0.578
3	0.777	0.858	0.858
4	0.552	0.584	0.584
5	0.811	0.875	0.874
6	0.684	0.747	0.748

CHAPTER 5

DATA COLLECTION FROM EDC PREDICTIONS

USF and UF researchers have analyzed static load tests and EDC-based predictions for 27 test piles tested during 2008-2017. The predictions of the EDC-FDOT method for these test piles are shown in Tables 5.1-5.4. Specific notes on the EDC-based method predictions at the various phases of pile installations follow. Tables 5.5 and 5.6 show the EDC-FDOT method predictions from McVay et. al. (2013) for piles #10 and #12

In the development of the EDC-FDOT method, skin friction was initially modeled using a linear soil-pile interaction. Some of the earlier test piles were modeled this way, and the soil in which they were embedded was treated as homogeneous in order to arrive at a quick solution. The justification for such treatment can be found in Tran et al. (2011). Following this, a model was developed where the skin friction on the pile was characterized using a multi-linear model on pile segments (Tran et al., 2012). This allowed for predicting the skin friction in layered soil deposits (i.e., non-homogeneous). The EDC-FDOT predictions in this current effort are based on the latter model.

Table 5.1: Results from EDC-based predictions – EOID

Pile No./Date	FDOT Method			UF Method		
	Tip (Kip)	Skin (Kip)	Total (Kip)	Tip (Kip)	Skin (Kip) †	Total (Kip)
1 7/20/2017	77	375	452	N/A	N/A	N/A
2 6/17/2017	123	60	183	N/A	N/A	N/A
3 6/22/2017	39	169	208	128	207	335
4 N/A	44	289	333	130	397	527
5 N/A	N/A	N/A	N/A	N/A	N/A	N/A
6 5/5/2017	203	525	728	350	1295	1645
7 N/A	196	420	616	310	1318	1628
8 10/4/2012	N/A	N/A	N/A	65	223	288
9 9/18/2012	N/A	N/A	N/A	39	620	659
10 1/25/2010	180	270	450	212	377	589

Table 5.1: Results from EDC-based predictions – EOID (contd.)

11 N/A	N/A	N/A	N/A	N/A	N/A	N/A
12 1/27/2010	76	N/A	N/A	40	229	269
13 2/24/2014	150	175	325	128	160	288
14 3/26/2014	N/A	N/A	N/A	68	N/A	N/A
15 3/26/2014	N/A	N/A	N/A	73	484	557
16 4/22/2014	118	543	661	194	577	771
17 5/15/2014	700	N/A	N/A	866	218	1084
18 4/9/2010	N/A	137	N/A	N/A	N/A	N/A

Table 5.1: Results from EDC-based predictions – EOID (contd.)

19 4/21/2010	N/A	97	N/A	574	40	617
20 N/A	N/A	N/A	N/A	N/A	N/A	N/A
21 5/6/2010	N/A	112	N/A	503	39	543
22 12/19/2008	280	200	480	308	155	463
23 8/1/2008	N/A	158	N/A	N/A	220	N/A
24 7/28/2008	N/A	194	N/A	N/A	200	N/A
25 8/21/2008	N/A	216	N/A	N/A	150	N/A
26 N/A	N/A	N/A	N/A	N/A	N/A	N/A
27 8/26/2008	N/A	N/A	N/A	N/A	215	N/A

† calculated (skin = total – tip).

N/A indicates that data are not available

Table 5.2: Results from EDC-based predictions – BOR1

Pile No./ Date	FDOT Method			UF Method		
	Tip (Kip)	Skin (Kip)	Total (Kip)	Tip (Kip)	Skin (Kip) †	Total (Kip)
1 7/31/2017	166	574	740	N/A	N/A	N/A
2 6/26/2017	52	372	424	N/A	N/A	N/A
3 7/5/2017	60	437	497	N/A	N/A	N/A
4 N/A	73	488	561	N/A	N/A	N/A
5 N/A	N/A	N/A	N/A	N/A	N/A	N/A
6 5/9/2017	287	906	1193	N/A	N/A	N/A
7 N/A	282	1369	1651	N/A	N/A	N/A
8 10/5/2012	53	505	558	91	341	432
9 9/19/2012	87	759	846	107	577	684
10 2/1/2010	186	382	568	137	466	603
11 N/A	N/A	N/A	N/A	N/A	N/A	N/A
12 1/27/2010* 1 hr restrike	N/A	N/A	N/A	61	310	371

Table 5.2: Results from EDC-based predictions – BOR1 (contd.)

13 2/27/2014	200	425	625	187	414	601
14 4/1/2014	200	1250	1450	265	N/A	N/A
15 4/1/2014	330	1080	1410	158	1308	1466
16 4/22/2014 * 1.5 hr restrike	280	1040	1320	251	1092	1343
17 5/15/2014	N/A	900	N/A	346	865	1211
18 4/12/2010	N/A	180	N/A	N/A	171	N/A
19 4/26/2010	225	166	391	392	78	448
20 N/A	N/A	N/A	N/A	N/A	N/A	N/A
21 5/10/2010	174	197	371	290	184	471
22 1/5/2009	N/A	N/A	N/A	202	550	752

37

Table 5.2: Results from EDC-based predictions – BOR1 (contd,)

23 N/A	N/A	N/A	N/A	N/A	N/A	N/A
24 N/A	N/A	N/A	N/A	N/A	N/A	N/A
25 N/A	N/A	N/A	N/A	N/A	N/A	N/A
26 N/A	N/A	N/A	N/A	N/A	N/A	N/A
27 N/A	N/A	N/A	N/A	N/A	N/A	N/A

† calculated (skin = total – tip).

N/A indicates that data are not available

Table 5.3: Results from EDC-based predictions – BOR2

Pile No./ Date	FDOT Method			UF Method		
	Tip (Kip)	Skin (Kip)	Total (Kip)	Tip (Kip)	Skin (Kip) †	Total (Kip)
1 8/8/2017	199	520	719	N/A	N/A	N/A
2 7/6/2017	74	400	474	N/A	N/A	N/A
3 7/11/2017	104	416	520	N/A	N/A	N/A
4N/A	94	469	563	N/A	N/A	N/A
5 N/A	N/A	N/A	N/A	N/A	N/A	N/A
6 N/A	370	1264	1634	N/A	N/A	N/A
7 N/A	N/A	N/A	1711	N/A	N/A	N/A
8 N/A	N/A	N/A	N/A	N/A	N/A	N/A
9 N/A	N/A	N/A	N/A	N/A	N/A	N/A
10 2/21/2010** post STL	N/A	N/A	N/A	94	480	574
11 N/A	N/A	N/A	N/A	N/A	N/A	N/A
12 2/24/2010	90	483	573	67	520	587

Table 5.3: Results from EDC-based predictions – BOR2 (contd.)

13 N/A	N/A	N/A	N/A	N/A	N/A	N/A
14 N/A	N/A	N/A	N/A	N/A	N/A	N/A
15 N/A	N/A	N/A	N/A	N/A	N/A	N/A
16 N/A	N/A	N/A	N/A	N/A	N/A	N/A
17 N/A	N/A	N/A	N/A	N/A	N/A	N/A
18 N/A	N/A	N/A	N/A	N/A	N/A	N/A
19 5/3/2010	N/A	N/A	N/A	425	67	487
20 N/A	N/A	N/A	N/A	N/A	N/A	N/A
21 5/14/2010	N/A	N/A	N/A	405	29	428
22 N/A	N/A	N/A	N/A	N/A	N/A	N/A
23 N/A	N/A	N/A	N/A	N/A	N/A	N/A

Table 5.3: Results from EDC-based predictions – BOR2 (contd.)

24 N/A	N/A	N/A	N/A	N/A	N/A	N/A
25 N/A	N/A	N/A	N/A	N/A	N/A	N/A
26 N/A	N/A	N/A	N/A	N/A	N/A	N/A
27 N/A	N/A	N/A	N/A	N/A	N/A	N/A

† calculated (skin = total – tip).

N/A indicates that data are not available

Table 5.4: Results from EDC-based predictions – BOR3

Pile No./ Date	FDOT Method			UF Method		
	Tip (Kip)	Skin (Kip)	Total (Kip)	Tip (Kip)	Skin (Kip) †	Total (Kip)
1 N/A	N/A	N/A	N/A	N/A	N/A	N/A
2 N/A	N/A	N/A	N/A	N/A	N/A	N/A
3 N/A	N/A	N/A	N/A	N/A	N/A	N/A
4 N/A	N/A	N/A	N/A	N/A	N/A	N/A
5 N/A	N/A	N/A	N/A	N/A	N/A	N/A
6 N/A	N/A	N/A	N/A	N/A	N/A	N/A
7 N/A	N/A	N/A	N/A	N/A	N/A	N/A
8 N/A	N/A	N/A	N/A	N/A	N/A	N/A
9 N/A	N/A	N/A	N/A	N/A	N/A	N/A
10 N/A	N/A	N/A	N/A	N/A	N/A	N/A
11 N/A	N/A	N/A	N/A	N/A	N/A	N/A

Table 5.4: Results from EDC-based predictions – BOR3 (contd.)

12 N/A	N/A	N/A	N/A	N/A	N/A	N/A
13 N/A	N/A	N/A	N/A	N/A	N/A	N/A
14 N/A	N/A	N/A	N/A	N/A	N/A	N/A
15 N/A	N/A	N/A	N/A	N/A	N/A	N/A
16 N/A	N/A	N/A	N/A	N/A	N/A	N/A
17 N/A	N/A	N/A	N/A	N/A	N/A	N/A
18 N/A	N/A	N/A	N/A	N/A	N/A	N/A
19 N/A	N/A	N/A	N/A	N/A	N/A	N/A
20 N/A	N/A	N/A	N/A	N/A	N/A	N/A
21 N/A	N/A	N/A	N/A	N/A	N/A	N/A
22 N/A	N/A	N/A	N/A	N/A	N/A	N/A

Table 5.4: Results from EDC-based predictions – BOR3 (contd.)

23 N/A	N/A	N/A	N/A	N/A	N/A	N/A
24 N/A	N/A	N/A	N/A	N/A	N/A	N/A
25 N/A	N/A	N/A	N/A	N/A	N/A	N/A
26 N/A	N/A	N/A	N/A	N/A	N/A	N/A
27 N/A	N/A	N/A	N/A	N/A	N/A	N/A

† calculated (skin = total – tip).

N/A indicates that data are not available

5.1 Notes on EDC predictions

Pile 3: UF method predictions were provided in emails from Radise International. The phase of installation that the predictions are from is indeterminable.

Pile 4: EDC EOID and BOR dates are indeterminable. UF method predictions were provided in emails from Radise International. The phase of installation that the predictions are from is indeterminable.

Pile 6: UF method predictions were provided in emails from Radise International. The phase of installation that the predictions are from is indeterminable.

Pile 7: EDC EOID and BOR dates are indeterminable. UF method predictions were provided in emails from Radise International. The phase of installation that the predictions are from is indeterminable.

Pile 10: UF method predictions reported in McVay et. al. (2013) and McVay and Wasman (2015) are from the BOR2 (Blow 659, 2/21/2010 after the SLT). UF and Fixed Jc EOID (Blow 631) and BOR1 (Blow 650) predictions are based on a selected blow within blows of consistent energy in pile.

Table 5.5: EDC-FDOT method predictions from McVay et. al. (2013) for pile #10

The blow numbers used were not reported.

Resistance	Skin (linear model) (kips)	Skin (nonlinear model) (kips)	Tip (kips)
EOID (1/25/2010)	270	NA	180†*
BOR1 (2/1/2010)	405†	382	186*

†value reported in McVay and Wasman (2015).

*average of 5 blows reported in McVay et. al. (2013).

Note: The FDOT prediction of the skin resistance for this test pile (pile 10) is based on the nonlinear soil model.

Pile 12: UF method predictions reported in McVay et. al. (2013) and McVay and Wasman (2015) are from the BOR2 (Blow 328, 2/24/2010). UF method EOID (Blow 306) and BOR1 (Blow 320) predictions reported by UF (Scott Wasman) are based on a selected blow within blows of consistent energy in pile.

Table 5.6: EDC-FDOT method predictions from McVay et. al. (2013) for pile #12

The blow numbers used were not reported.

Resistance	Skin (linear) (kips)	Skin (nonlinear) (kips)	Tip (kips)
EOID (1/27/2010)	360	NA	76*
BOR1 (1/27/2010)	NA	NA	NA
BOR2 (2/24/2010)	450†	483	90†*

†value reported in McVay and Wasman (2015).

*average of 5 blows at EOID and BOR2 reported in McVay et. al. (2013). McVay et. al. (2013) refers to BOR2 as BOR.

Note: The FDOT prediction of the skin resistance for this test pile (pile 12) is based on the nonlinear soil model.

Pile 13: UF method Predictions reported in McVay and Wasman (2015) are from the EIOD (Blow 670 on 2/24/2014) and BOR (Blow 688 on 2/27/2014).

Pile 14: This pile was a voided pile with EDCs installed 5 feet from the top of the pile in the solid section, on either side of the void and two locations near the tip of the pile, 5 feet and 2.5 feet from the tip. The pile was installed in the following sequence:

- Initially driven on 3/12/14
- restrike on 3/20/14
- restrike on 3/24/14 and EDC not recorded
- driven an additional 10 feet on 3/26/14
- restrike on 4/1/14
- The EOID was completed on 3/36/2014
- The BOR3 was taken on 4/1/2014
- The EDC monitoring consultant experienced issues reading the EDC for the solid section gauges on 3/20/2014 and data was not recorded.

EOID and BOR3 for tip resistance was the only prediction provided as the data came from the tip sensors in the tip/voided section EDC (the total resistance makes use of the accelerations from both EDC and since use of EDC around void is not standard practice, these were not considered). The UF tip resistance for EOID was from Blow 2212 of the predictions based on the tip/voided section EDC session report. The UF tip resistance for BOR3 was from Blow 976 of the predictions based on the tip/top EDC session report. The FDOT method tip and skin prediction values are from BOR3 Blow 976.

Pile 15: This pile was a voided pile with EDCs installed 5 feet from the top of the pile in the solid section, on either side of the void and two locations near the tip of the pile, 5 feet and 2.5 feet from the tip. The UF and Fixed Jc method predictions reported in McVay and Wasman (2015) are averages of blows 2134-2137 for EOID and blows 2139 – 2142 for BOR. These were averaged because the energy in the pile was not consistent. For the FDOT method blow 2141 was used for the tip resistance and blow 2142 for the skin resistance (both within the BOR). All predictions herein are from the tip/top EDC (use of EDC around void is not standard practice, these were not considered).

Pile 16: This pile was a voided pile with EDCs installed 5 feet from placed at the top of the pile in the solid section, on either side of the void and two locations near the tip of the pile, 5 feet and 2.5 feet from the tip. UF method prediction is the average of blows 1605-1608 in the EOID and blows 1610-1612 in the BOR. FDOT method predictions were available for both EOID and BOR. The EIOD predictions were based on blows 1595 (tip) and 1590 (skin). The BOR predictions were based on blow 1610.

Pile 17: This pile was a voided pile with EDCs installed 5 feet from placed at the top of the pile in the solid section, on either side of the void and two locations near the tip of the pile, 5 feet and 2.5 feet from the tip. The pile was installed in the following sequence:

- Initially driven to a tip elevation of -85.5 feet on 5/7/1 followed by restrikes 32 minutes later

- Driven to a tip elevation of -95.75 feet on 5/9/14 followed by restrikes 32 minutes later
- Driven to a tip elevation of -104.7 feet on 5/13/14 followed by restrikes 32 minutes later
- Driven to a tip elevation of -115.2 feet on 5/15/14 followed by restrikes 32 minutes later

The EOID and BOR were taken to be blows 1228 and 786, respectively, on 5/15/2014. Even though the pile was driven an additional 10 ft on 5/15/2014, the blow for BOR was selected because the pile had 2 days for setup and the BOR at the end of 5/15/2014 only had a 32 minute setup. For the BOR, UF and Fixed Jc method predictions averages of blows 786-788 recorded in the EDC sensors at the top of the pile (top/tip EDCs) were taken due to inconsistent energy in the pile. For the EOID UF and Fixed Jc method predictions averages of the final 8 blows (1148-1155) recorded in the EDC sensors at the tip of the pile (top/tip EDCs) were taken.

Pile 19: The FDOT method predictions for skin resistance in McVay et al. (2013) and McVay et al. (2015) are based on the linear soil model. The prediction at BOR is based on the nonlinear soil model and is 166 kips (McVay et. al., 2013). The UF and Fixed Jc method predictions are from Ref. C and Ref. D as the values reported in McVay and Wasman (2015) could not be reproduced because the Session Reports are not accessible.

Note: The FDOT prediction of the skin resistance for this test pile (pile 19) is based on the nonlinear soil model.

Pile 21: The FDOT method predictions for skin resistance in McVay et al. (2013) and McVay et al. (2015) are based on the linear soil model. The prediction at BOR is based on the nonlinear soil model and is 197 kips (McVay et. al., 2013). The UF and Fixed Jc method predictions are from Ref. E and Ref. F as the values reported in McVay and Wasman (2015) could not be reproduced.

Note: The FDOT prediction of the skin resistance for this test pile (pile 21) is based on the nonlinear soil model.

Pile 22: The FDOT method predictions are from McVay and Wasman (2015). The UF and Fixed Jc method predictions are averaged EOID and BOR blows with consistent energy in the pile. For EOID blows 1701-1704 and for BOR blows 1715-1721.

Pile 26: Session report not available.
Tables 4.7 and 4.8 were developed to demonstrate the EDC-FDOT method's predictions from the closest restrike prior to the corresponding static load tests (SLT), in terms of time and at EOID respectively.

Table 5.7: EDC-FDOT method at the closest re-strike prior to SLT:

Pile capacities evaluated at the closest re-strike to SLT under EDC-FDOT method				
Pile no.	Tip (kip)	Skin (kip)	Total Capacity (kip)	Date
1	166	574	740	7/31/2017
2	52	372	424	6/26/2017
3	60	437	497	6/30/2017
4	73	488	561	7/21/2017
5	-	-	-	-
6	287	906	1193	5/9/2017
7	282	1369	1651	6/12/2017
8	53	505	558	10/5/2012
9	87	759	846	9/19/2012
10	186	382	568	2/1/2010
11	-	-	-	-
12	90	483	573	2/24/2010
13	200	425	625	2/27/2014
14	200	1250	1450	4/1/2014
15	330	1080	1410	4/1/2014
16	280	1040	1320	4/22/2014
17	-	900	-	5/15/2014
18	-	180	-	4/12/2010
19	225	166	391	4/26/2010
20	-	-	-	-
21	174	197	371	5/10/2010
22	280	200	480	12/19/2008
23	-	158	-	8/1/2008
24	-	194	-	7/28/2008
25	-	216	-	8/21/2008
26	-	-	-	-
27	-	-	-	-

'-' mark indicates that an EDC-FDOT prediction was not made.

Table 5.8: EDC-FDOT method at EOID

EDC-FDOT EOID method	
Pile #	Total capacity (kip)
1	452
2	183
3	208
4	333
5	-
6	728
7	616
8	-
9	-
10	450
11	-
12	436
13	325
14	-
15	-
16	661
17	-
18	-
19	-
20	-
21	-
22	480
23	-
24	-
25	-
26	-
27	-

'-' mark indicates that an EDC-FDOT prediction was not made

CHAPTER 6

STATISTICAL ANALYSIS AND CALCULATION OF RESISTANCE FACTORS – EDC

6.1 EDC-FDOT resistance bias

In the next phase, the bias factors were calculated for the following EDC-based resistance predictions:

1. EDC-FDOT method total capacity with the restrike closest and prior to SLT
2. EDC-FDOT method tip capacity with the restrike closest and prior to SLT
3. EDC-FDOT method skin friction capacity with the restrike most prior to SLT
4. EDC-FDOT method skin friction capacity (compression and tension test piles) with the restrike most prior to SLT
5. EDC-FDOT method total capacity at EOID

The bias factors were calculated according to Eqn. 4.1 and are listed in Tables 6.1 and 6.2. Because EDC UF method resistances were not reported for the latest series of load tests (Piles 1-7), the EDC UF method is not evaluated in this report.

Table 6.1: Bias factors for EDC-FDOT predictions closest re-strike prior to SLT

Pile #	Total capacity (kip)	Tip capacity (kip)	Skin friction capacity (kip)	λ total	λ tip	λ skin
	EDC-FDOT method					
1	740	166	574	1.0973	0.957831	1.137631
2	424	52	372	0.6486	1.076923	0.58871
3	497	60	437	1.4990	2	1.430206
4	561	73	488	1.2068	1.643836	1.141393
5	-	-	-	N/A	N/A	N/A
6	1193	287	906	N/A	N/A	N/A
7	1651	282	1369	N/A	N/A	N/A
8	558	53	505	0.8244	1.339623	0.770297
9	846	87	759	1.0118	1.758621	0.926219
10	568	186	382	0.9771	1.043011	0.945026
11	-	-	-	N/A	N/A	N/A
12	573	90	483	1.0785	1.277778	1.041408
13	625	200	425	N/A	N/A	N/A
14	1450	200	1250	1.0345	N/A	N/A
15	1410	330	1080	N/A	N/A	N/A
16	1320	280	1040	0.7803	N/A	N/A
17	-	-	900	N/A	N/A	N/A
18	-	-	180	-	-	1.177778
19	391	225	166	1.0946	1.004444	1.216867
20	-	-	-	N/A	N/A	N/A
21	371	174	197	1.0108	1.057471	0.969543
22	480	280	200	0.8125	0.796429	0.835
23	-	-	158	-	-	N/A
24	-	-	194	-	-	0.927835
25	-	-	216	-	-	0.314815
26	-	-	-	-	-	N/A
27	-	-	-	-	-	N/A

- The CAPWAP estimate of capacity based on the load at a certain displacement for pile 17 was included in the dataset of bias in Chapter 4. This could be done for the EDC FDOT method using the new software from SmartStructures (Radise), however a limitation with the new software is that old files cannot be run.
- Measured capacities evaluated by USF have been used for pile12.
- Piles 18, 23, 24, 25, 26 and 27 were tension test piles and the '-' mark indicates tip and total were not tested.
- N/A indicates that either there isn't a EDC-FDOT prediction or the capacity from SLT was not measured. N/A indicates that either there isn't a EDC-FDOT prediction or the capacity from SLT was not measured

Table 6.2: Bias factors for EDC-FDOT EOID predictions

EDC-FDOT EOID method		
Pile #	Total capacity (kip)	λ *total*
1	452	1.79646
2	183	1.502732
3	208	3.581731
4	333	2.033033
5	-	N/A
6	728	N/A
7	616	N/A
8	-	N/A
9	-	N/A
10	450	1.233333
11	-	N/A
12	436	1.4908
13	325	
14	-	N/A
15	-	N/A
16	661	1.565809
17	-	N/A
18	-	N/A
19	-	N/A
20	-	N/A
21	-	N/A
22	480	0.797917
23	-	N/A
24	-	N/A
25	-	N/A
26	-	N/A
27	-	N/A

Table 6.3: Summary of bias factor statistics for the EDC-FDOT method, including pile #2

Case	Description	Size of dataset	Mean of Bias	COV of Bias
1	EDC-FDOT-Closest re-strike prior to SLT, total capacity	13	1.006	0.214
2	EDC-FDOT -Closest re-strike prior to SLT, tip capacity	11	1.269	0.299
3	EDC-FDOT -Closest re-strike prior to SLT, skin friction capacity	11	1.00	0.230
4	EDC-FDOT -Closest re-strike prior to SLT, skin friction capacity (compression and tension)	14	0.958	0.291
5	EDC-FDOT – EOID total capacity	8	1.75	0.471

Table 6.4: Summary of bias factor statistics for the EDC-FDOT method, excluding pile #2

Case	Description	Size of dataset	Mean of Bias	COV of Bias
1	EDC-FDOT-Closest re-strike prior to SLT, total capacity	12	1.036	0.188
2	EDC-FDOT -Closest re-strike prior to SLT, tip capacity	10	1.288	0.307
3	EDC-FDOT -Closest re-strike prior to SLT, skin friction capacity	10	1.041	0.188
4	EDC-FDOT -Closest re-strike prior to SLT, skin friction capacity (compression and tension)	13	0.987	0.272
5	EDC-FDOT – EOID total capacity	7	1.785	0.495

6.2 Fitting of resistance data against the assumed lognormal distributions

Since the range of predicted resistances represents the lognormal distribution more closely, predicted resistances in Table 6.1 were plotted against the corresponding theoretical lognormal distributions as shown in Figure 6.1. In the case such as the EDC-FDOT method (Figure 6.1), the data seem to be reasonably well represented by a lognormal distribution.
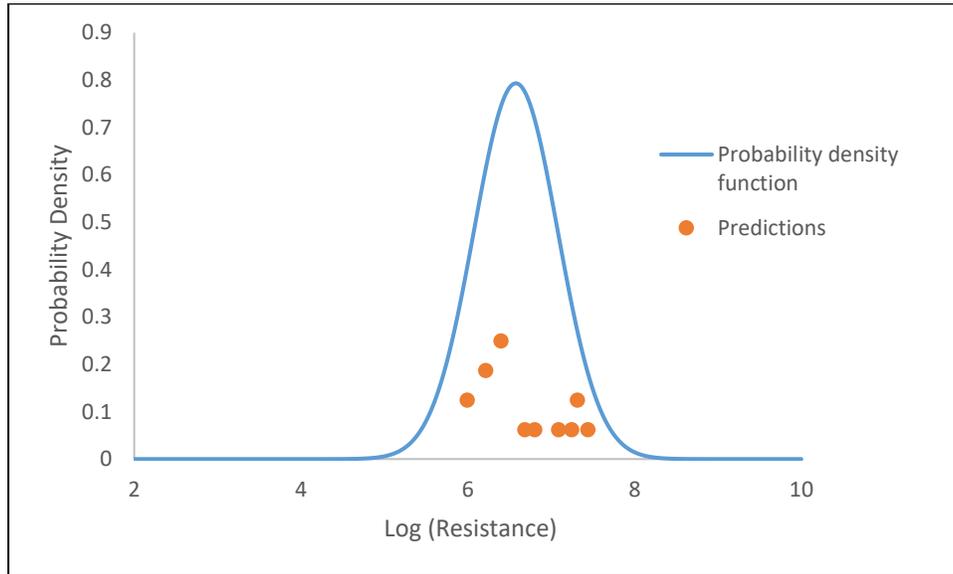
Figure 6.1: Probability density plot and probability density model fit to EDC-FDOT method total capacity with re-strike closest and prior to SLT

6.3 Results of the First-order second moment method

In the subsequent phase of the investigation, statistics of the bias factor were evaluated for EDC data obtained from the above methods. First, the FOSM (First-order Second Moment) method was used to compute the resistance factors for the EDC methods, as in the case of CAPWAP results. In the FOSM method for log-normally distributed load and resistance, the resistance factor (ϕ_R) can be calculated using Eqn. (4.4).

The calculated resistance factors for the EDC-FDOT predictions at the restrike closest and prior to the SLT for a range of target reliabilities (including pile #2 and excluding pile #2) are seen in Tables E.1 and E.3 in the Appendix E. They were also evaluated for the total pile capacity obtained from the EDC-FDOT method at EOID (Tables E.2 and E.4).

Finally, the resistance factors developed with the FOSM method were validated using (1) Monte-Carlo simulation of the load and resistance probability distributions corresponding to the respective statistics and (2) the AFOSM method.

Table 6.5: Summary of bias factor statistics and resistance factors with the FOSM method for a reliability index of 2.33, including pile #2

Case	Description	Size of dataset	Mean of Bias	COV of Bias	Resistance factor with FOSM method
1	EDC-FDOT-Closest re-strike prior to SLT, total capacity	13	1.006	0.214	0.648
2	EDC-FDOT -Closest re-strike prior to SLT, tip capacity	11	1.269	0.2993	0.691
3	EDC-FDOT -Closest re-strike prior to SLT, skin friction capacity	11	1.00	0.230	0.625
4	EDC-FDOT -Closest re-strike prior to SLT, skin friction capacity (compression and tension)	14	0.958	0.291	0.530
5	EDC-FDOT – EOID total capacity	8	1.75	0.471	0.657

Table 6.6: Summary of bias factor statistics and resistance factors with the FOSM method for a reliability index of 2.33, excluding pile #2

Case	Description	Size of dataset	Mean of Bias	COV of Bias	Resistance factor with FOSM method
1	EDC-FDOT-Closest re-strike prior to SLT, total capacity	12	1.036	0.188	0.698
2	EDC-FDOT -Closest re-strike prior to SLT, tip capacity	10	1.288	0.307	0.691
3	EDC-FDOT -Closest re-strike prior to SLT, skin friction capacity	10	1.041	0.188	0.702
4	EDC-FDOT -Closest re-strike prior to SLT, skin friction capacity (compression and tension)	13	0.987	0.272	0.568
5	EDC-FDOT – EOID total capacity	7	1.785	0.495	0.635

Table 6.7: Summary of bias factor statistics and resistance factors with the FOSM method for a reliability index of 2.1, including pile #2

Case	Description	Size of dataset	Mean of Bias	COV of Bias	Resistance factor with FOSM method
1	EDC-FDOT-Closest re-strike prior to SLT, total capacity	13	1.006	0.214	0.693
2	EDC-FDOT -Closest re-strike prior to SLT, tip capacity	11	1.269	0.2993	0.750
3	EDC-FDOT -Closest re-strike prior to SLT, skin friction capacity	11	1.00	0.230	0.670
4	EDC-FDOT -Closest re-strike prior to SLT, skin friction capacity (compression and tension)	14	0.958	0.291	0.575
5	EDC-FDOT – EOID total capacity	8	1.75	0.471	0.736

Table 6.8: Summary of bias factor statistics and resistance factors with the FOSM method for a reliability index of 2.1, excluding pile #2

Case	Description	Size of dataset	Mean of Bias	COV of Bias	Resistance factor with FOSM method
1	EDC-FDOT-Closest re-strike prior to SLT, total capacity	12	1.036	0.188	0.744
2	EDC-FDOT -Closest re-strike prior to SLT, tip capacity	10	1.288	0.307	0.750
3	EDC-FDOT -Closest re-strike prior to SLT, skin friction capacity	10	1.041	0.188	0.748
4	EDC-FDOT -Closest re-strike prior to SLT, skin friction capacity (compression and tension)	13	0.987	0.272	0.614
5	EDC-FDOT – EOID total capacity	7	1.785	0.495	0.715

6.4 Results of the Monte Carlo simulation

Monte-Carlo simulations were also run for a target reliably of 2.33 to validate the resistance factors developed using the FOSM methods for cases 1-5. The corresponding resistance statistics are shown in Tables 6.3 and 6.4 and the load statistics defined with respect to Eqn. (4.4) are reproduced in Table 6.9. The resistance factors determined based on convergence on the target reliability (2.33 and 2.1) are listed in Tables 6.10-6.13 (with and without Pile #2 in the data set). Monte-Carlo simulation process is described in detail in the Appendix D

Table 6.9: General values of the variables involved in the analysis

Coefficient	Value
Dead Load/Live Load (Q_D/Q_L)	3
Assumed Live Load (kip)	100[*]
Assumed Dead Load (kip)	300[*]
Dead Load Factor (γ_D)	1.25
Live Load Factor (γ_L)	1.75
Factored load	425
Coefficient of Variation of Dead Load (COV_{QD})	0.1
Coefficient of Variation of Live Load (COV_{QL})	0.18
Bias Factor of Dead Load (λ_{QD})	1.05
Target reliability	2.33
Bias Factor of Live Load (λ_{QL})	1.15

Table 6.10: Bias of resistance, COV of resistance and resistance factors from the MC method for a reliability index of 2.33, including pile #2

Case	Description	Size of dataset	Mean of Bias	COV of Bias	Resistance factor with MC method
1	EDC-FDOT-Closest re-strike prior to SLT, total capacity	13	1.006	0.214	0.741
2	EDC-FDOT -Closest re-strike prior to SLT, tip capacity	11	1.269	0.299	0.765
3	EDC-FDOT -Closest re-strike prior to SLT, skin friction capacity	11	1.00	0.230	0.709
4	EDC-FDOT -Closest re-strike prior to SLT, skin friction capacity (compression and tension)	14	0.958	0.291	0.59
5	EDC-FDOT – EOID total capacity	8	1.75	0.471	0.70

Table 6.11: Bias of resistance, COV of resistance and resistance factors from the MC method for a reliability index of 2.33, excluding pile #2

Case	Description	Size of dataset	Mean of Bias	COV of Bias	Resistance factor with MC method
1	EDC-FDOT-Closest re-strike prior to SLT, total capacity	12	1.036	0.188	0.809
2	EDC-FDOT -Closest re-strike prior to SLT, tip capacity	10	1.288	0.307	0.763
3	EDC-FDOT -Closest re-strike prior to SLT, skin friction capacity	10	1.041	0.188	0.814
4	EDC-FDOT -Closest re-strike prior to SLT, skin friction capacity (compression and tension)	13	0.987	0.272	0.634
5	EDC-FDOT – EOID total capacity	7	1.785	0.495	0.676

Table 6.12: Bias of resistance, COV of resistance and resistance factors from the MC method for a reliability index of 2.1, including pile #2

Case	Description	Size of dataset	Mean of Bias	COV of Bias	Resistance factor with MC method
1	EDC-FDOT-Closest re-strike prior to SLT, total capacity	13	1.006	0.214	0.781
2	EDC-FDOT -Closest re-strike prior to SLT, tip capacity	11	1.269	0.299	0.82
3	EDC-FDOT -Closest re-strike prior to SLT, skin friction capacity	11	1.00	0.230	0.75
4	EDC-FDOT -Closest re-strike prior to SLT, skin friction capacity (compression and tension)	14	0.958	0.291	0.631
5	EDC-FDOT – EOID total capacity	8	1.75	0.471	0.779

Table 6.13: Bias of resistance, COV of resistance and resistance factors from the MC method for a reliability index of 2.1, excluding pile #2

Case	Description	Size of dataset	Mean of Bias	COV of Bias	Resistance factor with MC method
1	EDC-FDOT-Closest re-strike prior to SLT, total capacity	12	1.036	0.188	0.848
2	EDC-FDOT -Closest re-strike prior to SLT, tip capacity	10	1.288	0.307	0.821
3	EDC-FDOT -Closest re-strike prior to SLT, skin friction capacity	10	1.041	0.188	0.852
4	EDC-FDOT -Closest re-strike prior to SLT, skin friction capacity (compression and tension)	13	0.987	0.272	0.677
5	EDC-FDOT – EOID total capacity	7	1.785	0.495	0.753

6.5 Reliability analysis using the AFOSM method

Based on the theoretical concepts related to the AFOSM method illustrated in the Appendix C, a performance function (G), which defines the failure region on the resistance (*R*) versus load (*Q*) space, was employed to determine the resistance factors for the target reliability for cases 1-5. The corresponding resistance statistics are shown in Tables 6.3 and 6.4 while the load statistics defined with respect to Eqn. (4.4) are reproduced in Table 6.9.

Table 6.14: Bias of resistance, COV of resistance and resistance factors from AFOSM for a reliability index of 2.33, including pile #2

Case	Description	Size of dataset	Mean of Bias	COV of Bias	Resistance factor with AFOSM method
1	EDC-FDOT-Closest re-strike prior to SLT, total capacity	13	1.006	0.214	0.741
2	EDC-FDOT - Closest re-strike prior to SLT, tip capacity	11	1.269	0.299	0.765
3	EDC-FDOT - Closest re-strike prior to SLT, skin friction capacity	11	1.00	0.230	0.71
4	EDC-FDOT - Closest re-strike prior to SLT, skin friction capacity (compression and tension)	14	0.958	0.291	0.59
5	EDC-FDOT – EOID total capacity	8	1.75	0.471	0.701

Table 6.15: Bias of resistance, COV of resistance and resistance factors from AFOSM for a reliability index of 2.33, excluding pile #2

Case	Description	Size of dataset	Mean of Bias	COV of Bias	Resistance factor with AFOSM method
1	EDC-FDOT-Closest re-strike prior to SLT, total capacity	12	1.036	0.188	0.809
2	EDC-FDOT - Closest re-strike prior to SLT, tip capacity	10	1.288	0.307	0.765
3	EDC-FDOT - Closest re-strike prior to SLT, skin friction capacity	10	1.041	0.188	0.813
4	EDC-FDOT - Closest re-strike prior to SLT, skin friction capacity (compression and tension)	13	0.987	0.272	0.635
5	EDC-FDOT – EOID total capacity	7	1.785	0.495	0.677

Table 6.16: Bias of resistance, COV of resistance and resistance factors from AFOSM for a reliability index of 2.1, including pile #2

Case	Description	Size of dataset	Mean of Bias	COV of Bias	Resistance factor with AFOSM method
1	EDC-FDOT-Closest re-strike prior to SLT, total capacity	13	1.006	0.214	0.78
2	EDC-FDOT - Closest re-strike prior to SLT, tip capacity	11	1.269	0.299	0.822
3	EDC-FDOT - Closest re-strike prior to SLT, skin friction capacity	11	1.00	0.230	0.75
4	EDC-FDOT - Closest re-strike prior to SLT, skin friction capacity (compression and tension)	14	0.958	0.291	0.631
5	EDC-FDOT – EOID total capacity	8	1.75	0.471	0.78

Table 6.17: Bias of resistance, COV of resistance and resistance factors from AFOSM for a reliability index of 2.1, excluding pile #2

Case	Description	Size of dataset	Mean of Bias	COV of Bias	Resistance factor with AFOSM method
1	EDC-FDOT-Closest re-strike prior to SLT, total capacity	12	1.036	0.188	0.848
2	EDC-FDOT - Closest re-strike prior to SLT, tip capacity	10	1.288	0.307	0.819
3	EDC-FDOT - Closest re-strike prior to SLT, skin friction capacity	10	1.041	0.188	0.852
4	EDC-FDOT - Closest re-strike prior to SLT, skin friction capacity (compression and tension)	13	0.987	0.272	0.677
5	EDC-FDOT – EOID total capacity	7	1.785	0.495	0.755

6.6 Summary of calculated resistance factors for different cases of the EDC-FDOT data

A comparison of the calculated resistance factors using the methods presented are shown in Tables 6.18-6.21. The comparisons show agreement between the MC and AFOSM methods and those factors are generally greater than those from the FOSM method. This has also been shown by Paikowsky (2004) and Kwak et al (2010).

Table 6.18: Comparison of resistance factors from FOSM, MC, and AFOSM methods for a reliability index of 2.33 with the data sets of the bias resistance, including Pile #2

Case	Resistance factor with FOSM method	Resistance factor with MC method	Resistance factor with AFOSM method
1	0.648	0.741	0.741
2	0.691	0.765	0.765
3	0.625	0.709	0.71
4	0.530	0.59	0.59
5	0.657	0.70	0.701

Table 6.19: Comparison of resistance factors from FOSM, MC, and AFOSM methods for a reliability index of 2.33 with the data sets of the bias resistance, excluding pile #2

Case	Resistance factor with FOSM method	Resistance factor with MC method	Resistance factor with AFOSM method
1	0.698	0.809	0.809
2	0.691	0.763	0.765
3	0.702	0.814	0.813
4	0.568	0.634	0.635
5	0.635	0.676	0.677

Table 6.20: Comparison of resistance factors from FOSM, MC, and AFOSM methods for a reliability index of 2.1 with the data sets of the bias resistance, including pile #2

Case	Resistance factor with FOSM method	Resistance factor with MC method	Resistance factor with AFOSM method
1	0.693	0.781	0.78
2	0.750	0.82	0.822
3	0.670	0.75	0.75
4	0.575	0.631	0.631
5	0.736	0.779	0.78

Table 6.21: Comparison of resistance factors from FOSM, MC, and AFOSM methods for a reliability index of 2.1 with the data sets of the bias resistance, excluding pile #2

Case	Resistance factor with FOSM method	Resistance factor with MC method	Resistance factor with AFOSM method
1	0.744	0.848	0.848
2	0.750	0.821	0.819
3	0.748	0.852	0.852
4	0.614	0.677	0.677
5	0.715	0.753	0.755

CHAPTER 7

CONCLUSIONS AND RECOMMENDATIONS

The results of this study showed that the resistance factors computed by FOSM, Monte-Carlo and AFOSM methods for the EDC-FDOT predictions are slightly higher than those for the CAPWAP predictions. In order to investigate the adequacy of the sample sizes that were available for the these computations, the following additional analysis was performed to review the ninety-five percent confidence interval.

7.1 Determination of the confidence interval of prediction of the bias factors

The following expression (Devore, 2008) can be used to determine the confidence interval of either predictive method based on the mean of the resistance bias factors assuming the bias factors are normally distributed with a sample mean of λ_s and a standard deviation of σ_s.

$$\lambda = \bar{\lambda}_s + \frac{z\sigma_s}{\sqrt{n}} \tag{7.1}$$

where λ is the true or the population mean and **z** is the standard normal variable corresponding to a desired confidence interval, which is the absolute difference (margin of error) that one needs to assure between the sample mean of the bias and the true bias, for a given sample size of **n.**
If the variable (i.e., bias) is log-normally distributed as assumed in this work, one can use Eqn. 4.3 to estimate the sample standard deviation to be used in Eqn. (7.1). Once the z value is computed based on the margin of error in the natural logarithmic value of bias (λ), the standard deviation and the number of tests used, one can determine the confidence interval from a standard normal distribution table.

Table 7.1 indicates the confidence levels involved in predicting the resistance factors at a reasonable accuracy with respect to the two methods (CAPWAP and EDC-FDOT). The case considered for both prediction methods was the total resistance (tip + skin friction) at the closest restrike prior to the static load test. The selected margin of error in the mean bias factor was **0.1**, which corresponds to an accuracy of plus or minus 0.1 of the bias factor. Based on the sensitivity discussion in Appendix G, it can be shown that the margin of error of 0.1 in bias corresponds to a resistance factor margin of error of approximately **0.068** for the two considered prediction scenarios. In other words, the max difference in resistance factors for all cases in Table 6.1 is 0.068.

Table 7.1 shows a significant disparity between the sizes of the data sets used for the two methods. This is because, as stated in the introductory section of Chapter 3, CAPWAP data from piles tested during 2008-2017 were supplemented with those from McVay et al. (2000). It must also be noted that, since these data were obtained, the computational schemes relevant to both CAPWAP and EDC predictions have evolved in reliability and accuracy due to continuous modifications that have resulted from field verification.

Table 7.1: Confidence levels for a margin of error of 0.068 in the resistance factor with the available sample sizes

Prediction method	Mean bias factor	Coeff. of variation of bias	Standard deviation of logarithm of bias (Eqn. 4.3)	Sample size available	Confidence level (%) (Eqn. 7.1)
CAPWAP total resistance closest to and prior to restrike (Case 6- including pile #2)	1.246	0.342	0.333	91	98
CAPWAP total resistance closest to and prior to restrike (Case 6- excluding pile #2)	1.254	0.337	0.358	90	97
EDC-FDOT method total resistance closest to and prior to restrike (Case 1-including pile #2)	1.006	0.214	0.211	13	83
EDC-FDOT method total resistance closest to and prior to restrike (Case 1 - excluding pile #2)	1.036	0.188	0.178	12	90

Finally, the following conclusions can be reached from this study:

- The results in Table 7.1 demonstrate that all of the resistance factors derived from the available data sets (Cases 6 and 1 respectively for PDA and EDC) corresponding to each prediction method would have an approximate margin of error of 0.068 at confidence levels of 83% to 98%.

- The results in Table 7.1 are based on the assumption that the data set is representative of the populations of bias for each method. PDA is ubiquitous throughout North America while EDC has seen limited use (e.g., Louisiana, Florida, North Carolina). The data sets for each method are predominantly from test piles in Florida (8-Florida, 1-Mississippi and 4-Louisiana). Therefore, the results herein apply specifically to piles driven in Florida.

- The data set of CAPWAP total resistance in Table 7.1 is based on a database of square concrete and steel pipe piles tested throughout Florida.

- The data set of bias-CAPWAP includes multiple CAPWAP predictions for the same test pile as indicated in Perez (1998) on pg. 27 "The difference between the number of piles and cases is due to the multiple attempts to determine the same pile's capacity" in an effort to assess appropriate resistance factors for different dynamic methods of estimating driven pile capacity in Florida.

- The data set of EDC-FDOT total resistance in Table 6.1 is based on 8 square concrete piles tested 8 sites in Florida.

- The data set of bias EDC-FDOT includes an average of multiple predictions on the skin and tip estimates for 1 test pile.

The advantage of the population of resistance bias being larger (due to more piles of different types and multiple estimates of the same pile) benefits the measure of accuracy of the method as demonstrated in a comparison of the CV of the first CAPWAP data set in Table 7.1 and the CAPWAP data set in Figure 7.1. Some points of the data set in Figure 7.1 are:

- The pre 2000 data set in Figure 7.1 is from CAPWAP BOR for piles with measured capacities from static load tests or Osterberg tests as presented in Perez (1998). The data set consists of 23 piles, 22 piles installed in Florida (17 static and 5 Osterberg load tests), 1 pile in Mississippi (Osterberg test), and all solid concrete. The 5 Osterberg load tests conducted in Florida experienced skin failure.

- The measured and predicted data for the pre 2000 data (Perez, 1998), which excludes the 5 Osterberg load tests in Florida, and the 2008-2017 data is shown in Figure 7.1.

- Since the data set of the EDC-FDOT method is small (n = 13), the assumption that it is representative of the population is not reasonable (91.6 level of significance) and more load tests of driven piles (solid and voided concrete, steel pipe piles, H-piles) with EDC are recommended.
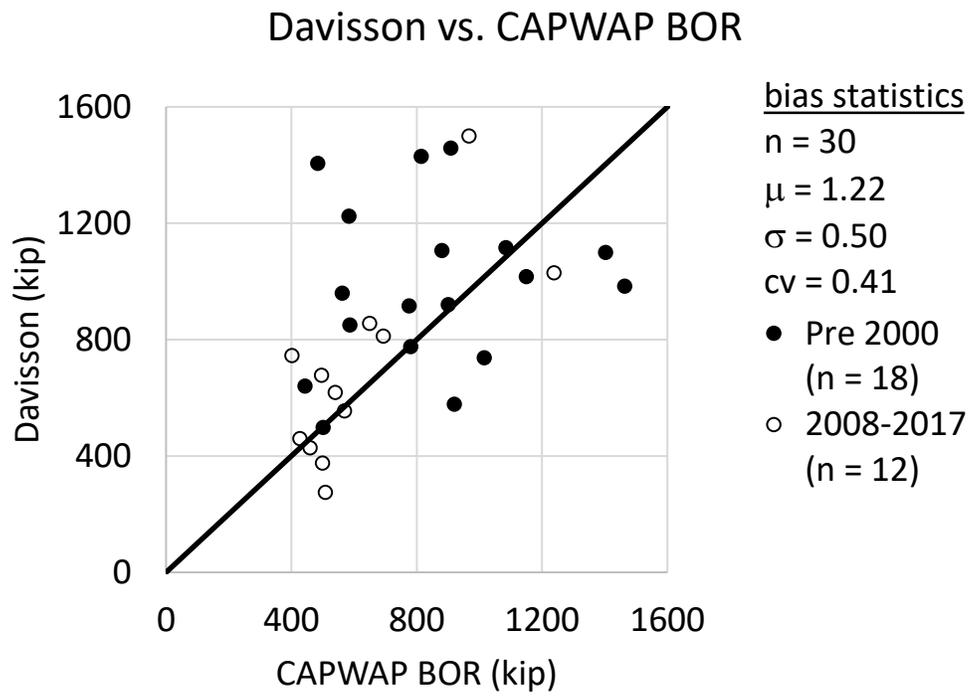
Figure 7.1: Davisson and CAPWAP BOR for 30 test piles in Florida, Mississippi, and Louisiana

REFERENCES

Bastidas, E. and Soubra A,H. (2014), *Reliability Analysis Methods*, Hicks, M.J. and Jommi, C., ALERT Doctoral School, *Stochastic Analysis and Inverse Modeling*, 978-2-95425517-5-2. http://alertgeomaterials.edu.<in2p3-01084369v2> , pp. 53-77.

Devore, J.L., "*Probability and Statistics for Engineering and Science*", Cengage Learning, 7th Edition, 2008.

Haque, M., Murad Abu-Farsakh, Qiming Chen, and Zhongjie Zhang (2014). "*Case Study on Instrumenting and Testing Full-Scale Test Piles for Evaluating Setup Phenomenon:,* Transportation Research Record 2462, Journal of the Transportation Research Board, http://trrjournalonline.trb.org/doi/10.3141/2462-05.

Kwak K, Kim, K.J. Huh, J., lee, J.H., and Park, J.H. (2010). , "Reliability-based calibration of resistance factors for static bearing capacity of driven steel pipe piles, Canadian Geotechnical Journal, 47, 528-538.

McVay, M. C., Birgisson, B., Zhang, L., Perez, A., and Putcha, S. (2000), "Load and Resistance Factor Design (LRFD) for Driven Piles Using Dynamic Methods—A Florida Perspective," *Geotechnical Testing Journal,* GTJODJ, Vol. 23, No. 1, March 2000, pp. 055–066.

McVay, M.C., D. Bloomquist, and K.T. Tran. (2013). "Embedded Data Collector (EDC) Evaluation Phase II – Comparison with Instrumented Static Load Tests", Final Report,)", Final Report, Florida Department of Transportation, Tallahassee, Florida,

McVay, M. and Wasman, S. (2015) "Embedded Data Collector (EDC) Phase II Load and Resistance Factor Design (LRFD)", Final Report, Florida Department of Transportation, Tallahassee, Florida,

Paikowsky, S. G., (2004). Load and Resistance Factor Design (LRFD) for Deep Foundations. *NCHRP Report (507)*, Transportation Research Board, Washington D.C.

Perez, A. P. (1998) "Load Resistance Factor Design (LRFD) for Driven Piles based on Dynamic Methods with Assessment of Skin and Tip resistance from PDA Signals". University of Florida Master thesis,198 pp.

Tran K. T, McVay M., Herrera R., and Lai P. (2011), "A New Method for Estimating Driven Pile Static Skin Friction with Instrumentation at the Top and Bottom of the Pile" Soil Dynamics and Earthquake Engineering, 2011; 31: 1285-1205.

Tran K. T, McVay M., Herrera R., and Lai P. (2012), Estimation of Nonlinear Static Skin Friction on Multiple Pile Segments Using Measured Hammer Impact Response at the Top and Bottom of Pile, Computers and Geotechnics, 2012, 41: 79-89.
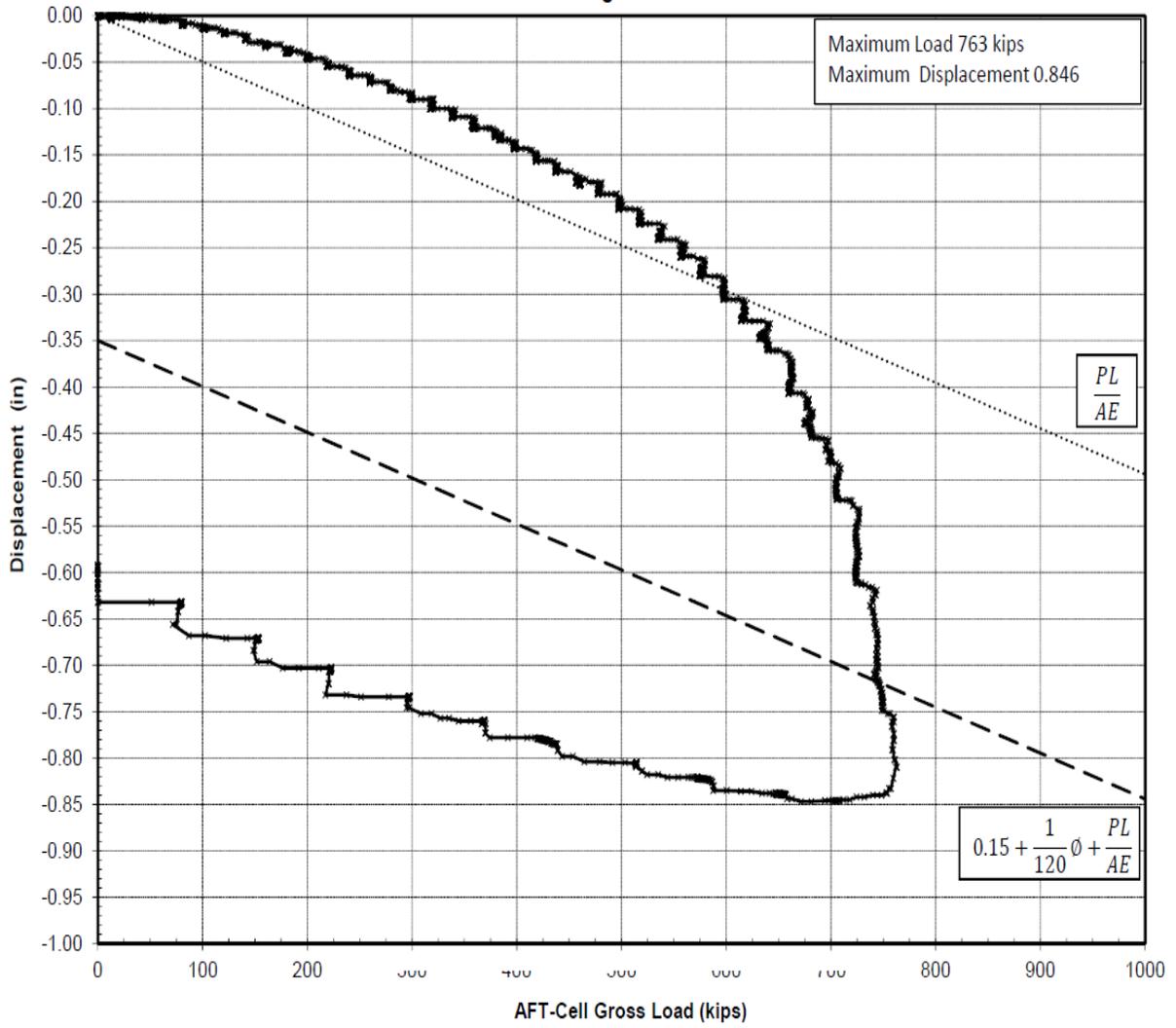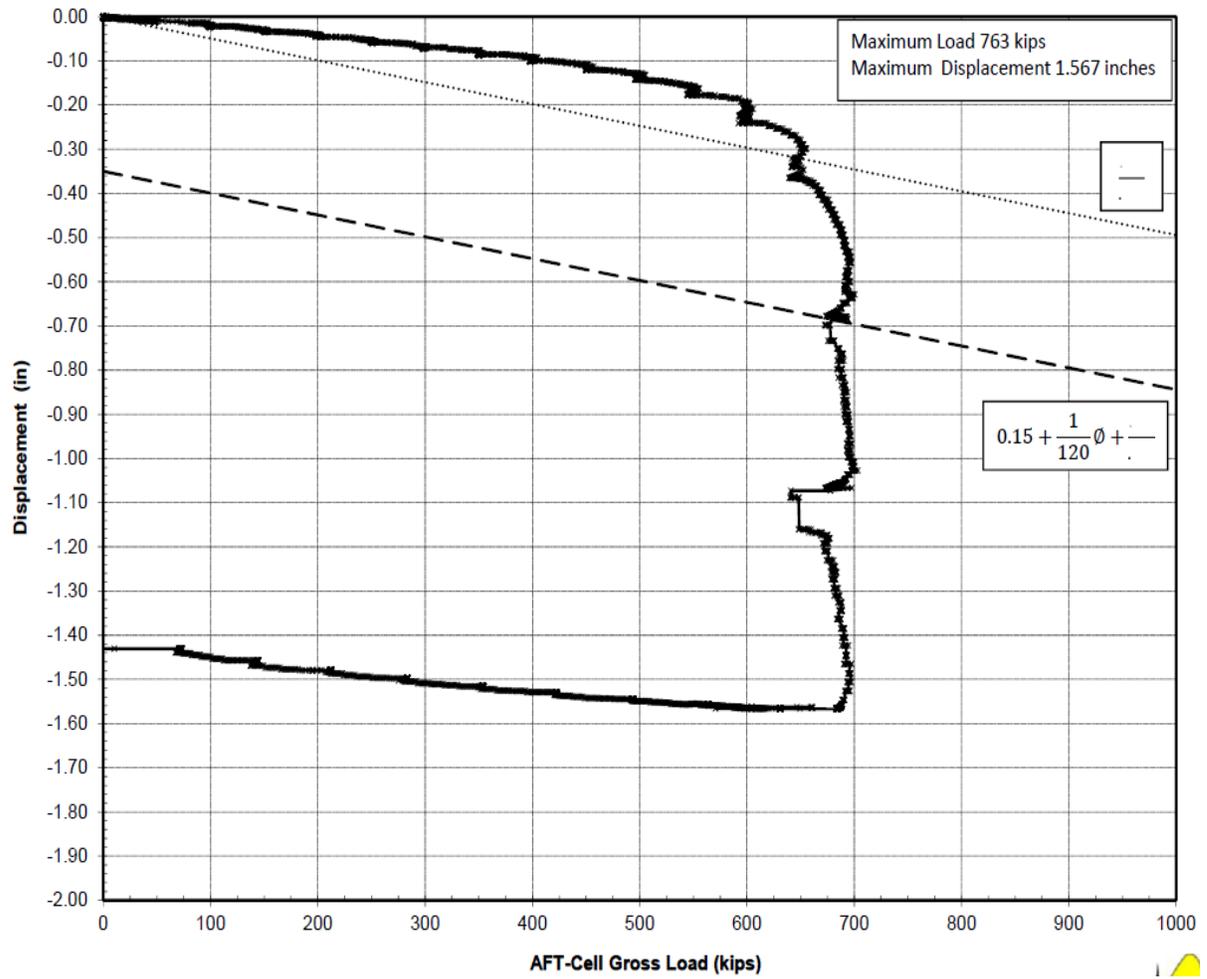
RESULTS OF STATIC LOAD TESTS
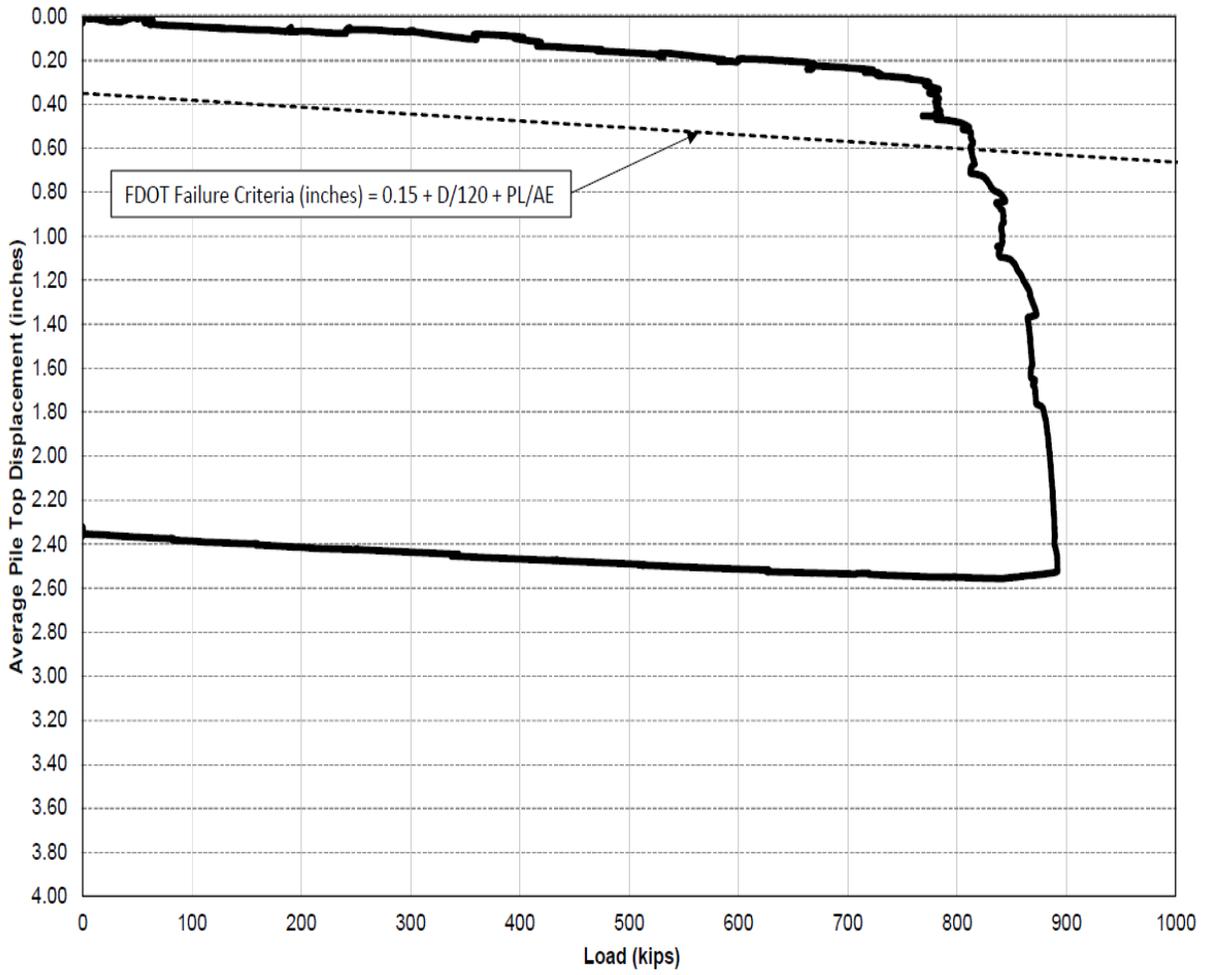
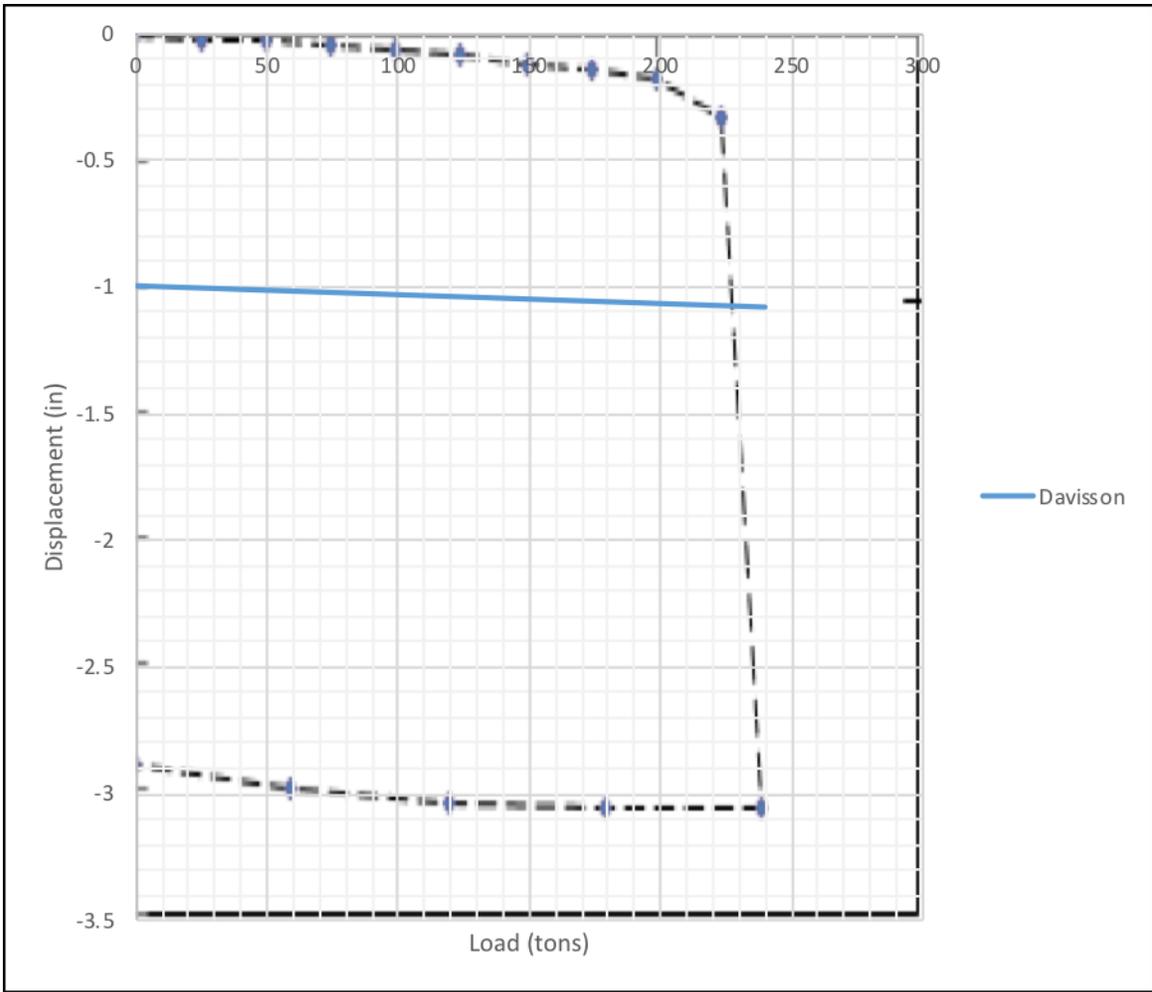**Figure A1: Load-displacement curve for pile 1**
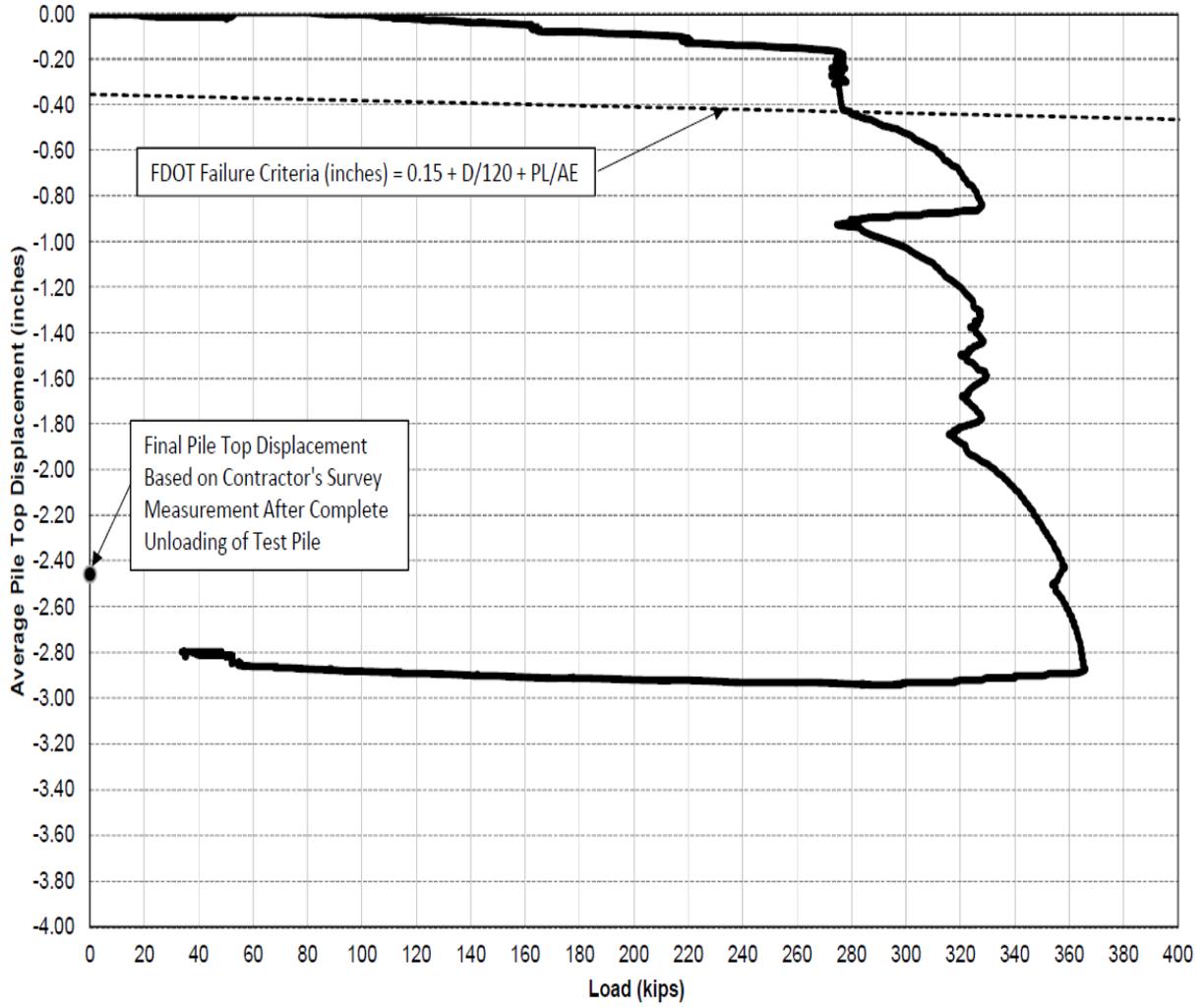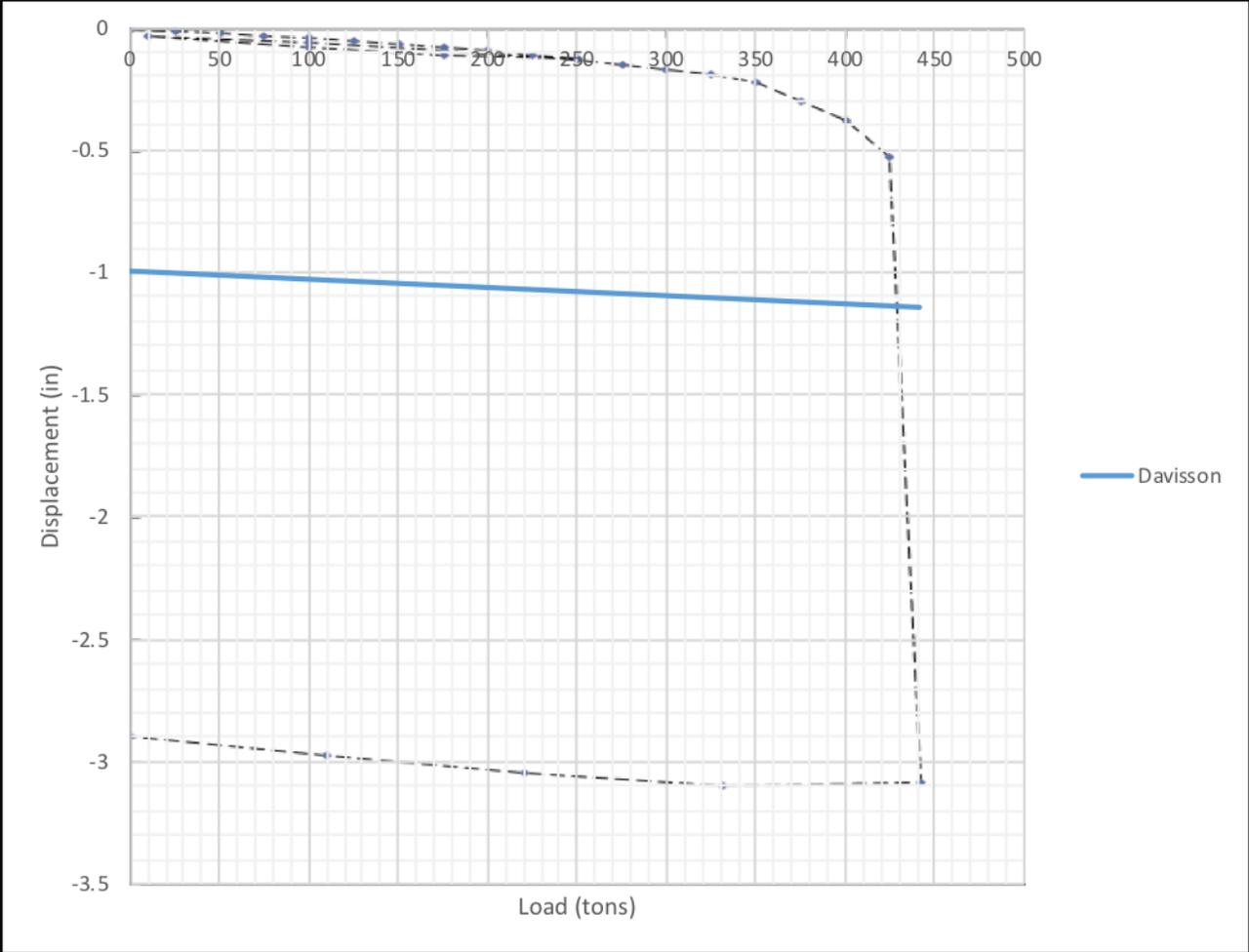
Figure A2: Load-displacement curve for pile 2

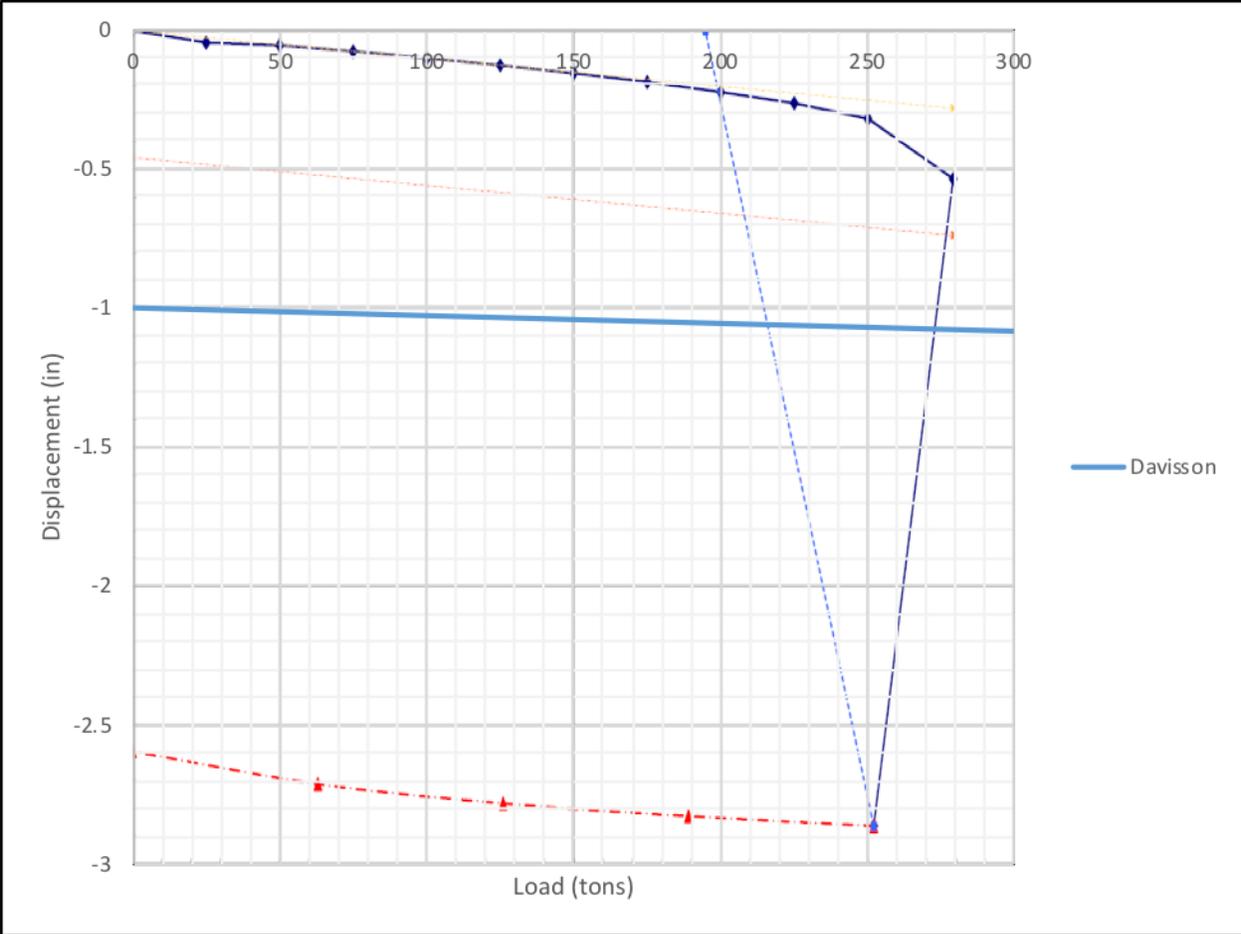**Figure A3: Load-displacement curve for pile 3**

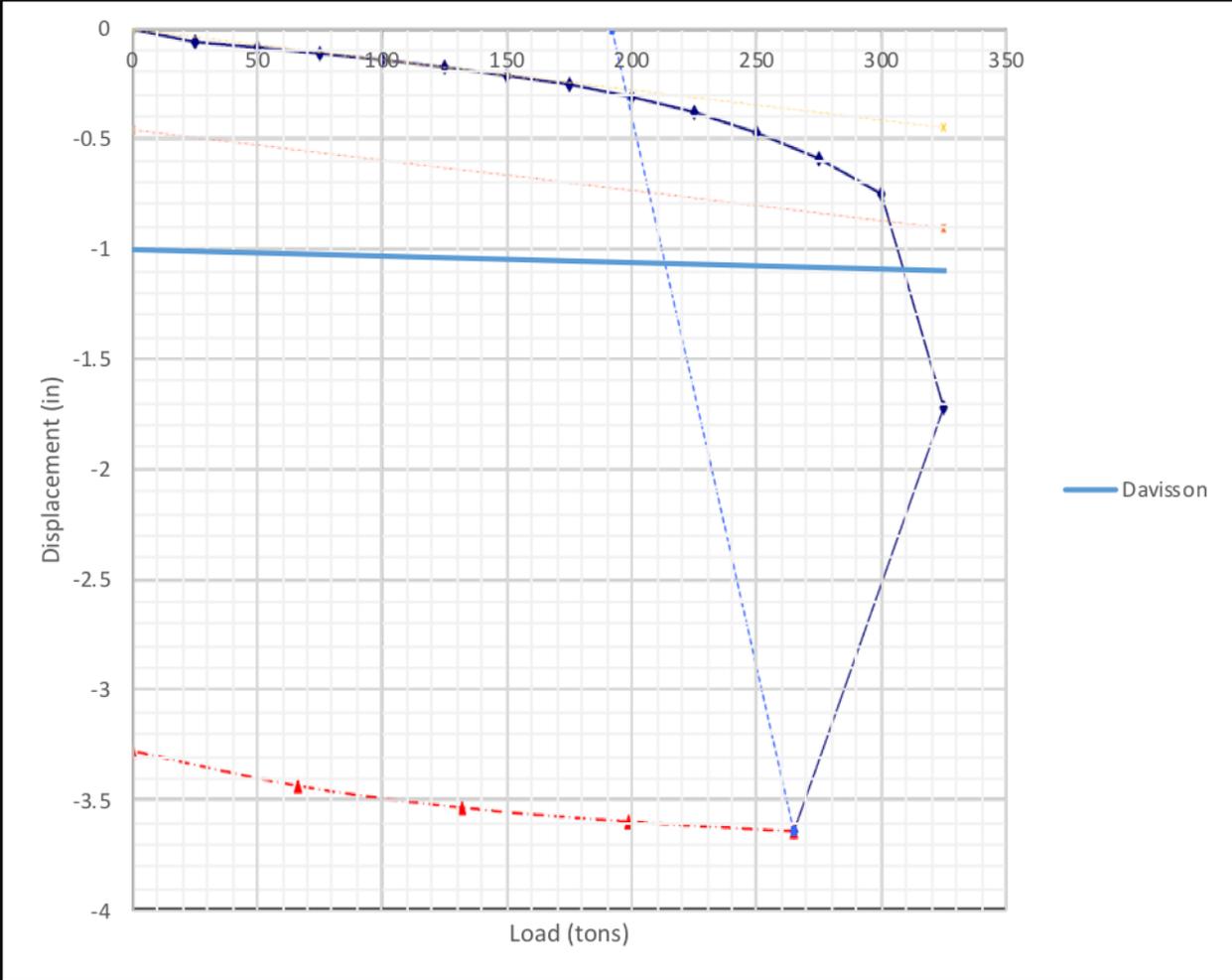**Figure A4: Load-displacement curve for pile 4**

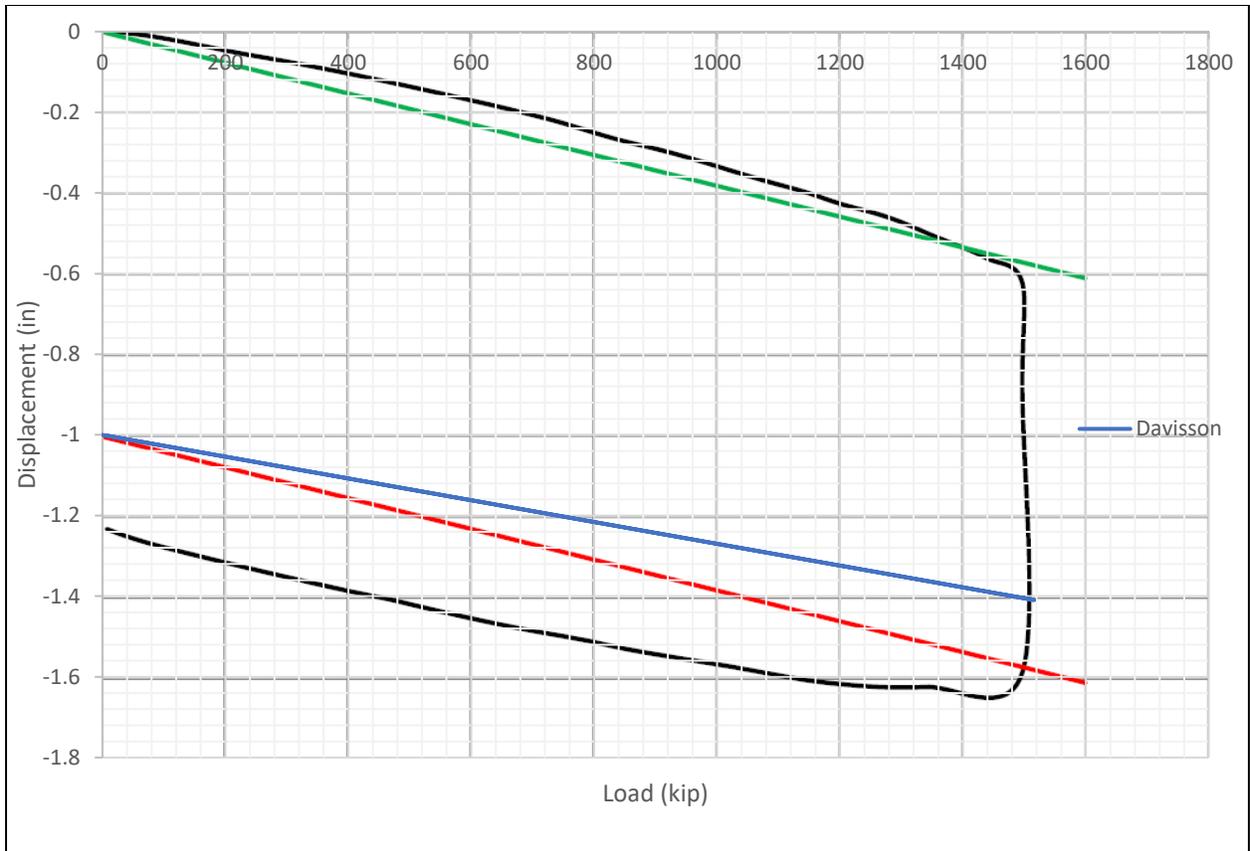**Figure A5: Load-displacement curve for pile 8**

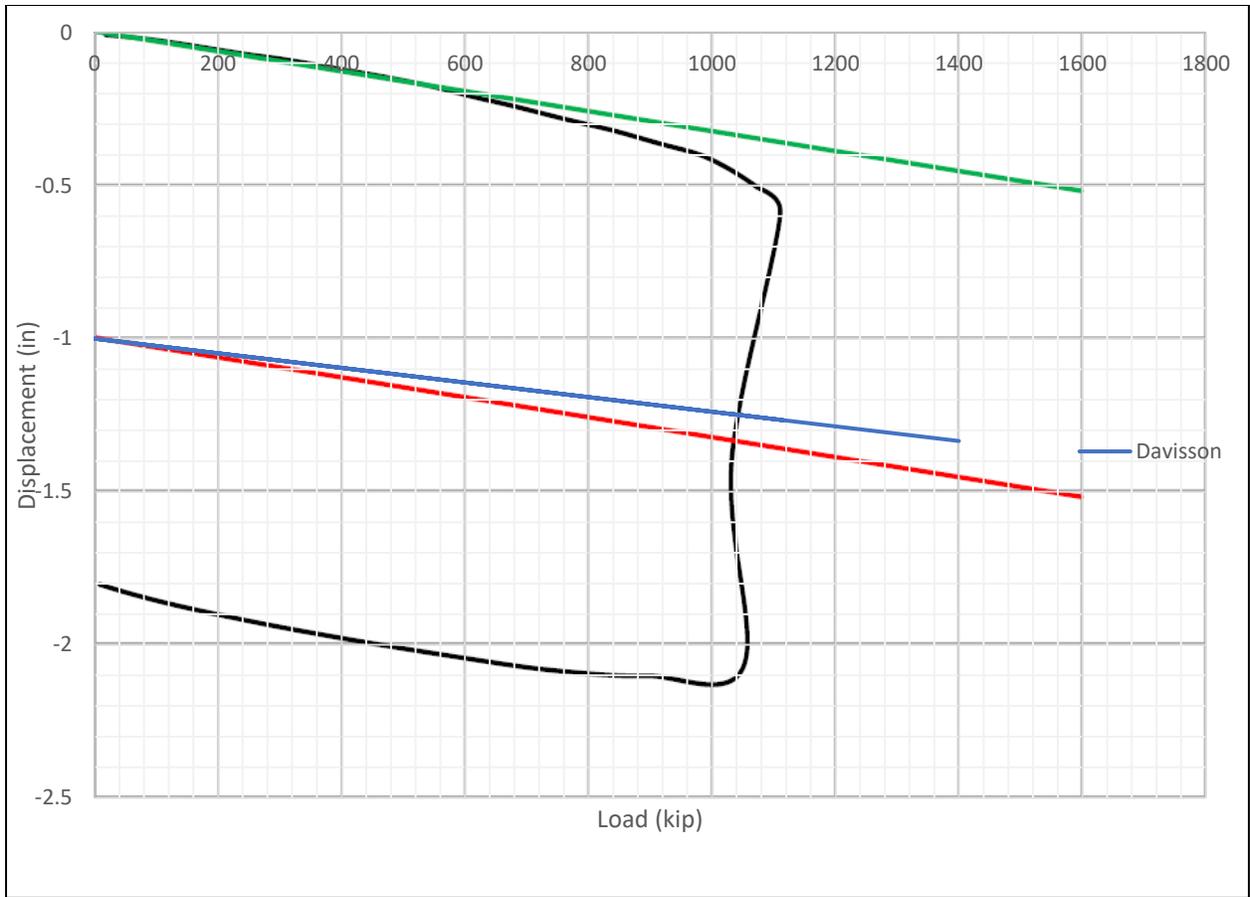**Figure A6: Load-displacement curve for pile 9**

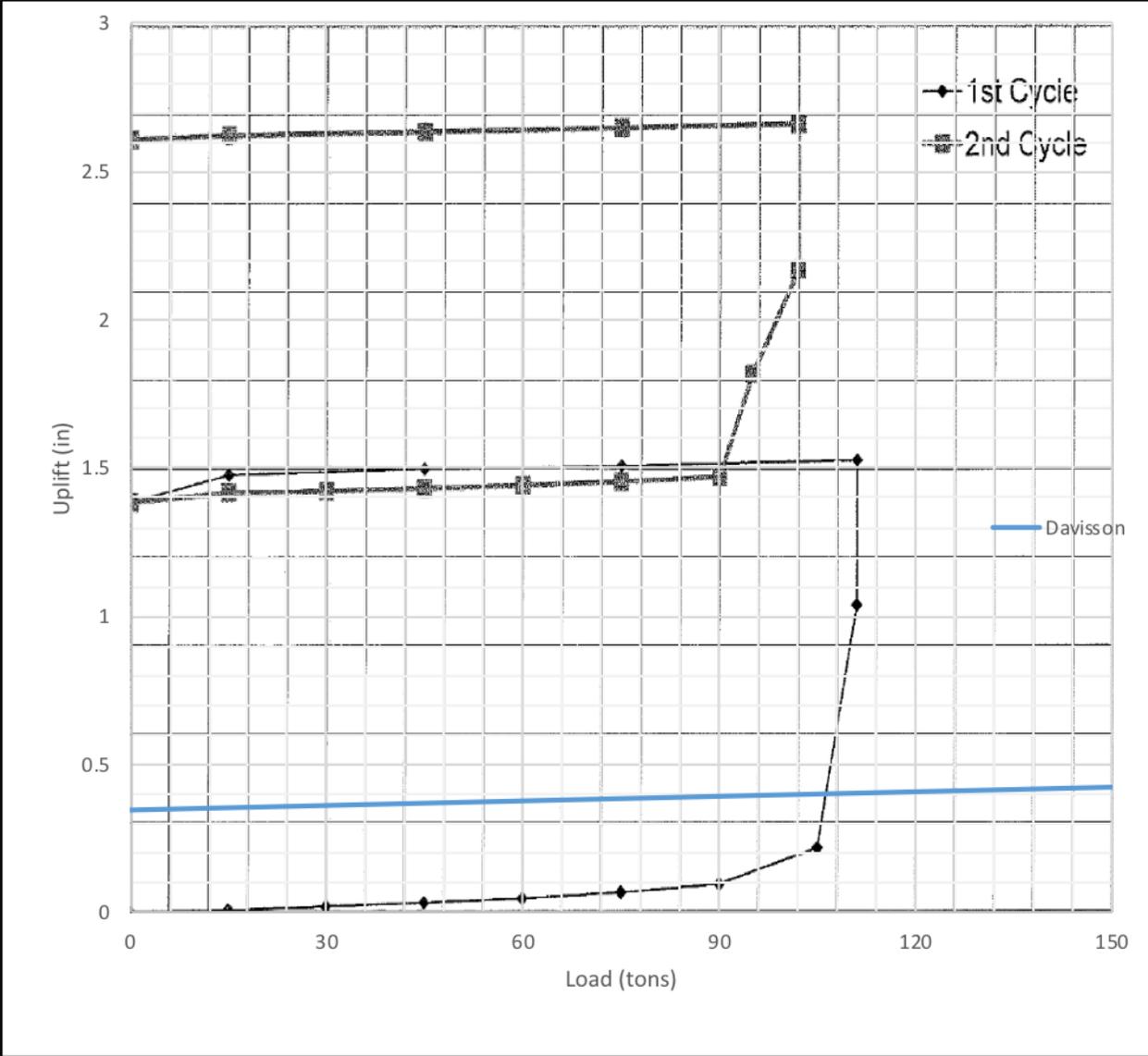**Figure A7: Load-displacement curve for pile 10**

Figure A8: Load-displacement curve for pile 12

Figure A9: Load-displacement curve for pile 14

Figure A10: Load-displacement curve for pile 16

Figure A11: Load-displacement curve for pile 18
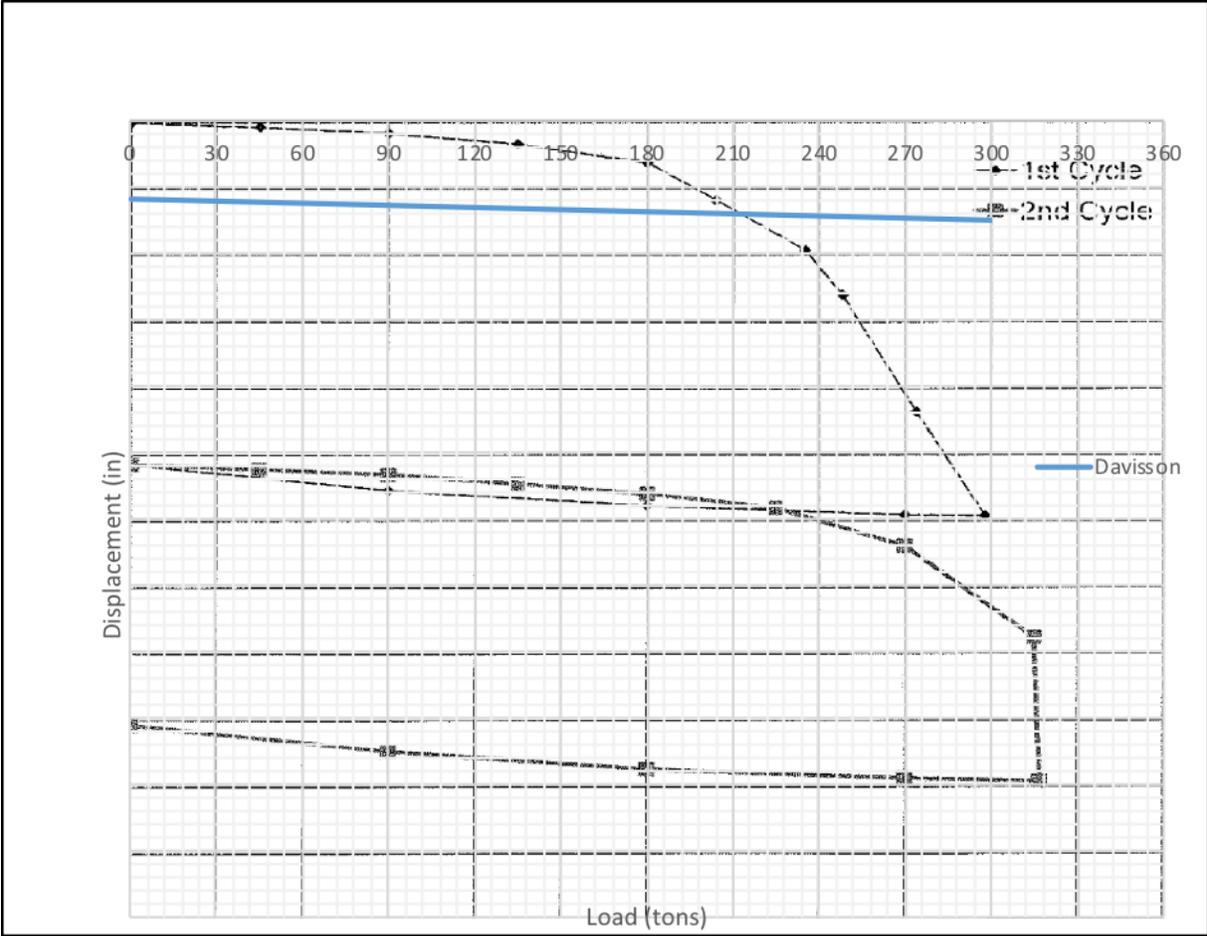
Figure A12: Load-displacement curve for pile 19
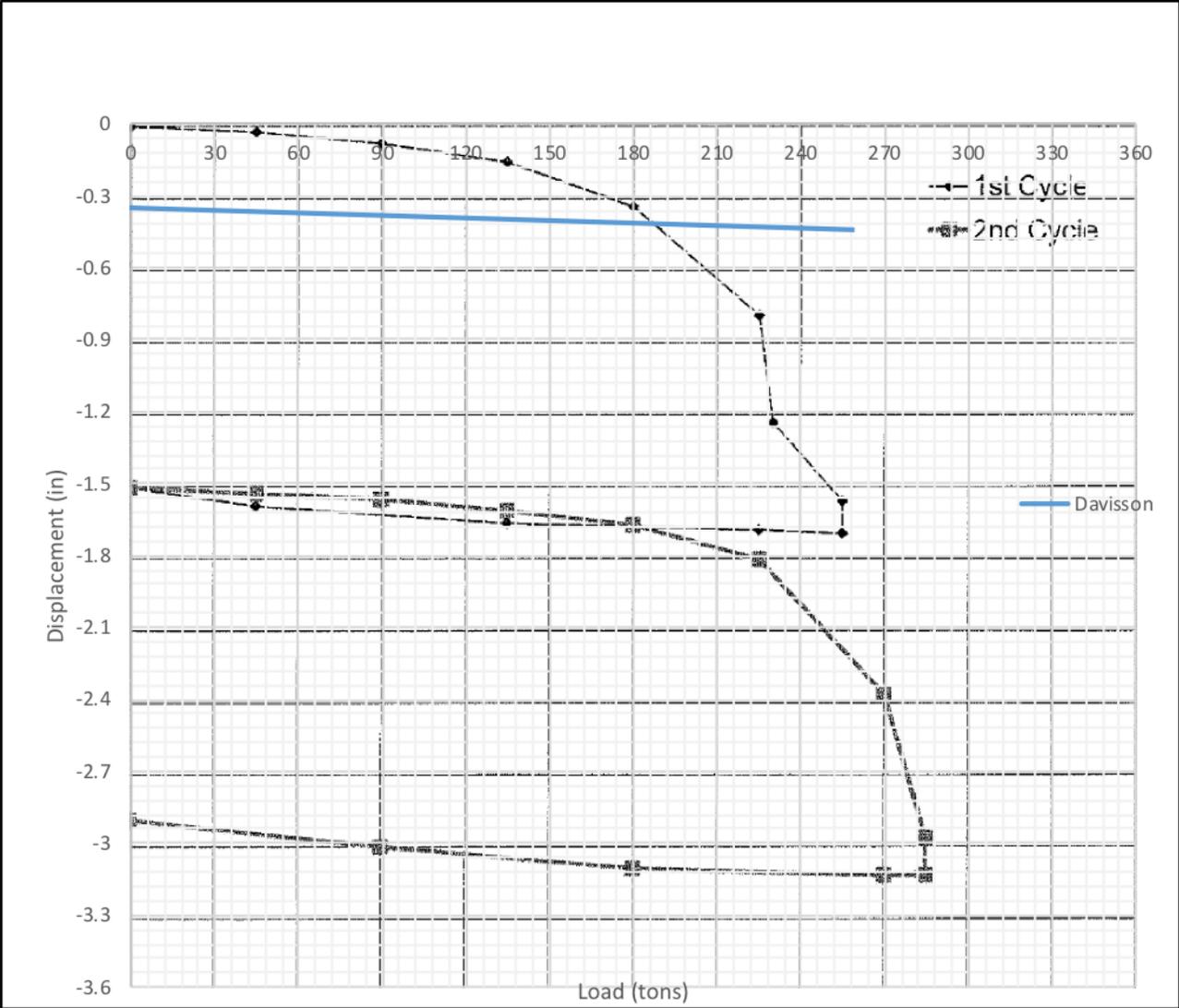
Figure A13: Load-displacement curve for pile 21
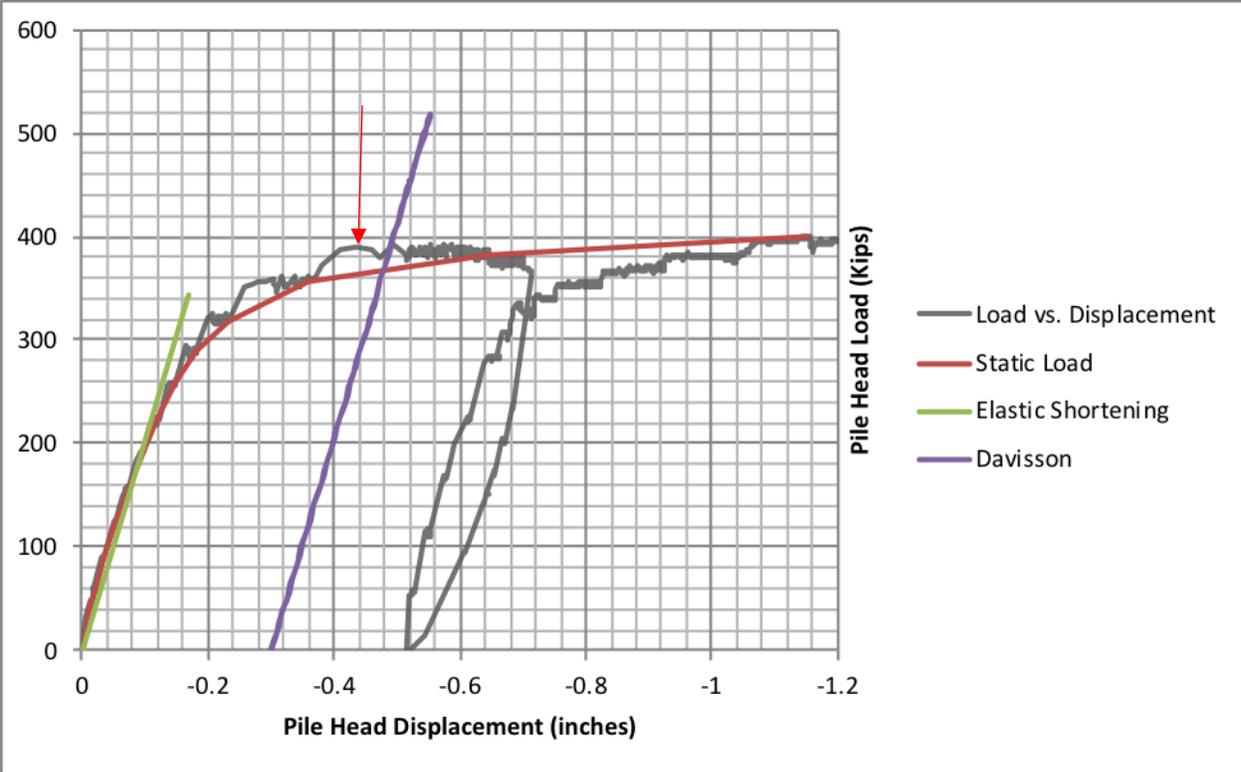
Figure A14: Load-displacement curve for pile 22
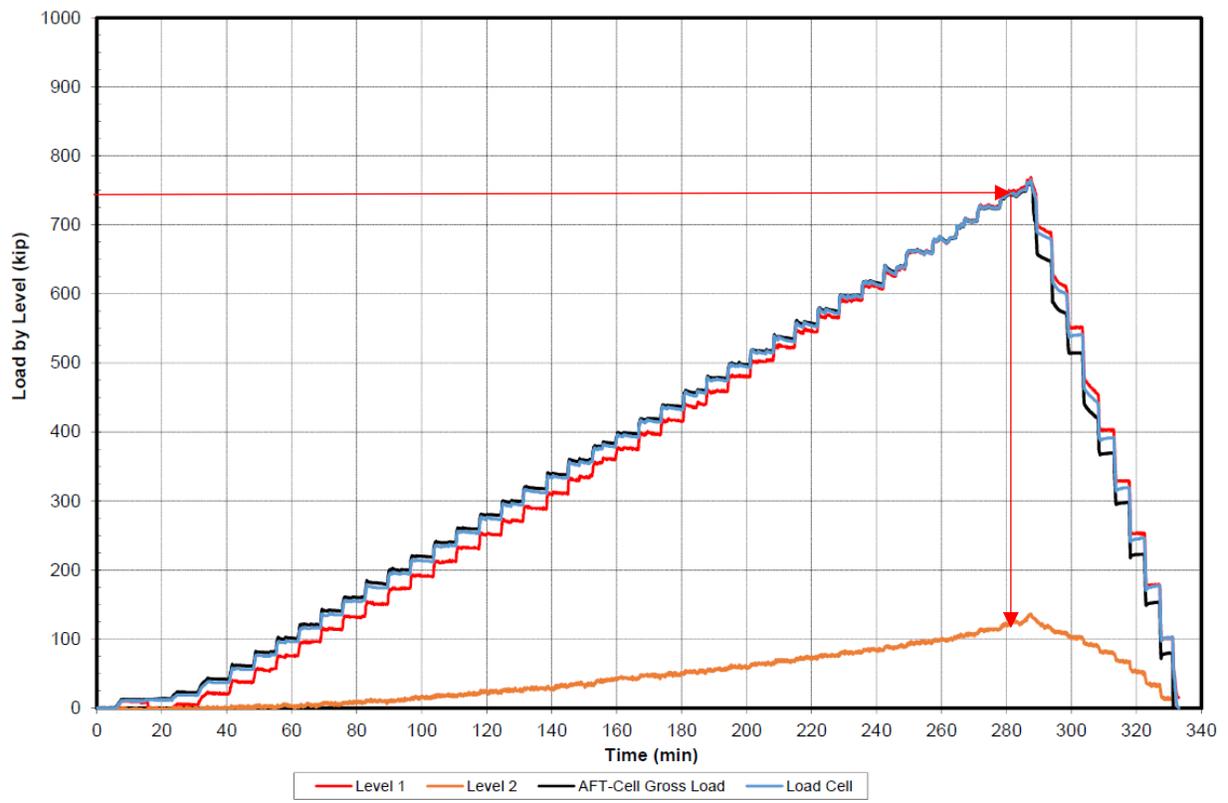
Figure A15: Load distribution vs. time for pile 3
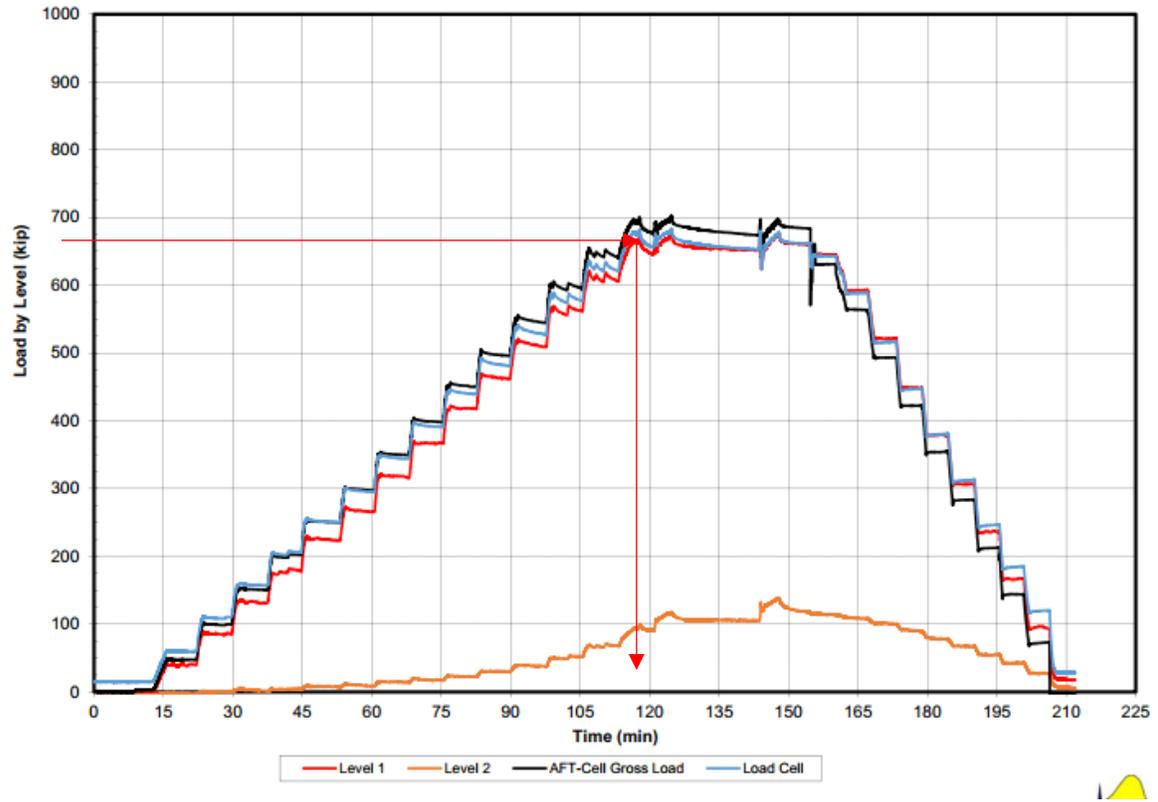
Figure A16: Load distribution vs. time for pile 4
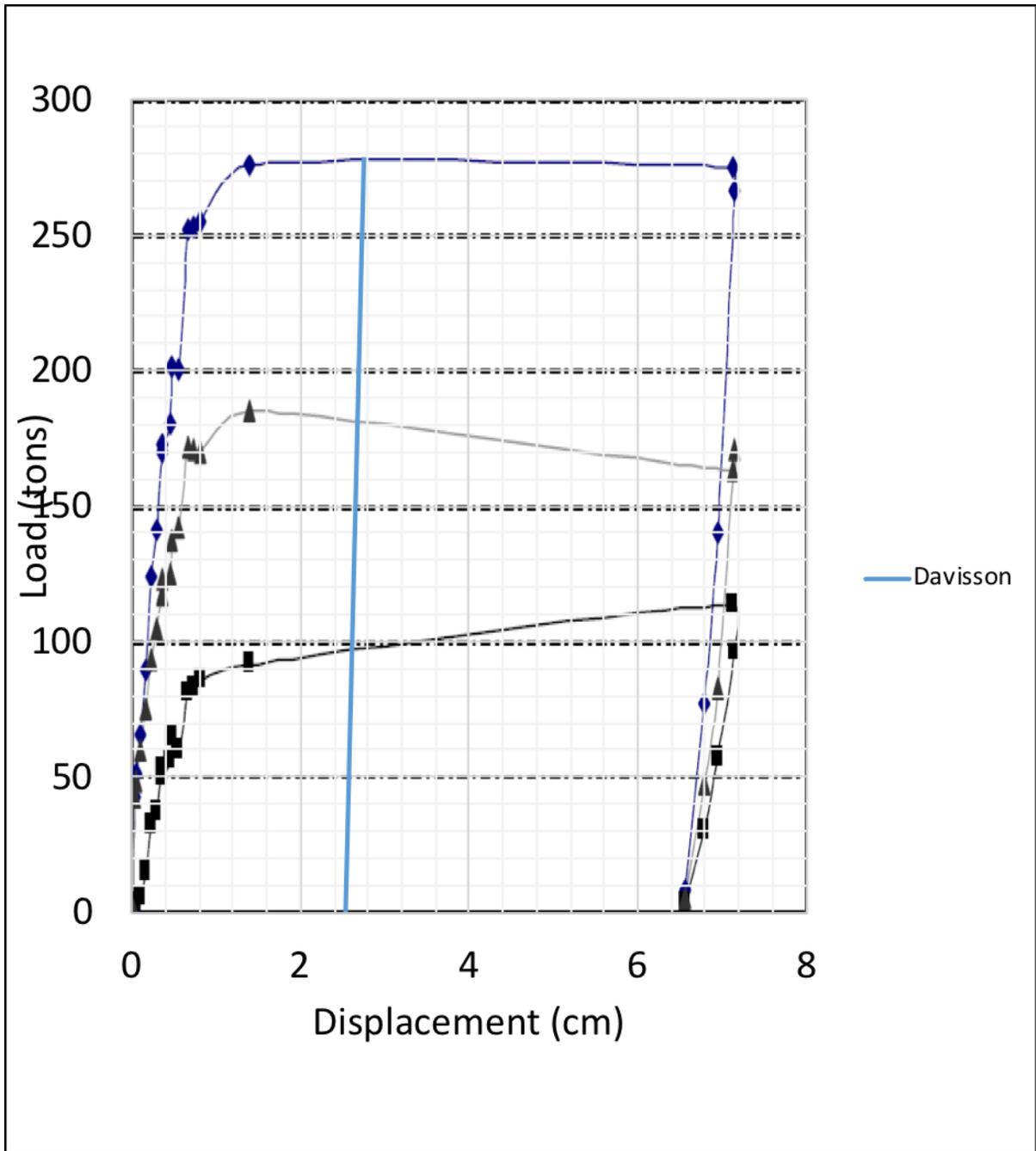
Figure A17: Tip capacity estimation for pile 10
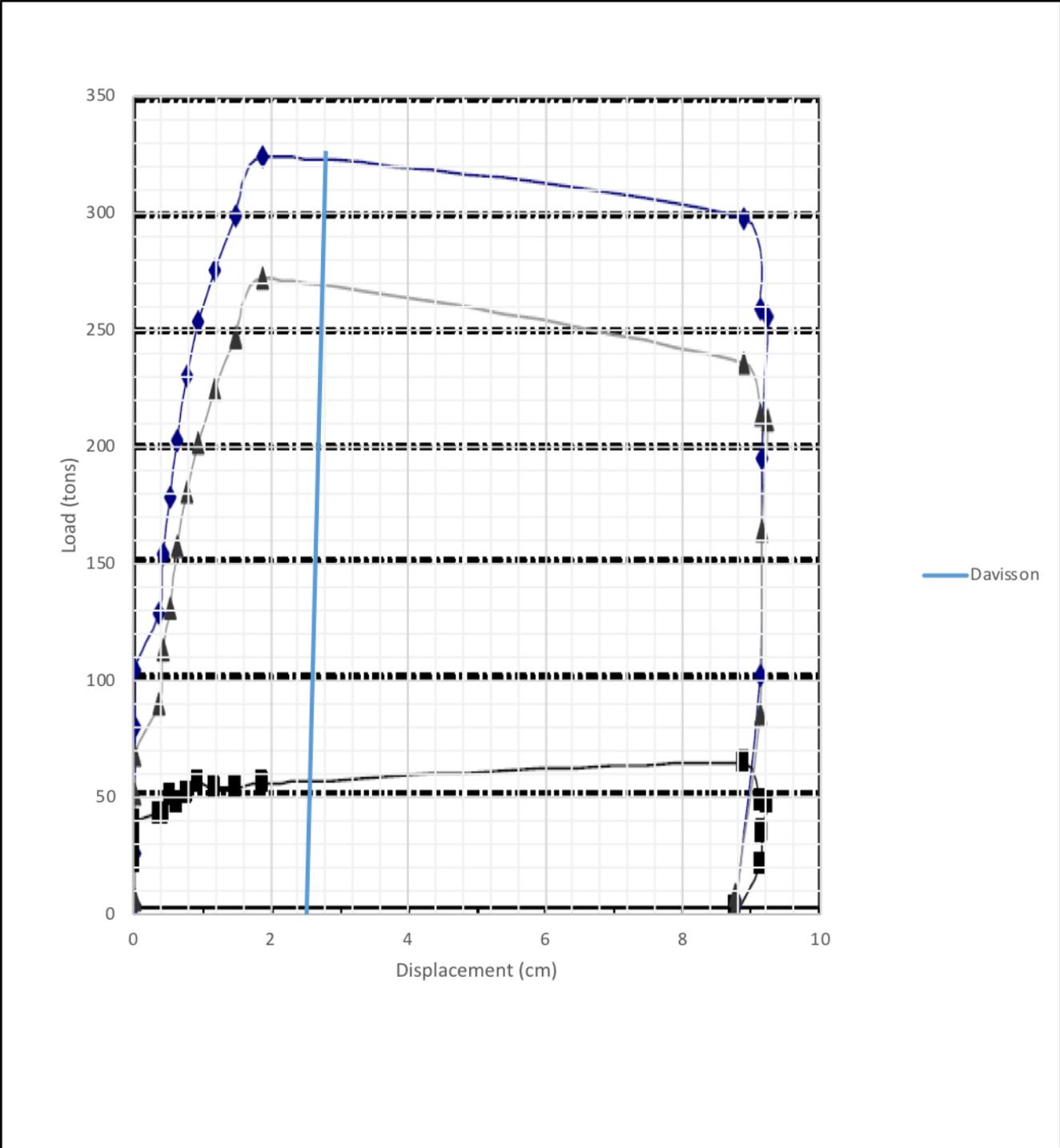
Figure A18: Tip capacity estimation for pile 12
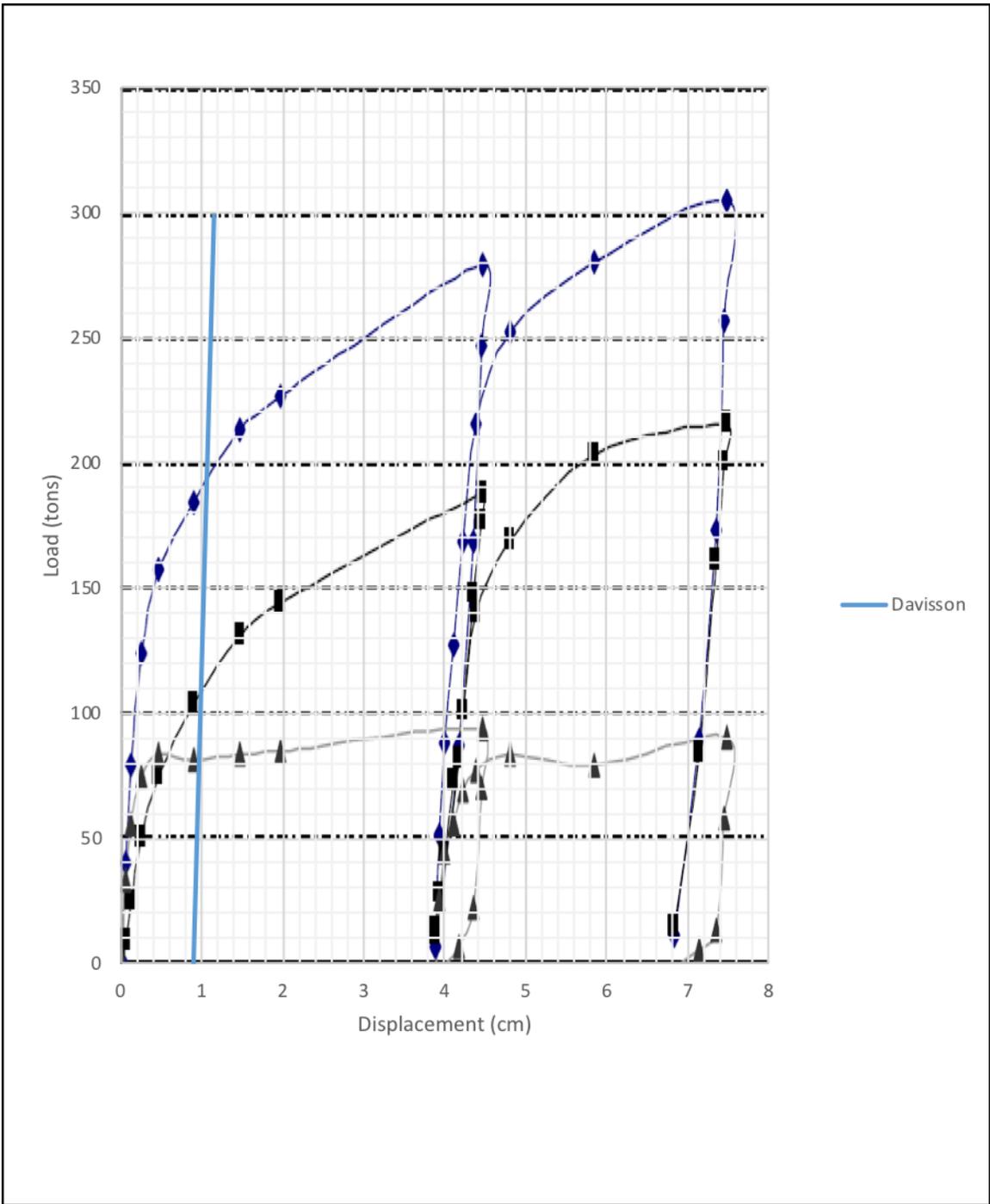
Figure A19: Tip capacity estimation for pile 19
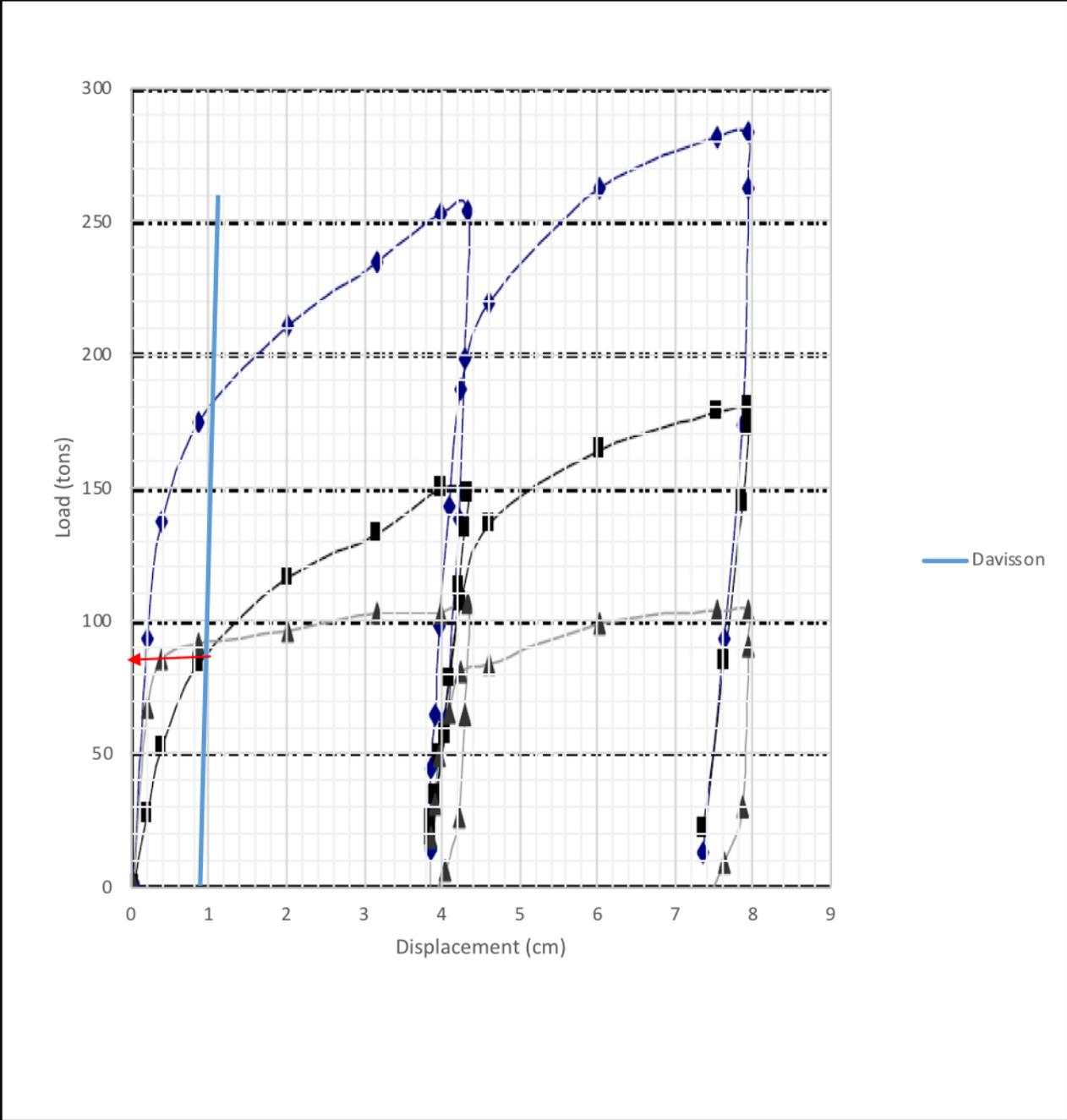
Figure A20: Tip capacity estimation for pile 21
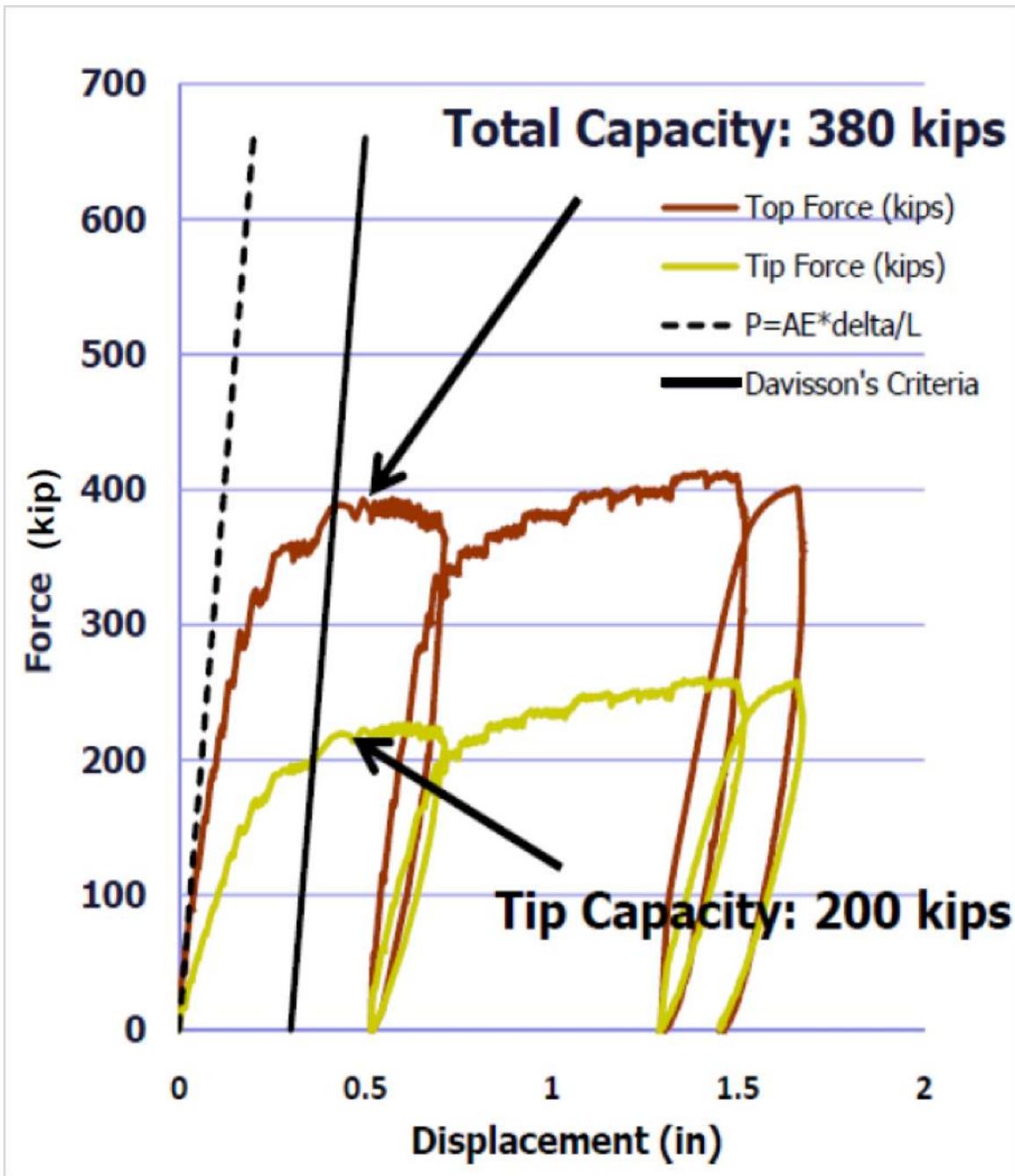
Figure A21: Tip capacity estimation for pile 22

APPENDIX B

TARGET RELIABILITY VERSUS RESISTANCE FACTOR DATA - CAPWAP

Table B.1: CAPWAP total capacity, closest restrike prior to SLT (2008-2017 data), including pile #2 (Case 1)

| λ_R	COV_R	β	ϕ_R
1.125	0.321	1	0.962729
		1.1	0.927423
		1.2	0.893411
		1.3	0.860647
		1.4	0.829084
		1.5	0.798679
		1.6	0.769389
		1.7	0.741173
		1.8	0.713992
		1.9	0.687807
		2	0.662583
		2.1	0.638284
		2.2	0.614876
		2.33	0.585724
		2.4	0.570604
		2.5	0.549678
		2.6	0.52952
		2.7	0.5101
		2.8	0.491393
		2.9	0.473372
		3	0.456012

Table B.2: CAPWAP tip capacity, closest restrike prior to SLT (2008-2017) data), including pile #2 (Case 2)

λ_R	COV_R	β	ϕ_R
0.963694	0.379553	1	0.773344
		1.1	0.741561
		1.2	0.711086
		1.3	0.681862
		1.4	0.65384
		1.5	0.626969
		1.6	0.601202
		1.7	0.576494
		1.8	0.552802
		1.9	0.530084
		2	0.508299
		2.1	0.487409
		2.2	0.467378
		2.33	0.442563
		2.4	0.429752
		2.5	0.41209
		2.6	0.395155
		2.7	0.378915
		2.8	0.363343
		2.9	0.34841
		3	0.334092

Table B.3: CAPWAP resistance factors for skin capacity of compression piles at closest re-strike prior to SLT(2008-2017 data), including pile #2 (Case 3)

λ_R	COV_R	β	ϕ_R
1.174	0.331	1	0.993917
		1.1	0.95672
		1.2	0.920915
		1.3	0.88645
		1.4	0.853274
		1.5	0.821341
		1.6	0.790602
		1.7	0.761014
		1.8	0.732533
		1.9	0.705118
		2	0.678729
		2.1	0.653328
		2.2	0.628877
		2.33	0.598454
		2.4	0.582687
		2.5	0.56088
		2.6	0.539889
		2.7	0.519683
		2.8	0.500234
		2.9	0.481513
		3	0.463493

Table B.4: CAPWAP resistance factors for skin friction capacity (of compression and tension piles) at closest restrike prior to SLT (2008-2017 data), including pile #2 (Case 4)

λ_R	COV_R	β	ϕ_R
1.297	0.513	1	0.891893
		1.1	0.846315
		1.2	0.803066
		1.3	0.762027
		1.4	0.723086
		1.5	0.686134
		1.6	0.651071
		1.7	0.617799
		1.8	0.586228
		1.9	0.55627
		2	0.527843
		2.1	0.500869
		2.2	0.475273
		2.33	0.443944
		2.4	0.427939
		2.5	0.40607
		2.6	0.385319
		2.7	0.365628
		2.8	0.346944
		2.9	0.329214
		3	0.31239

Table B.5: CAPWAP resistance factors for total pile capacity at EOID (2008-2017 data and McVay et al (2000) data), including pile #2 (Case 5)

λ_R	COV_R	β	ϕ_R
1.569	0.368	1	1.275458

		1.1	1.224157
		1.2	1.17492
		1.3	1.127663
		1.4	1.082307
		1.5	1.038775
		1.6	0.996994
		1.7	0.956893
		1.8	0.918406
		1.9	0.881466
		2	0.846012
		2.1	0.811985
		2.2	0.779325
		2.33	0.738824
		2.4	0.717895
		2.5	0.68902
		2.6	0.661307
		2.7	0.634708
		2.8	0.609179
		2.9	0.584677
		3	0.561161

Table B.6: CAPWAP resistance factors for total pile capacity at closest restrike prior to SLT (2008-2017 data and McVay et al (2000) data), including pile #2 (Case 6)

λ_R	COV_R	B	ϕ_R
1.246	0.341	1	1.043486
		1.1	1.003647
		1.2	0.965329
		1.3	0.928474
		1.4	0.893026
		1.5	0.858931
		1.6	0.826138
		1.7	0.794597
		1.8	0.764261
		1.9	0.735082
		2	0.707018
		2.1	0.680024
		2.2	0.654062
		2.33	0.621787
		2.4	0.605073
		2.5	0.581972
		2.6	0.559753
		2.7	0.538382
		2.8	0.517828
		2.9	0.498058
		3	0.479042

Table B.7: CAPWAP total capacity closest restrike prior to SLT (2008-2017 data), excluding pile #2 (Case 1)

λ_R	COV_R	β	ϕ_R
1.178	0.277	1	1.055448

		1.1	1.020188
		1.2	0.986106
		1.3	0.953163
		1.4	0.92132
		1.5	0.890541
		1.6	0.86079
		1.7	0.832033
		1.8	0.804237
		1.9	0.777369
		2	0.751399
		2.1	0.726296
		2.2	0.702032
		2.33	0.671697
		2.4	0.655909
		2.5	0.633997
		2.6	0.612817
		2.7	0.592344
		2.8	0.572555
		2.9	0.553427
		3	0.534939

Table B.8: CAPWAP tip capacity closest restrike prior to SLT (2008-2017 data), excluding pile #2 (Case 2)

λ_R	COV_R	β	ϕ_R
1.009	0.355	1	0.832153

		1.1	0.799528
		1.2	0.768183
		1.3	0.738067
		1.4	0.709132
		1.5	0.681331
		1.6	0.65462
		1.7	0.628956
		1.8	0.604298
		1.9	0.580607
		2	0.557844
		2.1	0.535974
		2.2	0.514962
		2.33	**0.488872**
		2.4	0.475376
		2.5	0.456739
		2.6	0.438833
		2.7	0.421628
		2.8	0.405099
		2.9	0.389217
		3	0.373958

Table B.9: CAPWAP resistance factors for skin capacity of compression piles at closest re-strike prior to SLT (2008-2017 data), excluding pile #2 (Case 3)

λ_R	COV_R	β	ϕ_R
1.245	0.27	1	1.123386

		1.1	1.086431
		1.2	1.05069
		1.3	1.016126
		1.4	0.982699
		1.5	0.950371
		1.6	0.919107
		1.7	0.888871
		1.8	0.85963
		1.9	0.831351
		2	0.804002
		2.1	0.777553
		2.2	0.751974
		2.33	**0.719975**
		2.4	0.703313
		2.5	0.680176
		2.6	0.6578
		2.7	0.636161
		2.8	0.615233
		2.9	0.594994
		3	0.57542

Table B.10: CAPWAP resistance factors for skin friction capacity (of compression and tension piles) at closest restrike prior to SLT (2008-2017 data), excluding pile #2 (Case 4)

λ_R	COV_R	β	ϕ_R
1.351	0.485	1	0.960159
		1.1	0.913078
		1.2	0.868306
		1.3	0.825729

		1.4	0.78524
		1.5	0.746737
		1.6	0.710121
		1.7	0.675301
		1.8	0.642188
		1.9	0.610699
		2	0.580754
		2.1	0.552277
		2.2	0.525197
		2.33	0.491968
		2.4	0.474954
		2.5	0.451665
		2.6	0.429518
		2.7	0.408457
		2.8	0.388429
		2.9	0.369383
		3	0.960159

Table B.11: CAPWAP resistance factors for total pile capacity at EOID (2008-2017 data and McVay et al (2000) data), excluding pile #2 (Case 5)

λ_R	COV_R	β	ϕ_R
1.569	0.368	1	1.275458
		1.1	1.224157
		1.2	1.17492
		1.3	1.127663

		1.4	1.082307
		1.5	1.038775
		1.6	0.996994
		1.7	0.956893
		1.8	0.918406
		1.9	0.881466
		2	0.846012
		2.1	0.811985
		2.2	0.779325
		2.33	**0.738824**
		2.4	0.717895
		2.5	0.68902
		2.6	0.661307
		2.7	0.634708
		2.8	0.609179
		2.9	0.584677
		3	.561161

Table B.12: CAPWAP resistance factors for total pile capacity at closest restrike prior to SLT (2008-2017 data and McVay et al (2000) data(, excluding pile #2 (Case 6)

λ_R	COV_R	B	ϕ_R
1.245	0.337	1	1.054767
		1.1	1.014816
		1.2	0.976377

		1.3	0.939395
		1.4	0.903814
		1.5	0.86958
		1.6	0.836643
		1.7	0.804954
		1.8	0.774464
		1.9	0.74513
		2	0.716907
		2.1	0.689752
		2.2	0.663627
		2.33	0.631137
		2.4	0.614307
		2.5	0.591038
		2.6	0.568652
		2.7	0.547113
		2.8	0.52639
		2.9	0.506452
		3	0.487269

APPENDIX C

ILLUSTRATION OF THE AFOSM (HASOFER-LIND) METHOD

γ_D x Mean of Nominal Dead Load + γ_L x Mean of Nominal Live Load = $\emptyset_R$ x Mean of Nominal Resistance

$$\mu_{nR} = \left(\frac{\gamma_D Q_D + \gamma_L Q_L}{\phi_R} \right) \tag{C1}$$

Mean of measured total load $= \lambda_{DL}$ *x Mean of Nominal Dead Load* $+$ λ_{LL} *x Mean of Nominal Live Load*

$$\mu_S = \lambda_{QD} Q_D + \lambda_{QL} Q_L \qquad \text{(C2)}$$

Mean of measured resistance $= \lambda_R$ *x Mean of Nominal Resistance*

$$\mu_R = \lambda_R \left(\frac{\gamma_D Q_D + \gamma_L Q_L}{\phi_R} \right) \qquad \text{(C3)}$$

Then, COV of the total load was calculated using equation (C4).

COV of measured total load $= \sqrt{\text{COVQD}^2 + \text{COVQL}^2}$

$$COV_S = \sqrt{COV_{QD}^2 + COV_{QL}^2} \qquad \text{(C4)}$$

By combining (A2.a) and (A4.a), one obtains

$$\sigma_S = [\lambda_{DL} Q_D + \lambda_{LL} Q_L] \sqrt{COV_{QD}^2 + COV_{QL}^2} \qquad \text{(C5)}$$

If the coefficient of variation of the measured resistance is COV_R

$$\sigma_R = \lambda_R \left(\frac{\gamma_D Q_D + \gamma_L Q_L}{\phi_R} \right) COV_R \qquad \text{(C6)}$$

The AFOSM method of deriving the reliability index provides a unique solution. In this method, both R and S are normalized using the following transformations:

$$\text{If } R' = \frac{R - \mu_R}{\sigma_R} \qquad \text{(C7a)}$$

$$\text{and } S' = \frac{S - \mu_S}{\sigma_S} \qquad \text{(C7b)}$$

Then, g(R,S), the performance function is defined as

104

$$g = R - S \tag{C8a}$$

Or, in the expanded form

$$g = (R'\sigma_R + \mu_R) - (S'\sigma_S + \mu_S) \tag{C8b}$$

It is seen that the non-failure region ($g(R',S') > 0$) and the failure regions($g(R',S') > 0$) are separated by the *limit state surface* ($g(R',S') = 0$)

It can be shown that the reliability index β can be defined as the minimum distance between the origin of the (R',S') axes system and the surface ($g(R',S') = 0$)·

The following equation can be used to express the reliability index β

$$\beta = \frac{\Sigma_1^n\left[x_i'^*\left[\frac{\partial g}{\partial x_i'}\right]^*\right]}{\sqrt{\Sigma_1^n\left[\frac{\partial g}{\partial x_i'}\right]^{2*}}} \tag{C9}$$

Where X_i are the β fundamental variables that compose R and S while "*" indicates the values evaluated at the point on the $g(R',S')=0$ surface which is at the minimum distance from the origin of (R'-S') coordinates. This is known as the *design point* and determined based on Eqn. (C10).

$$x_i'^* = -\alpha\beta \tag{C10}$$

where the directional cosines are computed by

$$\beta = \frac{\left[\frac{\partial g}{\partial x_i'}\right]^*}{\sqrt{\Sigma_1^n\left[\frac{\partial g}{\partial x_i'}\right]^{2*}}} \tag{C11}$$

The location of the design point on the orginal (R-S) coordinates can be found by the following

expression, using the relations in Eqn. (C7).

$$x_i = \mu_{X_i} - \alpha_i\beta\sigma_{X_i} \tag{C12}$$

Specific variables associated with the current problem

In the LRFD problem, the following identification is made of the fundamental variables:

Load (S) – dead load Q_D and live load Q_L
Resistance - R

Then using Eqn. (B8.b) one obtains the following partial derivatives to be used in Eqns, (C9) and (C11).

$$\frac{\partial g}{\partial R} = \sigma_R \tag{C13a}$$

$$\frac{\partial g}{\partial S} = -\sigma_S \tag{C13b}$$

Based on Eqn. (C11), the directional cosines can be written as

$$\alpha_R = \frac{\sigma_R}{\sqrt{(\sigma_R)^2 + (-\sigma_S)^2}} \tag{C14a}$$

$$\alpha_S = \frac{\sigma_S}{\sqrt{(\sigma_R)^2 + (-\sigma_S)^2}} \tag{C14b}$$

Similarly, the reliability index β (Eqn. can be expressed as

$$\beta = \frac{R/\sigma_R - S/\sigma_S}{\sqrt{(\sigma_R)^2 + (-\sigma_S)^2}} \tag{C15}$$

Since the (C9)-(C12) must be evaluated at the design point (*) and the design point is, in fact, the target of the computation, the procedure has be an iterative one. The following iterative procedure is recommended typically.

It must be noted that in cases where the probability distributions of the load or the resistance do not follow normal the distributions, equivalent mean and standard deviation values have to be used at each design point x* based on the following equations:

$$\mu_X^N = x^* - \emptyset^{-1}(F_X(x^*))\sigma_X^N \tag{C16}$$

$$\sigma_X^N = \frac{\emptyset[\emptyset^{-1}(F_X(x^*))]}{f_X(x^*)} \tag{C17}$$

Step 1

Assume normalized values of (*n-1*) fundamental variables X_i^* and determine the nth normalized variable X_i^* based on the fact that the design point is on the *g(R-S)=0* surface.

<u>Step 2</u>

Compute the reliability index from Eqn. (C15)

<u>Step 3</u>

Compute the directional cosines from Eqn. (C14) and update the design point based on Eqn. (C10).

<u>Step 4</u>

Determine the (n-1) of the n original X_i values based on Eqn. (C12) and transform them using Eqn. (C7).

<u>Step 5</u>

Update the last (n^{th}) X_i value based on the same criterion as in step 1.

Repeat the above process iteratively, until the reliability index converges.

APPENDIX D

DESCRIPTION OF THE MONTE-CARLO SIMULATION PROCESS

Table D1 displays the values of the variables used in the simulation.

Table D.1: General values of the variables involved in the analysis

Coefficient	Value
Dead Load/Live Load (Q_D/Q_L)	3
Assumed Live Load (kip)	100^*

Assumed Dead Load (kip)	300*
Dead Load Factor (γ_D)	1.25
Live Load Factor (γ_L)	1.75
Factored load	425
Coefficient of Variation of Dead Load (COV_{QD})	0.1
Coefficient of Variation of Live Load (COV_{QL})	0.18
Bias Factor of Dead Load (λ_{QD})	1.05
Target reliability	2.33
Bias Factor of Live Load (λ_{QL})	1.15

With the Monte-Carlo simulation, the first task was to develop the lognormal distributions of measured total load and measured resistance. The process was initiated using equation (C1) to compute the mean nominal resistance:

$$\gamma_D \ x \ Mean \ of \ Nominal \ Dead \ Load + \ \gamma_L \ x \ Mean \ of \ Nominal \ Live \ Load =$$
$$\emptyset_R \ x \ Mean \ of \ Nominal \ Resistance \tag{D1}$$

*It must be noted that any magnitude of loads (or the load scaling factor) can be assumed as long as the ratio of Q_D/Q_L is maintained. This is because, as seen in Eqn. (C1), the magnitude of the corresponding resistance will also be determined by the magnitude of the loads.

Next, the mean values of measured resistance and load were calculated using equations (D2) and (C3).

$$Mean \ of \ measured \ total \ load = \ \lambda_{DL} \ x \ Mean \ of \ Nominal \ Dead \ Load +$$
$$\lambda_{LL} \ x \ Mean \ of \ Nominal \ Live \ Load \tag{D2}$$

$$Mean \ of \ measured \ resistance = \ \lambda_R \ x \ Mean \ of \ Nominal \ Resistance \tag{D3}$$

Then, COV of the total load was calculated using equation (D4).

$$COV \ of \ measured \ total \ load = \ \sqrt{COVQD^2 + COVQL^2} \tag{D4}$$

In the next step, the mean and standard deviation values of the lognormal distributions of measured resistance and total load were calculated using equations (D5-D8):

$$Mean \ of \ the \ lognormal \ distribution \ of \ measured \ resistance =$$
$$\ln \frac{Mean \ of \ measured \ resistance}{\sqrt{1+(COV \ measured \ resistance)^2}} \tag{D5}$$

$Mean\ of\ the\ lognormal\ distribution\ of\ measured\ total\ load =$

$$\ln \frac{Mean\ of\ measured\ total\ load}{\sqrt{1+(COV\ measured\ total\ load)^2}} \tag{D6}$$

$Standard\ deviation\ of\ the\ lognormal\ distribution\ of\ measured\ resistanc =$

$$\sqrt{\ln(1 + (COV\ measured\ resistance)^2)} \tag{D7}$$

$Standard\ deviation\ of\ the\ lognormal\ distribution\ of\ measured\ total\ load =$

$$\sqrt{\ln(1 + (COV\ measured\ total\ load)^2)} \tag{D8}$$

Using the above mean and standard deviation values, the lognormal distributions of measured total load and measured resistance were developed for Cases 1 of CAPWAP and EDC-FDOT predictions (Figs. D1 and D3) and the Monte-Carlo simulation was performed with each set of distributions in the following manner. In each trial, a load value and a resistance value were selected randomly from the load distribution and the resistance distribution respectively. In a given trial, if the selected load is greater than the resistance, that pair represented a failure condition. Otherwise, it was classified as a non-failure condition. Similarly, for the above case 1, one hundred thousand such trials were performed to derive the plots comparing the load and resistance values (Figs. D2 and D4). It must be noted that, in Fig. D2 and D4, the tan colored lines indicate the load = resistance condition. Finally, the probability of failure was computed using equation (D9):
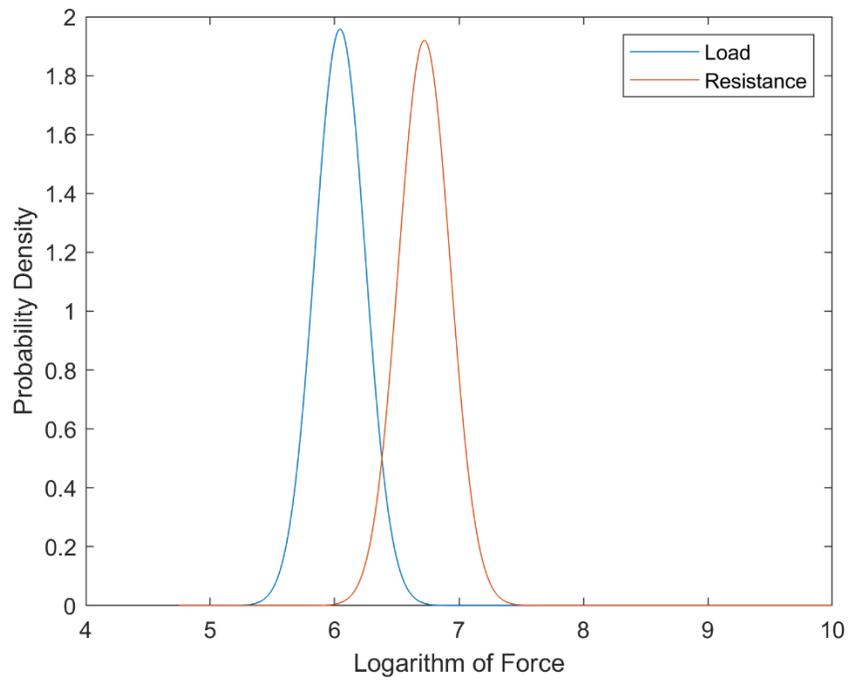
$$Probability\ of\ failure = \frac{Number\ of\ tests\ that\ failed}{Total\ number\ of\ tests\ performed} x100 \tag{D9}$$
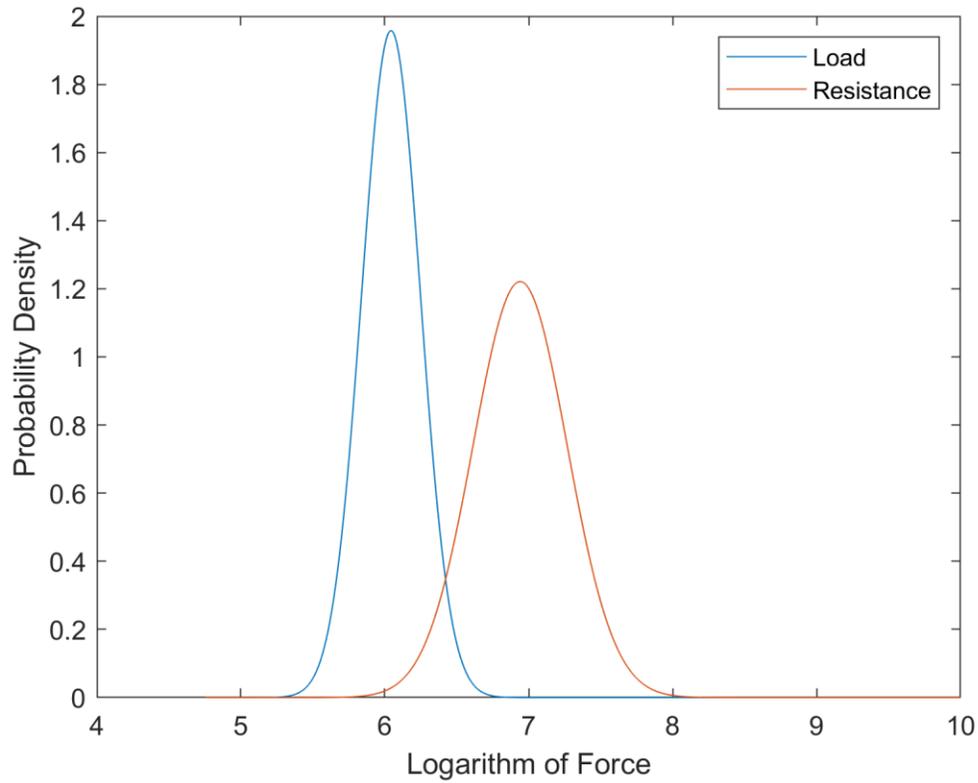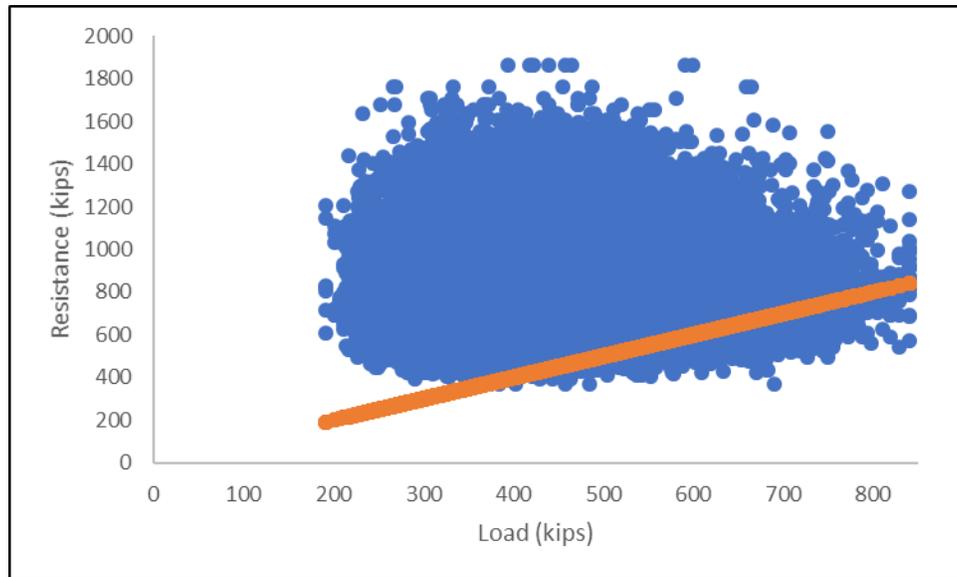
Figure D.1: Probability density function for Case 1 – CAPWAP Predictions- Closest and prior to restrike
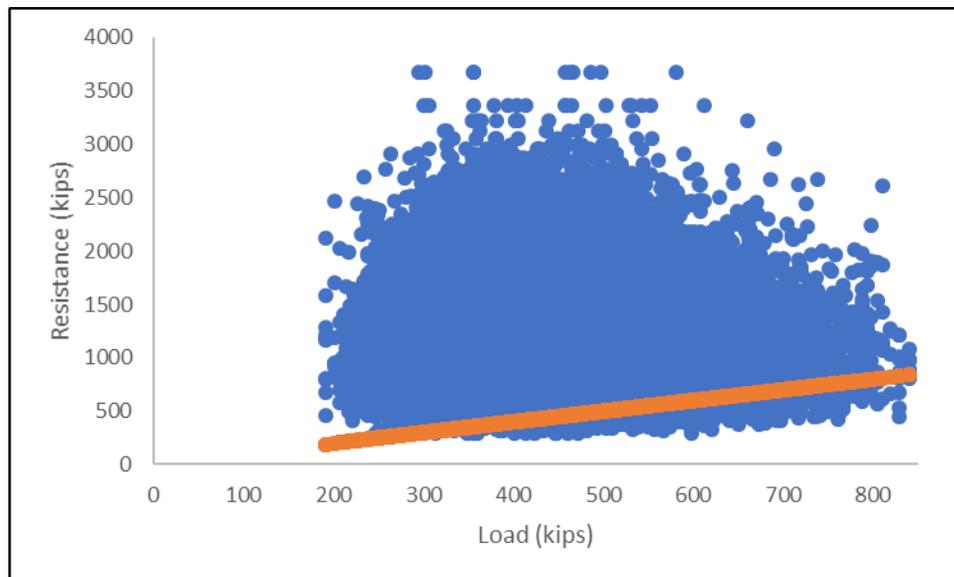
Figure D.2: Load vs. resistance for Case 1 - CAPWAP Predictions- Closest and prior to restrike

Figure D.3: Probability density functions for Case 1-EDC FDOT -Predictions- Closest and prior to restrike

Figure D.4: Load vs. resistance for Case 1- EDC –FDOT Predictions– Closest and prior to restrike

APPENDIX E

TARGET RELIABILITY VERSUS RESISTANCE FACTOR DATA - EDC

Table E.1: EDC-FDOT method resistance factors for total pile capacity at closest restrike prior to SLT, including pile #2 (Case 1)

λ_R	COV_R	β	ϕ_R
1.0059	0.213925	1	0.957569
		1.1	0.929852
		1.2	0.902937
		1.3	0.876801
		1.4	0.851422
		1.5	0.826778
		1.6	0.802847
		1.7	0.779608
		1.8	0.757042
		1.9	0.735129
		2	0.713851
		2.1	0.693188
		2.2	0.673124
		2.33	0.647906
		2.4	0.634721
		2.5	0.616349
		2.6	0.598508
		2.7	0.581184
		2.8	0.564362
		2.9	0.548026
		3	0.532164

Table E.2: EDC-FDOT method resistance factors for total pile capacity at EOID, including pile #2 (Case 5)

λ_R	COV_R	β	ϕ_R
1.7502	0.4718	1	1.258605
		1.1	1.197251
		1.2	1.138887
		1.3	1.083368
		1.4	1.030555
		1.5	0.980318
		1.6	0.932529
		1.7	0.88707
		1.8	0.843826
		1.9	0.802691
		2	0.763561
		2.1	0.726339
		2.2	0.690931
		2.33	0.647469
		2.4	0.62521
		2.5	0.594732
		2.6	0.56574
		2.7	0.538161
		2.8	0.511926
		2.9	0.486971
		3	0.463232

Table E.3: EDC-FDOT method resistance factors for total pile capacity at closest restrike prior to SLT, excluding pile #2 (Case 1)

λ_R	COV_R	β	ϕ_R
1.0356	0.18808	1	1.008359
		1.1	0.980889
		1.2	0.954167
		1.3	0.928173
		1.4	0.902887
		1.5	0.878291
		1.6	0.854364
		1.7	0.831089
		1.8	0.808448
		1.9	0.786424
		2	0.765
		2.1	0.744159
		2.2	0.723887
		2.33	0.698356
		2.4	0.684983
		2.5	0.666323
		2.6	0.64817
		2.7	0.630513
		2.8	0.613336
		2.9	0.596627
		3	0.580374

Table E.4: EDC-FDOT method resistance factors for total pile capacity at EOID, excluding pile #2 (Case 5)

λ_R	COV_R	β	ϕ_R
1.785	0.495	1	1.253785
		1.1	1.191377
		1.2	1.132076
		1.3	1.075726
		1.4	1.022181
		1.5	0.971302
		1.6	0.922955
		1.7	0.877014
		1.8	0.833361
		1.9	0.79188
		2	0.752464
		2.1	0.715009
		2.2	0.679419
		2.33	0.635788
		2.4	0.613466
		2.5	0.58293
		2.6	0.553915
		2.7	0.526343
		2.8	0.500144
		2.9	0.475249
		3	0.451594

COMPARISON OF FOSM AND AFOSM METHODS OF RELIABILITY INDEX CALCULATIONS

FOSM is the abbreviation for First-order Second Moment method whereas **AFOSM** is that for Advanced First-order Second Moment method. Both are First-order Reliability Methods implying that they use the first and the second moments of the probability distribution function (pdf) of the performance function, G.

As an example, if G is expressed as R-S where R and S are the resistance and the load respectively, and the pdf of G is $\mathbf{f_G(g)}$, then the first, second and the nth moments of $f_G(g)$ can be written as follows:

$$M_1 = \mu(g) = \int_{-\infty}^{\infty} g . f_g(g) dg \tag{F1}$$

$$M_2 = Va(g) = \int_{-\infty}^{\infty} [g - \mu]^2 . f_g(g) dg \tag{F2}$$

$$M_n = \int_{-\infty}^{\infty} [g - \mu]^n . f_g(g) dg \tag{F3}$$

One realizes that in order to correctly represent the entire distribution of G, one must use all the possible moments of $f_G(g)$, an exercise which is impractical. Therefore, in most reliability computational methods such as **FORM**, the analysts use just M_1 and M_2 to represent the entire pdf distribution of G, thus approximating the reliability assessments.

FOSM and AFOSM are both FORMs implying that both of them only use the mean (μ_g) and std. deviation (σ_g) of G to determine the reliability coefficient β. However, they do differ in the method of calculation adopted in deriving the reliability coefficient β.

Process of determining β in FOSM:

1. G is expressed in R and S, the simplest forms being $G = R$- S (if R and S are normally distributed) and $G = R/S$ (if R and S are log-normally distributed).

2. $f_G(g)$ is expressed as a joint distribution of R and S as $f_{R,S}(r,s)$.

3. Assuming independence between R and S, $f_{R,S}(r,s)$.can be separated into the product of $f_R(r)$ and $f_S(s)$.

4. In order to find the mean of G or $\mu(g)$, the first moment equation (F1) can be rewritten as

$$M_1 = \mu(g) = \iint_{-\infty}^{\infty} g f_R(r) f_S(s) \tag{F4}$$

5. In order to find the variance of G or $Va(g)$, the second moment equation (C2) can be rewritten as

$$M_2 = Va(g) = \iint_{-\infty}^{\infty} (g - \mu)^2 f_R(r) f_S(s) \tag{F5}$$

6. G is expressed using the Taylor series expansion about its mean value as follows:

$$g = g(\mu_R, \mu_S) + \frac{\partial g}{\partial R}(g - \mu_R) + \frac{\partial g}{\partial S}(g - \mu_S) + higher\ order\ terms\ with\ second\ partial$$
$$derivatives \tag{F6}$$

If the higher order terms of Eqn. (F6) are truncated and substituted in Eqns. (F4) and (F5), one can obtain μ(g) and Va(g) as follows:

$$\mu(g) = g(\mu_R, \mu_S) \tag{F7a}$$

$$Va(g) = \left[\frac{\partial g}{\partial R}\right]^2 Va(R) + \left[\frac{\partial g}{\partial S}\right]^2 Va(S) \tag{F7b}$$

If G=R-S, it is easily seen that the second partial derivatives are zero in Eqn. (F6) and hence

$$\mu(g) = \mu_R - \mu_S \tag{F7c}$$

and

$$Va(g) = [\sigma_R]^2 + [\sigma_S]^2 \tag{F7d}$$

7. If R and S are normally distributed, then G=R-S is also normally distributed, providing the reliability index β as

$$\beta = \mu(g)/\sqrt{Va(g)} \tag{F8a}$$

where
$$P_f = \emptyset[-\beta] \tag{F8b}$$

and ɸ is the cumulative standard normal variate.

It is seen that similar arguments apply to G=R/S if R and S are log-normally distributed

Limitations of the FOSM method:

i. If *G* is a nonlinear function of *R* and *S*, then the higher order terms in Eqn. (F6) will not be zero and hence Eqns. (F7c) and (F7d) will provide approximate estimates.

ii. Similarly, not all the alternative functional forms of G will allow the truncation of the higher order terms in Eqn. (F6) without generating a significant error.

iii. R and S will have to be either normally or log-normally distributed.

iv. Only the first and the second moments of G are used for the computation of β since it is a FORM method.

Comparison with AFOSM

As illustrated in Appendix C, in the AFOSM method on the other hand, the derivation of the reliability index provides a unique solution, since both R and S are normalized using the transformation in (C7a) and (C7b)

$$\text{If } R' = \frac{R - \mu_R}{\sigma_R} \tag{C7a}$$

$$\text{and } S' = \frac{S - \mu_S}{\sigma_S} \tag{C7b}$$

and the reliability index is determined as in Eqn. (C9) from the shortest distance from the origin of R' Vs S' plot to the limit state surface where $g(B', S')=0$.

Strengths/Limitations of the AFOSM method:

i. Since no truncation of the higher order terms is needed (e.g. in Eqn. (F6)) the reliability index β will be exact.
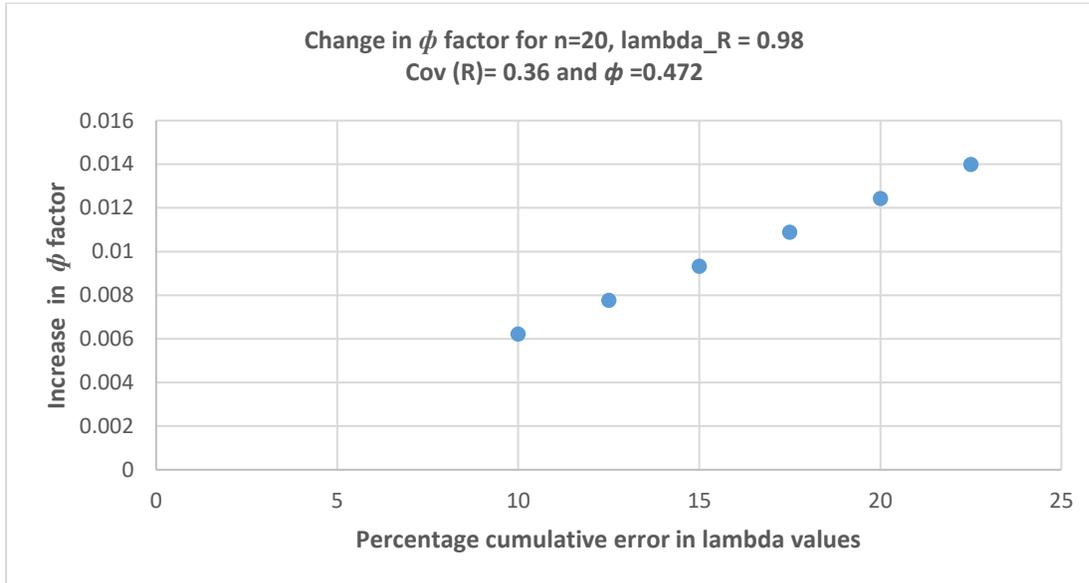
ii. Similarly, all the alternative functional forms of G will produce the same reliability index β since the truncation of the higher order terms is not needed.

iii. Typically R and S will have to be either normally or log-normally distributed. However, as illustrated in the Appendix C this method can be modified to accommodate R and S distributions that are not normal or lognormal.

iv. Only the first and the second moments of G are used for the computation of β since it is also a FORM method.

APPENDIX G

EFFECT OF SLT (OR CAPWAP OR EDC) ERRORS ON THE ϕ_R FACTORS

Change in ϕ factor for n=20, lambda_R = 0.98
Cov (R)= 0.36 and ϕ =0.472

Increase in ϕ factor (y-axis)
Percentage cumulative error in lambda values (x-axis)

Figure G1. Effect of SLT (or PDA or EDC) errors on the ϕ_R factors

The above plot was developed for a typical data set of 20 piles that we have generated with an average bias factor of 0.98, coefficient of variation of bias of 0.36 yielding a ϕ_R of **0.472**. Assume a simple example where a number of SLT values (R_m in Eqn (G1) on the next page) of 1000 kip were overestimated by a cumulative value of 250 kip. This could be the result of an extremely impossible scenario of overestimating 5 SLT values (out of 20 piles) by 50 kip each. Usually this would not happen unless there is a systematic error, since random estimation errors ($d\lambda_{i,}$ in Eqn. (G2)) do not necessarily have the same sign.

The above plot shows that the error in ϕ_R would be about 0.016 with ϕ_R changing to about **0.488** even in this extremely erroneous hypothetical situation.

In addition, the following facts must be noted:

    i.   Underestimation of SLT values will result in a negative change in ϕ_R of the same order of magnitude.

    ii.   It is realized from Eqn. (G1) that the effect of overestimation of SLT values will be equivalent to that of underestimation of PDA/EDC values and vice versa. Hence errors in predictions can also be handled by the same analytical approach.

Finally, instead of doing a cumbersome parametric study which involves many possibilities, convenient plots such as the one above can be generated conveniently using a calculus-based error analysis that is illustrated below.

<u>Derivation</u>

For any i^{th} pile, the bias factor can be expresses by Eqn. (G1)

$$\lambda_i = \left[\frac{R_m}{R_n}\right]$$ (G1)

Where R_m and R_n are the measured and the nominal resistances respectively.

The change in the ϕ_R factor due to an overestimation of the λ value for any pile ***I***, ***d***λ_i, can be obtained from Eqn. (G2). According to Eqn. (G1), this overestimation can be due to an overestimation of R_m or an underestimation of R_n. Conversely, underestimation of R_m or an overestimation of R_n will result in an underestimation of λ_i (negative ***d***λ_i)

$$d\phi_R = \sum_{i=1}^{n} \frac{\partial \phi_R}{\partial \lambda_i} d\lambda_i$$ (G2)

where n = number of piles

The mean and the coefficient of variation of the λ values for an n number of piles can be expressed as follows:

$$\lambda_R = \frac{\Sigma \lambda_i}{n}$$ (G3)

$$COV_R = \frac{\sigma \ (std.deviation) of [\lambda_i]}{\lambda_R}$$ (G4a)

$$\sigma_R = \sqrt{\frac{\Sigma(\lambda_i - \lambda_R)^2}{(n-1)}}$$ (G4b)

$$COV_R = \sqrt{\frac{\Sigma(\lambda_i - \lambda_R)^2}{(n-1)}} \frac{1}{\lambda_R}$$ (G4c)

From Eqn. (G3)

$$\frac{\partial \lambda_R}{\partial \lambda_i} = \frac{1}{n}$$ (G5)

From Eqn. (G4a)

$$\frac{\partial Cov_R}{\partial \lambda_i} = \frac{n(\lambda_i - \lambda_R)\lambda_R - (n-1)\sigma_R^2}{n(n-1)\sigma_R \lambda_R^2}$$ (G6)

Consider the resistance factor expression given in Eqn. (4.4)

$$\phi_R = \frac{\lambda_R[\gamma_D Q_D + \gamma_L Q_L]\sqrt{\frac{(1+COVQ_D^2 + COVQ_L^2)}{(1+COV_R^2)}}}{[\lambda_{QD}Q_D + \lambda_{QL}Q_L]e^{\beta_T \sqrt{\ln[(1+COVQ_D^2 + COVQ_L^2)(1+COV_R^2)]}}}$$ (3.4)

When the following conventional values are substituted, $Q_D/Q_L = 2$, $\gamma_D = 1.25$, $\gamma_L = 1.75$, $COV_{QD} = 0.1$, $COV_{QL} = 0.2$, $\lambda_{QD} = 1.05$ and $\lambda_{QL} = 1.15$, for a target reliability index β_T of 2.33, Eqn. (3.4) becomes

$$\phi_R = \frac{[1.34]\lambda_R}{e^{2.33\sqrt{\ln[(1.05)(1+COV_R^2)]}}\sqrt{1+COV_R^2}} \tag{G7}$$

$$\frac{\partial \phi_R}{\partial \lambda_i} = 1.34\left[\frac{\left(\frac{\partial \lambda_R}{\partial \lambda_i}\right)}{e^{2.33\sqrt{\ln[(1.05)(1+COV_R^2)]}}\sqrt{1+COV_R^2}} - \lambda_R\left|\frac{\frac{2.33COV_R}{\ln[(1.05)(1+COV_R^2)](1.05)(1+COV_R^2)}\left(\frac{\partial Cov_R}{\partial \lambda_i}\right)}{e^{2.33\sqrt{\ln[(1.05)(1+COV_R^2)]}}\sqrt{1+COV_R^2}} + \right.\right.$$

$$\left.\left. \frac{COV_R\left(\frac{\partial Cov_R}{\partial \lambda_i}\right)}{e^{2.33\sqrt{\ln[(1.05)(1+COV_R^2)]}}\sqrt{1+COV_R^2}}\right|\right]$$

$$\frac{\partial \phi_R}{\partial \lambda_i} = 1.34\left[\frac{\left(\frac{\partial \lambda_R}{\partial \lambda_i}\right)-\lambda_R COV_R\left(\frac{2.22}{(1+COV_R^2)\ln[(1.05)(1+COV_R^2)]}+\frac{1}{1+COV_R^2}\right)\left(\frac{\partial Cov_R}{\partial \lambda_i}\right)}{e^{2.33\sqrt{\ln[(1.05)(1+COV_R^2)]}}\sqrt{1+COV_R^2}}\right] \tag{G8}$$

One can evaluate $\frac{\partial \phi_R}{\partial \lambda_i}$ by substitution from Eqns. (G5) and (G6).

Finally, using Eqn. (G2), the expected change in ϕ_R due to overestimation or underestimation errors in λ_i can be obtained.